U. S. DEPARTMENT OF THE INTERIOR
U. S. GEOLOGICAL SURVEY

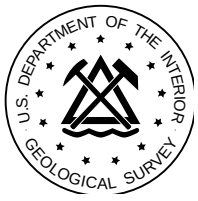

DENSE THREE-DIMENSIONAL ARRAY NEAR GARNI, ARMENIA AS PART OF THE JOINT EURASIAN SEISMIC STUDIES PROGRAM

(OBJECTIVES, ARRAY DESIGN, ARCHIVED DATA, AND PRELIMINARY WAVE-SLOWNESS ANALYSIS)

edited by

Gary Glassmoyer
and
Roger D. Borcherdt

OPEN-FILE REPORT 93-216

Menlo Park, California
February 1993

DENSE THREE-DIMENSIONAL ARRAY NEAR GARNI, ARMENIA AS PART OF THE JOINT EURASIAN SEISMIC STUDIES PROGRAM

(Objectives, Array Design, Archived Data, and Preliminary Wave-Slowness Analysis)

CONTENTS

CHAPTER I

Summary and Objectives
for
a Dense Three-Dimensional Array near
Garni, Armenia

J. Filson, R. D. Borcherdt, W. H. K. Lee, E. Cranswick,
C. Dietel, E. Sembera, J. Mori, and J. Sena
(U. S. Geological Survey)

L. Hakhverdian, R. Amirbekian, V. Aharonian, K. Safarian, H. Galagian, and G. Apoian
(Yerevan Seismic Station)

R. Banfill
(Small Systems Support, Big Water, Utah)

INTRODUCTION

Within two weeks following a major earthquake in December 1988 a team of seismologists and engineers from the United States went to Armenia to investigate the cause and effects of that tragic event. A modest but sustained cooperative effort between seismologists in Armenia and in the U. S. Geological Survey (USGS) has grown from that initial post-earthquake investigation. In 1989 the USGS began to participate in what is now called the Joint Seismic Program (JSP) between the United States and what was then the Union of Soviet Socialist Republics (USSR). This program is led on the U. S. side by the Incorporated Research Institutions for Seismology (IRIS) and on the Soviet side by the Institute of Physics of the Earth. In 1989 the Soviet side suggested that among other things the JSP project should include detailed studies of the seismicity of certain earthquake-prone areas of the Soviet Union. Kirgizia and Armenia were offered as places where arrays of seismometers could be installed for this purpose. As a participant in theJSP and as the organizer of the post-earthquake investigation in Armenia, the USGS was chosen to take up the array work in Armenia.

OBJECTIVES

During the 1988 post-earthquake investigation Armenian colleagues suggested that a portable seismic station be installed at a geophysical observatory near Garni, about 20 km east of the capital, Yerevan (Figure 2-3). A trip to this site revealed a two-story building with a horizontal tunnel, or adit, running from the basement about 200 meters into the hill behind the building. This tunnel had been constructed for the purpose of obtaining geophysical observations relevant to earthquake prediction. The tunnel was lined with concrete and had several small rooms with piers suitable for seismic recording (Figure 2-5). The tunnel is described in more detail in the next chapter.

Given this excellent facility and the charge from the Joint Seismic Program, a USGS team went to Armenia in June 1990 with the purpose of installing a dense seismometer array in and around this tunnel. Other than taking advantage of an exceptional site, the scientific justification for the array can be seen in Figure 2-4. The Garni site lies on the northern edge of a long, steep valley that runs northeast-southwest opening to the southwest onto the larger and broader valley of the Araks River about 10 km south of Yerevan. There is concern that the topography of the narrow valley near Garni is controlled by an active fault. A Roman temple at Garni was destroyed by a “great” earthquake in 1679. If the valley follows the course of an active fault, then this fault represents a considerable hazard to Yerevan, a city of 1.2 million people, with construction of the type that was destroyed in Spitak and Leninakan in 1988 killing over 25,000 people. The purpose of the array is to detect and locate if possible any local seismicity associated with a larger pattern of strain release along this fault. Of course a wider microearthquake network would have been more suitable for this task, but was not considered possible given the time allowed and the funds provided.

The recording scheme is built around the General Earthquake Observtion Systems (GEOS) developed and described by Borcherdt *et. al.* (1985). A PC-based system developed by W. H. K. Lee is also used for recording-backup and display of the data. The seismometers used are 1 Hz Mark Products L-4Cs deployed in three-component sets. The fact that the tunnel is set into a hill provided the opportunity to establish sites on the hill above the tunnel and thus provide a three dimensional array geometry. The GEOS and PC recorders were set up in the observatory building with cable

connections to the seismometer sites. The total aperture of the array is less than 1 km. More detailed descriptions of the array geometry and recording system specifications are given in the next chapter.

(The array deployment was completed within a two-week period during June 1990. Anyone who has ever participated in a similar exercise in a foreign country will appreciate the difficulties endured and the problems that had to be met and overcome. A full description of the effort will probably be wasted on anyone who has not. However, it must be said that the task could not have been completed without the help of Armenian colleagues and their families. We slept in an abandoned dormitory with no running water or other facilities. Our food was bought, cooked, and served by the wives and friends of the Armenians working with us on the project. Our Armenian colleagues carried gear, dug pits, pulled cable, mixed concrete, and generally shared in all of the labor intensive activities.)

SUMMARY

Since the installation of the dense array nearly one thousand events have been recorded at one or more of the array sites. The array has operated since July 1990 with some gaps in recording caused by strains on the infrastructure of Armenia due to the breakup of the Soviet Union and military actions resulting from disputes with Azerbaijan over contested territory. This report documents the recordings of the array and shows examples of the types of events that are available for study. Data from the array has been placed on optical disks and is available on these disks from the USGS and also through the IRIS Data Management Center in Seattle, Washington. Data from the array has proven amenable to three-dimensional analysis as described in Chapter V. The analysis of the local seismicity is not yet complete. It is clear that there is considerable local activity, occurring at times of day random enough that it cannot be due to blasting. Accurate location of these events with an array this small remains a problem of study.

CHAPTER II

Site Selection, Array Design, and Recording Instrumentation for the Dense Three-Dimensional Array near Garni, Armenia

R. D. Borcherdt, J. Filson, W. H. K. Lee, E. Cranswick,
C. Dietel, G. Glassmoyer, E. Sembera, and J. Mori
(U. S. Geological Survey)

L. Hakhverdian, R. Amirbekian, V. Aharonian, K. Safarian, H. Galagian, and G. Apoian
(Yerevan Seismic Station)

R. Banfill
(Small Systems Support, Big Water, Utah)

SUMMARY

Scientific objectives and logistic constraints were primary considerations in site selection and design of the dense three-dimensional array near Garni, Armenia. Principle scientific objectives concerned the need for high-frequency discrimination studies and the need to monitor seismicity for improved seismic hazard analyses for the capitol city of Yerevan with a population of 1.2 million. Principle logistic constraints concerned availability of supplies, fuel, transportation resources and site security. Instrumentation selection was based on availability of resources, familiarity, and reliability.

SITE SELECTION

The site selected for array installation was developed for geophysical monitoring purposes in the 1970s as a cooperative effort involving the USSR and Armenian Academies of Science. The facility is known as the Garni Observatory. Logistic difficulties concerned with availability of transportation vehicles and fuel were considered sufficient to preclude establishment of isolated multiple monitoring stations that might require regular visits for power maintenance.

Garni is located approximately 20 kilometers east of the capitol city of Yerevan in a moderately remote region. The location relative to other landmarks is shown at different map scales in Figures 2-1, 2-2, 2-3 and 2-4. The observatory site is located at the base of a large hill which in turn forms the boundary for a small valley used for minor agricultural farming. The area near the observatory is used primarily for the grazing of a small dairy herd.

The site consists of an elaborate two-dimensional horizontal tunnel complex (Figure 2-5) leading from the basement of the two-story observatory building (Figure 2-7), and about four hectares of property. The site is under the jurisdiction of local cooperating scientific officials and is relatively secure from vandalism. The extensive two-dimensional tunnel configuration at the observatory provided a unique opportunity to establish an array to serve as both a three-dimensional array for high-frequency discrimination studies and as an array to assist in monitoring seismicity for improved seismic hazard analyses for Yerevan.

Seismic studies conducted at this site as part of the joint U. S. - U. S. S. R. cooperative studies following the devastating earthquakes of December 7, 1988 (Borcherdt *et al.*, 1989), showed that the site is relatively well isolated from local cultural noise sources.

ARRAY DESIGN

The array design was developed to incorporate the two-dimensional configuration of the tunnel as shown in Figure 2-5. Using the length of the shortest arm of the tunnel as the minimum dimension of the array (~60 m), the array was designed within geometric constraints of the tunnel and available cable to resemble a nested tripartite configuration. The array is centered on a tetrahedron, consisting of sites G1A, G1B, G2B and G4A, with minimum distances between sensors being roughly 60 meters. Three-component sensors are located in a nested configuration with spacings of about 60, 120, 200, and 480 meters. The final vertical and horizontal apertures of the array are 87 and 823 meters,

respectively. The final configuration of the array as defined by the locations of the three-component sensors is shown in Figure 2-6.

To increase the aperture of the array the initial design included an additional three sites located at distances of about 1.5 km from the center of the array. The lack of appropriate housing in the area and scarcity of available resources led to the establishment of sites G6A and G7A. The first subsequent revisit of the site a few months later showed that continued maintenance of sites G6A and G7A was also an extreme imposition on local resources. As a result these stations were withdrawn from the array.

INSTRUMENTATION

Sensors -- Three single-component velocity transducers (1 Hz, Mark Products L-4C) oriented vertical, north-south, and east-west (refer to Table 2-1 for actual sensor orientations and positions) were emplaced at each of the array nodes indicated in Figure 2-6. Each of the sensors was emplaced on a concrete pad (~ 0.5 x 0.8 x 0.1 m) prepared at each site with leveling platforms and housings (Figures 2-9 and 2-10) according to specifications used for emplacement of sensors in the Central California Network. Sensor signals were transmitted over cables to a central recording area located in a secure room (Figure 2-8) on the second floor of the observatory building (Figure 2-7). It was necessary to use locally available unshielded cable for location G4B, because one large reel of shielded U. S. supplied cable was lost in shipping.

Recording Instrumentation -- Array recording capabilities were designed to permit on-site data playback and analysis capability by local scientists and technicians. They were designed to provide redundancy in recording, playback, and event-timing capabilities. IBM compatible personal computers (PCs) were selected because of their wide availability and the local inaccessibility to other types of computer hardware. Subsequent array operation confirmed this conclusion and showed that even the replacement of common components such as hard disks was beyond the capacity of local resources.

The array was designed so that seismic-event signals are recorded simultaneously at 200 samples per second (sps) both in 16-bit digital format using GEOS and in 12-bit digital format using a PC. Two sets of three-component signals are recorded on each six-channel GEOS recorder. In addition, each set of six analog sensor signals upon being amplified and filtered for anti-aliasing by GEOS is multiplexed and recorded on the PC. Detailed performance specifications of the GEOS and the personal computer system are provided by Borcherdt *et al*. (1985), and Lee *et al*. (1988), respectively.

Timing -- Timing for the array was also designed to include redundancy. A master Omega receiver was used to establish absolute time for a master clock. In order to optimize relative timing each GEOS in the Garni Observatory was linked so as to synchronize and determine clock skew measurements with respect to the time pulse of the same master clock. The GEOS permits the clock skew measurements to be written to tape at operator selected time intervals. As an additional constraint to improve relative accuracy, the array was designed such that all signals for each event were digitized by a single analog-to-digital converter and recorded on the PC. In addition, special Omega receiver boards were designed that would have permited each GEOS to independently synchronize to Omega. Nominal GEOS clock drift rates are less than 80 milliseconds per day.

Power -- To accommodate frequent power outages and variations in voltage levels, power was supplied through an uninterrupted power supply to the PC and through batteries for the GEOS. Ungrounded power lines in the Observatory required that special provisions be implemented to minimize electronic noise pick-up on signal cables. Electronic noise was a special problem for location G4B connected via unshielded cable and was most apparent at night, when electrical lights were being used. Power outages proved to be sufficiently severe so as to eventually damage PC hard disks and reduce on-site playback capabilities.

Data Playback -- To facilitate on-site data playback, GEOS hardware and software capabilities were augmented to permit data playback via PC. Capabilities were developed for the simultaneous archival of both GEOS and PC data using two PCs networked via LANtastic. One PC is used as a data acquisition system and the other as a data playback, archival, and analysis system. Software was developed for automatic data archival using a simple multi-tasking environment. PC-compatible optical disks were selected as the medium for data archival.

Previously developed GEOS playback software (RDGEOS) used on Digital Electronic Corporation mini-computers was converted for operation on PCs (PCGEOS). GEOS software was developed to permit each GEOS unit to serve as a field playback unit via RS-232 into the portable field PCs.

Table 2-1. Sensor Locations and Orientations

Station	Relative Position (meters from tunnel door)			Component Orientation (degrees clockwise from north)	
	North	East	Down	5 ("N")	6 ("E")
G1A	185.3	8.1	-0.7	2	92
G1B	180.0	53.0	-0.7	2	92
G2A	56.6	3.9	-0.1	2	92
G2B	125.1	-2.1	-0.7	2	92
G3A	4.8	0.9	0.0	2	92
G3B	100.4	1.4	-39.4	5	95
G4A	185.3	8.1	-60.5	5	95
G4B	384.5	16.7	-87.8	5	95
G5A	-37.0	-189.8	13.5	5	95
G5B	-63.7	167.0	-0.8	5	95
G6A	-332.7	-386.6	31.0	5	95
G7A	-159.5	344.7	12.1	5	95

Positions were determined assuming the tunnel is aligned 2.5 degrees east of north. Tunnel sensors were aligned with the tunnel axis. Surface sensors were aligned with magnetic north. Component 4 ("Vertical") is oriented with positive up. Location and orientation information was not recorded for preliminary stations GAA, GAB, GBA, GCA, GCB, GDA or GDB.

Figure 2-1. World view centered on Garni, Armenia.

Figure 2-2. Armenia and surrounding countries with bodies of water, political boundaries, major highways, selected cities, and the locations of the Spitak and Georgia Earthquakes on a half-degree latitude - longitude grid.

Figure 2-3. Northern Armenia with bodies of water, political boundaries, major highways, selected cities, Mount Ararat, and the epicenter of the 1988 Spitak Earthquake.

Scale 1:250,000; elevations in feet; from Defense Mapping Agency - Tactical Pilotage Chart F-4C, edition 4.

Figure 2-4. Map of the Garni - Yerevan region of Armenia. Circle marks Garni Observatory.

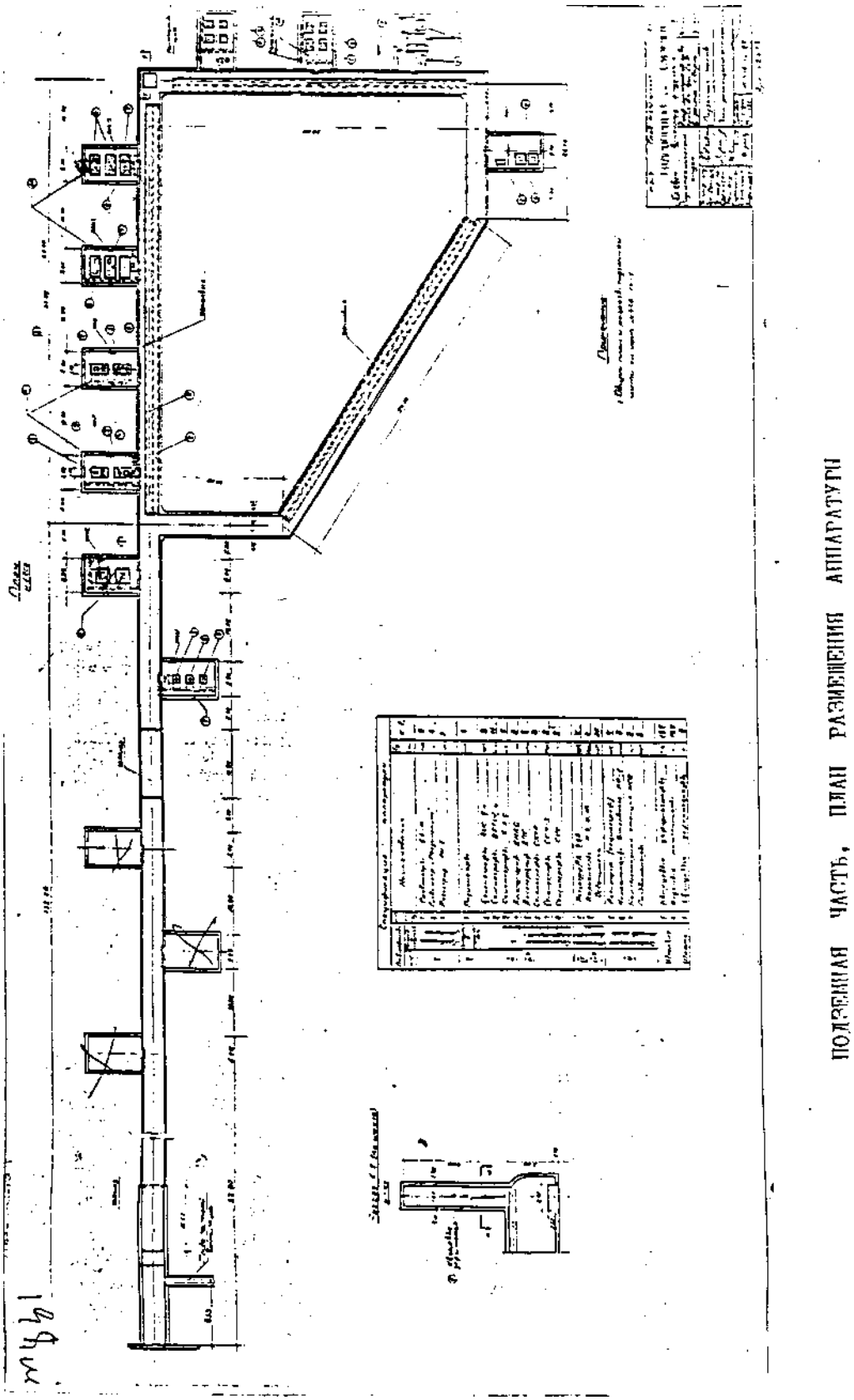

Figure 2-5. Plan view of the Garni Observatory Tunnel.

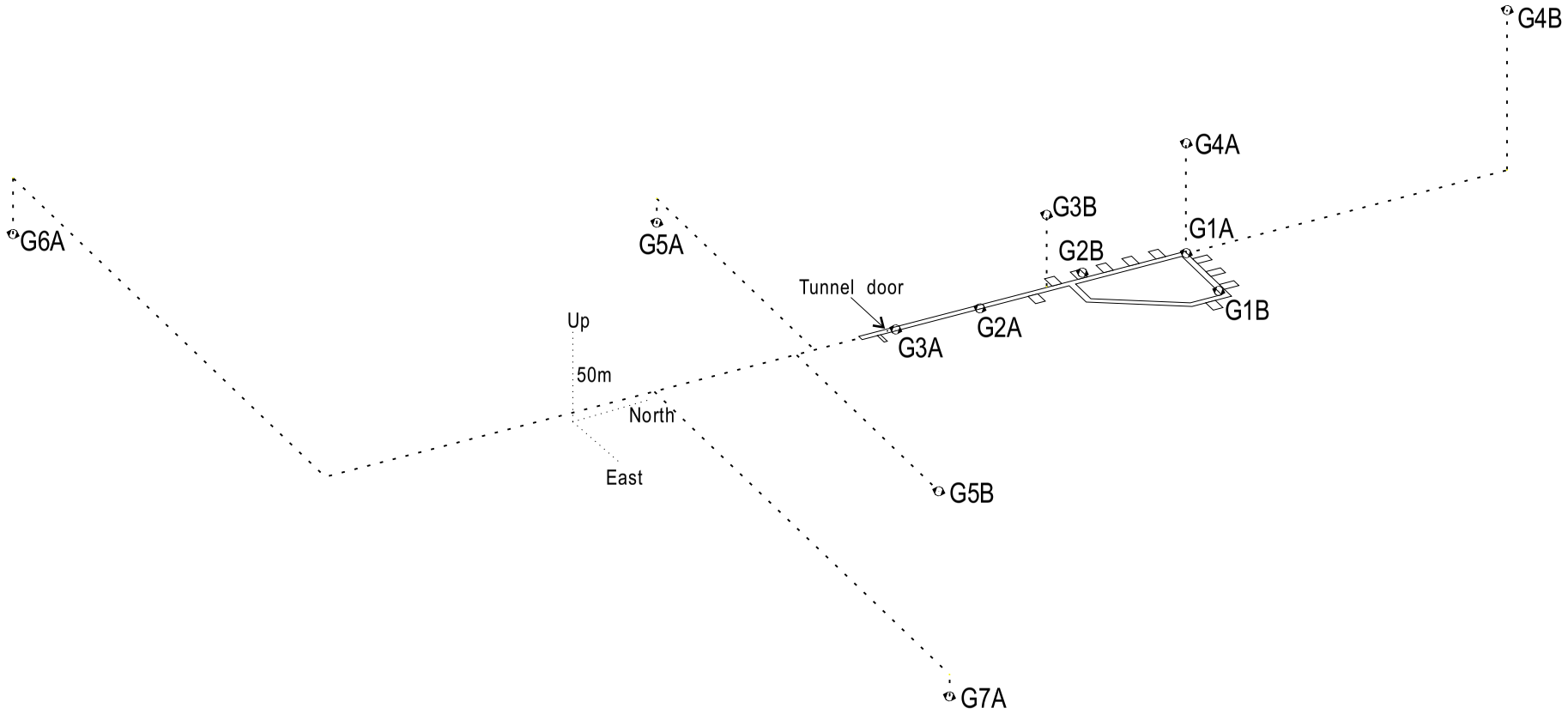

Figure 2-6. Oblique view of sensor locations with respect to the Garni Observatory Tunnel. Dashed lines indicate vertical, parallel to, and perpendicular to the tunnel axis. The tunnel door, which is the origin of the coordinate system used in Table 2-1, is at the small dot indicated by the arrow.

Figure 2-7. Two-story building at Garni Observatory.

Figure 2-8. Playback room at Garni Observatory.

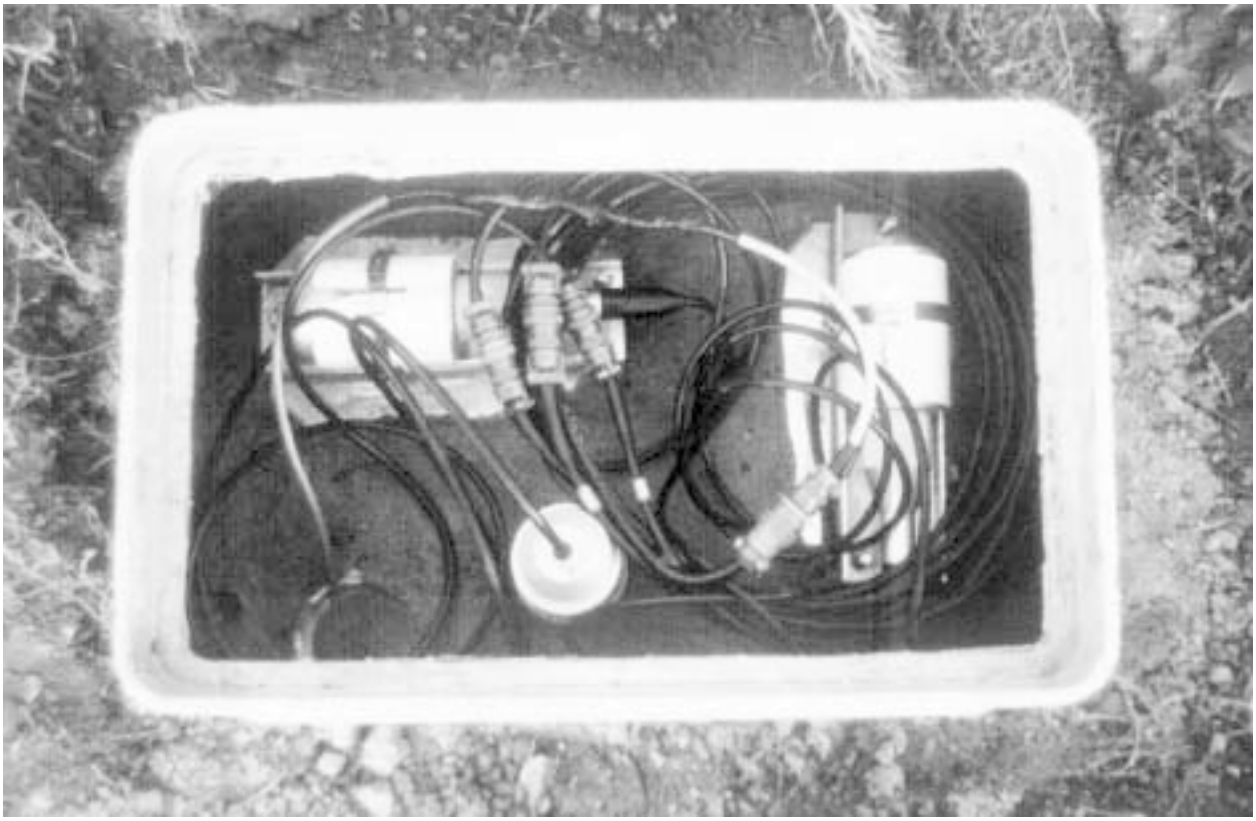

Figure 2-9. Three components of sensor deployment.

Figure 2-10. Sensor housing at a surface site.

CHAPTER III

Digital GEOS Data from Garni, Armenia as Archived on Optical Disk

G. Glassmoyer
(U. S. Geological Survey)

PROCESSING

As of this writing 245 GEOS tape cartridges from the Garni Array, representing the time period 26 June 1990 through 10 August 1992, have been played back at the National Strong Motion Data Center.

The playback procedure involves demultiplexing of the data on tape cartridge using the computer programs RDGEOS on a DEC VAX computer or PCGEOS on an IBM-compatible PC. These programs write separate time-series files to disk for each channel recorded on GEOS, plus a time-stamp file that contains the start times of each (0.42 second) block of data recorded on the GEOS.

Format

The format used for the digital data is a block-binary file consisting of two header blocks (512 bytes each), one 2-byte integer, the other 4-byte real, followed by the data as 2-byte integers. Integer and real values are stored in the format used by DEC PDP and VAX computers. 2-byte integer values are stored as low-byte-first, high-byte-second signed integers in two's-complement form. 4-byte real values are stored as high-word-first, low-word-second. The integers are in the same format as used by PCs, however the real values are not the same format as PC real values. Programs RECSEC or VECTOR, written by E. Cranswick and R. Banfill, can be used to read the data on a PC.

Filenames on the VAX are constructed from the station name and the start-of-record time. Characters 1-3 are the day-of-year (001-366), characters 4-5 the hour (00-23), characters 6-7 the minute (00-59), and character 8 represents the second (A-T, where A=0-2, B=3-5, ..., T=57-59). Character 9 is the component (4 is vertical, 5 and 6 are horizontal). The suffix is the station name. On the PC and the optical disk one less character is available for the filename so the hour is represented by a letter from A to X.

Fixes

Normally the GEOS can be relied upon to write to tape cartridge the complete recording sufficiently well to be read and accurately interpreted by the demultiplexing programs. It has been a recognized phenomenon that the GEOS instruments may occasionally fail in part or whole to write an accurate tape. These types of failures occurred in several forms in this study. In the case of data that can still be read by the programs, these failures can be grouped into two types: bit errors and block errors.

An exact correction can usually be made for bit errors. These are what are often referred to as “glitches.” The symptom is an occasional data value that is a large power of two different from the preceding and subsequent data values. The cause typically is memory board failures, but can also be in the analog-to-digital circuit. The computer program BITFIX is used to find and correct bit errors whenever the bit errors are sufficiently large compared to the true rate of change between data values.

Block errors usually cannot be fully corrected. These are instances where the data block to be written to GEOS tape cartridge either is not written, or that which is written is corrupt. During playback the demultiplexing program (RDGEOS or PCGEOS) attempts to identify missing data blocks by examining the data-block time stamps. When these are identified, the null data value (integer header offset 3 of Table 3-1a) is written to the data file in place of the missing data. The G5 recordings have several instances of these data gaps.

If the first data block of an event is corrupt, then the files created for that event will initially be given a name that does not indicate the true time of that event. Such files may also contain initial meaningless data. Such files are easily recognized by the program CHKTIME which compares the start-of-block time stamps, as written to the time-stamp files, to their expected time values. Start-of-record times have been corrected for these files using the program CHGTIME.

In addition to allowing files to be given the correct start times, the program CHKTIME, reading the time-stamp files, also verifies the integrity of timing within the recordings. By this means several recordings have been found to have faulty internal timing. The cause of these failings is not always certain, but often is the result of reading a corrupt data block in the midst of an event. Recordings that contain internal timing errors have been corrected to the degree possible by using null values to mark those samples where no data are available, or by removing extra null values that the demultiplexing programs may have mistakenly added. These corrections are made using the editing capability of the programs RAWRI2 and RAWWI2.

Recording parameters are stored in the two header blocks described in Table 3-1. The most critical values are shown in boldface. Many of these such as amplifier gain (see log-files in Figure 3-1) are derived from the GEOS cartridge. Other parameters such as station location or sensor orientation are added from the parameter list file GARNI.AHC. While usually accurate, there are instances where the polarity may be opposite from that which is indicated for vertical components. A careful evaluation of each clock correction in the manner described in the log-file section later should be made if these are important to a study.

PLOTS OF SELECTED EVENTS

Plots are included for those seismic events that were recorded at five or more three-component stations. These events are listed in Table 3-2, where the second-code of the filename is used to indicate those stations that recorded an event. The plots have been prepared using E. Cranswick's RECSEC program. They show each trace at equal amplitude, bundled by three-component station, for a duration proportional to the number of stations recording the event (5 seconds per station). The time (nominally UTC) of the first sample in each plot is indicated in large numbers on the right-hand side of the plot page. This is given as year (less 1900), day-of-year, hour, minute, second, and millisecond. The time scale at the top of the plot page is in seconds. Indicators on the right-hand side identify the individual trace. For example, G5B.V2 is station G5B's 2nd velocity channel - the first channel is up, the second is nominally north, and the third is nominally east. See Table 2-1 for actual horizontal orientations indicated for components 5 (=.V2) and 6 (=.V3). Numbers on the left-hand side of each trace indicate the maximum absolute value in digital counts through the end of the plotted portion of each trace (32767 is full-scale).

ORGANIZATION OF OPTICAL DISK

Two IBM-3363 write-once-read-many (WORM) optical disks have been prepared containing calibration records and seismic triggers as listed in Table 3-3. One disk contains the 1990 data and the other contains the data from 1991 through 10 August 1992. Data are organized into subdirectories by day-of-year of event. These subdirectories are within parent directories by year. Log-files created

by the demultiplexing programs from each tape are included in the LOG directory on the 1991-1992 disk. Also included are ORDARR files for use by the Cranswick and Banfill (WFPS) processing programs for each year. The WHERE list of Table 3-3 is also provided as text files for each year. Seismic triggers were selected by visual inspection and may still include such events as aircraft triggers or other signals that appear as possibly of seismic origin.

LOG-FILES

Four examples of log-files are provided in Figures 3-1a through 3-1d. These show most of the useful types of information that can be read from a log-file.

LOG28.G3 (Figure 3-1a) is a typical log-file from the program RDGEOS. The first line indicates the date and time the program was run and the program name and version. The log-file number (28) is added after the RDGEOS program has completed its operation, so it does not appear on this line which shows simply LOG.G3. Following is the channel/component naming description. The default refers to the log file itself as well as to the time-stamp files. Channel 1 data is component 4 of data for G3A, *etc*. The next lines indicate the tape/experiment number, location number, GEOS unit serial number, and the year. If any of these parameters change during the tape, such as the year, a new indication is made.

In the next line file numbers include all files be they data or clock files as counted by the demultiplexing program (RDGEOS). The event numbers (Evt) are data files as counted by the GEOS. The type can be a trigger, continuous record, manual record, sensor calibration, amplifier calibration, or a clock file. Clock files can be master-clock synchronization (synch), manual synch, WWVB synch, WWVB synch failures (VB Synch TMO), or WWVB corrections. The time indicated for data files is of the first sample, as measured by the internal GEOS clock and is shown as day-of-year, hour, minute, second, and millisecond. The time standard can be none, manual, WWVB, or external. For the Garni data the time standard shown in this column is probably not reliable. An indication of none means that the clock has not been set and shows the elapsed time since the GEOS was turned on (starting day 001). Manual (MAN.) would indicate an operator set the clock by hand, such as by reading the time off of a watch. WWVB would indicate the clock was set by interpreting a WWVB time code. External (EXT.) is the only time standard that properly should have been used in this data set, and indicates that the internal GEOS clock was set by an external clock. The clock correction (Corr) as it is stored in the data files is shown in seconds that should be subtracted from the internal GEOS time to get the corrected time. See the later clock-correction example for a more complete discussion. DR100 name is a generic representation of the the names of the data files as they would be stored on a VAX. Duration is an estimate of the length of the recording in minutes and seconds. Srate is the sampling rate in samples per second. Pre-event is the length of time in seconds of GEOS blocks that were filled before the active block of the tape turn-on decision. Volts is the recorder battery voltage at the time of a trigger.

The last four columns refer to parameters of the trigger algorithm. Trg ch is the trigger channel. STA is the short-term-average interval in seconds. LTA is the effective length of the long-term-average interval in seconds. Ratio is the threshold triggering level by which the short-term-average must exceed the long-term-average in order to trigger. Ratio is expressed in Fortran notation of 2 raised to a power. Motion type, amplifier gain, and anti-aliasing filter frequency are shown for each channel.

Examples

File 1 of G3 tape number 28 is a sensor calibration. It was recorded on GEOS unit number 5 beginning in the year 1991, day-of-year 121, hour 14, minute 47, second 27.382 according to the internal GEOS clock that was set by a master-clock. The clock correction stored for this record is 0.000 seconds. Channel 1 is ground-motion velocity recorded with 54 "decibels" (more accurately 2**(54/6) = 512 x) gain using a 7-pole, 50-hertz anti-aliasing filter, and given the filename 1211447J4.G3A (121O47J4.G3A on the PC optical disk). It was sampled at 1200 samples per second and is a little less than 37 seconds long. Battery voltage is not reported for calibrations.

File 2 is an amplifier calibration. The notation about 506 null values refers to this file; in ampliflier calibrations, however, it is due to a minor bug in the GEOS, and the data is complete without the nulls which have since been removed. In other data files each 506 null values represent a lost data block with the data value of -32768 being used in the place of the lost samples.

File 7 is a triggered event. The GEOS was set to trigger by comparing for channel 1 the short-term-average of 0.4 seconds data to 8 (= 2**3) times the long-term-average representing 20 seconds of data. The batteries providing power to the GEOS were at 26.66 volts. Optimum battery voltage is about 24 to 28 volts.

File 3 is a failure to read a WWVB time code. It should not have been set to try since no WWVB-encoded time-code was available.

File 4 is the all-important clock correction! Eight attempts are made by the GEOS to read the one-second pulse of an external signal. This need not be a WWVB signal. As measured by the internal GEOS clock these pulses were detected 1, 0, 0, 0, 1, 0, 0, and 0 milliseconds after the second so the internal and external clocks are in near-perfect agreement.

File 13 is also a clock correction. At its time the internal GEOS clock is 4 milliseconds fast relative to the external clock. For data files that follow the clock correction is recorded in the header as 0.004 seconds.

Clock-Correction Example

File 9 is a triggered recording of a magnitude 5.1 aftershock of the Ratchi, Georgia Earthquake. To get the best estimate of a clock correction for this event it is necessary to interpolate between two clock corrections. Using 0.25 milliseconds (the mean of the eight clock-correction measurements) from file 4 (121:14:56:44) and 4.00 milliseconds from file 13 (122:02:57:52) one can get by linear interpolation 3.5 milliseconds as a clock correction at 122:01:26:00. This 3.5 milliseconds would be subtracted from the 122:01:26:00.618 start-of-record time to get the external clock referenced time of 122:01:26:00.6145.

When similar calculations are made for units G1, G2 and G4 their clock corrections are found to be -0.7, -7.0, and 16.2 milliseconds, respectively, and their externally referenced start-of-record times are ...:01.8837, ...:01.0980, and ...:01.5068. All units are using the same external clock signal, a master clock, so relative times have thus been determined.

The absolute time could then also be determined since there is data in Table 3-4 indicating when the master clock was set to Omega-time. The master clock appears to have been synched to Omega sometime between 116:09:13 and 116:21:14. Later it was found to need adjusting by -5 milliseconds sometime between 125:23:47 and 126:08:05. The minimum estimate of drift for the master clock may be made by assuming the master clock was synched at 116:21:14 and was found to need an

adjustment of -4.5 milliseconds at 126:08:05. The maximum estimate of drift for the master clock may be made by assuming the master clock was synched at 116:09:13 and was found to need an adjustment of -5.5 milliseconds at 125:23:47. This yields a range of -2.5 to -3.2 milliseconds, averaging to -2.8 milliseconds. This master-clock correction should be added to the previously calculated relative clock corrections to get absolute clock corrections. Thus respectively for G1, G2, G3 and G4 the best absolute clock corrections would be -0.0035, -0.0098, 0.0007 and 0.0134 seconds to be subtracted from GEOS start-of-record times. These are different from the values -0.002, -0.006, 0.000 and 0.011 seconds that are stored by default in the headers. All clock corrections stored on the optical disks are the inaccurate default values. The destinctions are small in this case but may approach one full second during intervals when clock synchs are infrequent.

Under ideal circumstances, such as in this example, relative clock corrections could at best be accurate to 1 to 2 milliseconds and absolute clock corrections to 2 to 4 milliseconds. During the Spring of 1991 clock corrections were usually well recorded on all GEOSs. At other times, however, at least one recorder may have been misprogrammed, permitting only partial recovery of relative times. Also, the recording of master-clock resynchs (Table 3-4) was inconsistant, thus limiting the opportunities for the recovery of absolute time.

Other Examples

Following file 14 is a page break.

At the end of the log-file is the line indicating the number of files processed.

LOG03.G1 (Figure 3-1b) is a short example from the PCGEOS program, version 04.07.

The first 2 files on this tape are corrupted clock files. The first 6 words (cells) stored in each block are the start time for that block. PCGEOS attempted to search ahead in the files for intact time information, but found none, so these files were skipped.

The first file from this tape was corrupted. PCGEOS used default header information from file G1.GHD in the “grand-parent” directory for the file(s) it encountered before finding the readable header information in file 4 of this tape. The default header information uses serial number 99 and voltage equal to 20.00 as flags that the header information did not come from the tape.

File 5 is a master-clock synch. At 183:08:26 the GEOS internal clock was set to match the external clock. The remaining information on this line is not reliable.

LOG22.G1 (Figure 3-1c) begins with a master-clock synch, shows a faulty serial number and indicates an operator-initiated (continuous) recording.

LOG06.G2 (Figure 3-1d) begins with clock information extracted from the header of the first trigger. PCGEOS will use this information, which is from the last clock correction on the previous tape, as a starting point for the default value of the clock correction. There is a risk that this value can be very out-of-date and inaccurate (as it may be here). The other examples did not have this either because they were from RDGEOS, had a corrupted header, or began with a clock file.

Not shown is an example which ends with Physical End of Tape indicating that the tape was read all the way through instead of just to the end-of-tape mark. This would be the case for 100% full tapes.

KNOWN EVENTS

153 of the included events have been identified in the National Earthquake Information Center (NEIC) catalog. These are listed in Table 3-5 by date, Table 3-6 by distance, and Table 3-7 by magnitude. Body-wave magnitudes are used unless otherwise indicated. A travel-time plot of the larger events is shown in Figure 3-2.

Table 3-1a. GEOS Header Descriptions (2-Byte Integer).

Offset	Description (Units)	Value as Used in this Report
1	Number of extra integer header records (record size=512 bytes)	0
2	Number of ASCII header records	0
3	**'Undefined' integer value [INULL]**	**-32768**
4	Data type (positive=real, negative=integer, absolute value=number of bytes per sample)	-2
5	If =1 then (*) parameters are defined	1
10	**Event year**	
11	**Event day of year**	
12	**Hour of event**	
13	**Minute of event**	
14	**Second of event**	
15	**Millisecond of event**	
16	Microsecond of event	0
17	Sample number of first tickmark	unused
18	Detection amplitude of tickmark	unused
19	Number of tickmarks detected	unused
20	Serial number of recording unit	
21	Event sequence number	
27	First active channel number recorded on unit	
28	Actual channel number as recorded on unit	
29	Total number of channels recorded on unit	
30	Total number of components recorded for station I.D.	3
31	**Number of data records that follow**	
32	**Index of last sample in last record**	
33	Record size (bytes)	512
34	Playback program (1=RDGeos, 2=AfTape, 3=ANZA, 4=PCGEOS, 5=CrTape)	
35	Playback program version number	
36	Playback program ‘ sub-version’ number	
37	Recorder type (1=GEOS, 2=DR100, 3=Reftek 72-04, 4=Tustin A/D, 5=Synthetic)	1
38	Recorder version number	1
39	Recorder ‘ sub-version’ number (GEOS software number)	uncertain
40	Sensor unit serial number	unreported
41	**(*) Vertical orientation (degrees from up)**	
42	**(*) Horizontal orientation (degrees clockwise from north)**	
43-49	[ASCII] Sensor model (7A2)	unused
50	Location number	
51	Experiment number (tape number)	
52	Trigger algorithm type (1=STA/LTA)	
53	Trigger STA (tenths of seconds)	
54	Trigger LTA (seconds)	
55	Trigger ratio STA/LTA (power of two)	
56	Trigger component number	
57	Pre-event memory size (tenths of seconds)	
58	Post-trigger duration (seconds)	unreported
101	(*) Bugger processing history	unused
208	Directory number (study I.D. number)	unused
209	Sub-directory number (tape-set number)	unused
210-216	[ASCII] Filename (7A2)	
217-219	[ASCII] Study name (3A2)	unused
252	GEOS clock type (0=None, 1=WWVB, 2=External(master), 3=Manual)	
253	GEOS event type (0=Continuous, 1=Trigger, 2=Preset, 3=Calibration, 4=Amplifier calibration, 5=Sensor calibration)	
254	**Motion unit (1=Acceleration in cm/s^2, 2=Velocity in cm/s, 3=Displacement in cm, 50=Volumetric micro-strain)**	**2**
255	Component number (1-3:acceleration, 4-6:velocity, 7-9:displacement; 1,4,7:vertical)	
256	Number of samples in event (only valid when I031 $\leq$ 128)	

Table 3-1b. GEOS Header Descriptions (4-Byte Real).

Offset	Description (Units)	Value as Used in this Report
1	Number of extra real header records	0.
2	'Undefined' real value [RNULL]	1.7E38
5	**Sample rate (samples per second)**	**200.**
6	**(*) Component sample lag (seconds)**	
39	(*) [ASCII] Transducer type (1A4)	VEL
40	(*) Latitude (degrees north)	40.134
41	Local coordinate x (meters north)	
42	(*) Longitude (degrees east)	44.724
43	Local coordinate y (meters east)	
44	(*) Elevation (meters above sea-level)	1460.
45	Local coordinate z (meters down)	
46	**(*) Digitizing constant (counts/volt)**	**3276.8**
47	**(*) Anti-alias filter corner frequency (hertz)**	**50.**
48	**(*) Poles of anti-alias filter (roll-off=6dB/pole)**	**7.**
49	**(*) Transducer natural frequency (hertz)**	**1.**
50	**(*) Transducer damping coefficient**	**0.8**
51	**(*) Coil constant (volts/motion-unit)**	**1.**
52	**(*) Amplifier gain (dB)**	
60	**(*) Clock correction (seconds; subtract from event time to get true time)**	**uncertain**
61	Elapsed time since last update of clock correction (seconds)	uncertain
62	Recorder battery voltage (volts)	
63	Desired trigger ratio STA/LTA	unused
64	Actual value of STA at trigger	unused
65	Actual value of LTA at trigger	unused
66	Maximum value of STA/LTA during event	unused

Table 3-2a. Listing of events recorded at 5 or more stations.

EVENT	G1	G2	G3	G4	G5	G7
			Jul 1990			
1811602	R	R			R	
1821226	K	K	k		K	
1841647	G	G		G	G	
1850235	G	G	G	G	G	
1850700	N	O		N	N	
1850817	G		H	H	G	
1851021	K		K	K		
1851206	K	K		K		
1871129	E	E	E	E	E	
1871224			G	G	G	
1871936	C		G	G		
1880740	T		T	T	T	
1890310	R		R	R		
1891450	H		I	I	H	
1900855	D		D	D		
1910900	G		G	G		
1911254	G		H	I		
1930900	N	N	N	N	N	m
1930917	S	S	T	S	S	s
1931442	N	N	N	N	N	n
1931516	D	D	D	D	D	d
1940828	F		F	F	F	
1941043	S		S	S		
1941425	D		D	D	D	
1941516	E		E	E	E	
1950605	K		K	K	K	
1950735	Q		Q	Q	Q	
1951541			S	S	S	
1951627	N		N	O		
1970737	P	P	Q	Q	Q	
1970937	K	K	K	K		
1971155		E	E	E	54O	
1971159	T	T	A	A	A	
1971245	R	R	R	R		
1980403	O	O	O			
1980958	O	O		P	P	
1981146	M		M	L	L	
1981656	N		N	N	O	
1990827			H	H	H	
2010321	H	H		H	H	
2040815	P			Q	P	
2041224	A	A	A	A	A	
2041445	M	M	M	M	M	
2041527	H	I	I	I	I	
2042055	O		P	Q	O	
2051003	A			A	A	
2060741	N			N	N	
2061111	R	R		A	S	
2070658	P	P		P	P	
2070900	G	G		G	G	
2080532	J		J	J	J	
2081256	P	P	P	P	P	
2090058	H		I		H	
2110845	C	C	C	C	C	
2110920	P		N	N		
2111303	A		A	B	B	

EVENT	G1	G2	G3	G4	G5	G7
			Aug 1990			
2130726	A		B	B	A	
2130820	E	E	E	E	E	
2132218	M		M	M	M	
2140718	B	B	B	C	C	
2140734	A			A	A	
2140911	P		P	P	P	
2141214	R		Q	15H	R	
2150742	N	N	N	N		
2150856	P		P	Q	P	
2151131		J		I	J	
2201500	H	H	H	H	H	g
2220908	T		A	A		
2221157	N		N	O		
2221246	D		D	D		
2221555	L	L	L	L	L	l
2240029	L		L	L		
2242144	E		F		F	
2250620	A		B	B		
2250702	R	R	R	R	R	r
2252211	K	L	L	L	L	
2271313	P		P		P	
2280209	I		I	I	I	
2280506	M	N	M	N		
2280717	M		M	M		
2281147	F		F	F		
2302317	F		F	F	F	
2311829			P	Q	Q	
2312043	L	M	L	M	L	
2312140			E	E	E	
2320915	P		P	P	P	
2321127	H	I	I	I	I	
2321221	N		O	P	N	
2321236	E		E	E		
2330348	T		A		S	
2330728			N	N	N	
2331234	C		D	D		
2331507	F		F	G		
2351124			P	P	P	
2351827	P	P	Q	Q	Q	p
2352152	B	B	B	B	B	
2370705	P	P	P	P	P	
2371600	H	H	H	H	H	
2390142	K	K	K	K	K	
2390856	P	P	P	Q	P	
2391048	B	B	B	B	B	
2391108	L	L	L	L	L	
2391229	M	M			M	
2400335	M		M	N	M	
2400557	M		M	M	M	
2411109	N		O	O		
2411253	G		G	G		

EVENT	G1	G2	G3	G4	G5	G7
			Sep 1990			
2472255	P	P	P	P	P	
2510854	O	O	O	O	O	
2511938	D	E		D	D	
2531053	G	G			G	
2540703	E	E	E		E	
2601137	S	T	S	S	T	
2601347	R	R	R	R		
			Oct 1990			
2831211		P	P	P	P	
2831217		S	S	S	S	
2880749	T	S	T		T	
2881842	O	O	P	P	O	
2911121	R	R	R	R	R	
2921401	E	E	E	E	E	
3000549	C	B	B	C	B	
3021252	N		N	O	N	
3030913	P		P	P	P	
3030932	R		R		Q	
			Nov 1990			
3121935	I	I	I	J		
3200659	S		S	S	R	
3201500	L	L	L	L	L	
3251224	E	E	E	E	E	
3261136	M	M	M	M	M	
3310805	I	I	I		I	
3330518	F	F	F		F	
			Dec 1990			
3450823	J	I	J	J	I	
3460809	K		K	K		
3461153	J	I	J		J	
3490939	B	B	B	C		
3491038	J	J	J	J	J	
3491541	D	D	D	D	D	
3501546	A	A	A	A	A	
3510116	T	T	T	T	T	
3541304	B	B	B	B	B	
3572129		E	E	E	E	
3591320		T	T	T		
3601029		J	J	J	J	
3611328		I	I		H	
3620405		H	H		H	

Capital letter indicates both stations A & B. Lower case letter indicates station A only.
In 1971154O.G5 the event signal arrived during a sensor calibration.

Table 3-2b. Listing of events recorded at 5 or more stations.

EVENT	G1	G2	G3	G4	G5
		Jan 1991			
0011919		P	O		O
0070103		I	I	I	
0070435		M	M	M	M
0070615		T	T	T	
0070937		N	N	N	
0110604	K	K	K	K	
0312308	C	C	C	C	
		Feb 1991			
0321241	R	R	R		
		Mar 1991			
0801040	N	N	N		
0841345			T	t	T
0841353	N	N	N	n	N
0851132	T			t	T
0851150	K	K	K	k	K
0861351	R	R	R	r	
0862217	Q	Q		q	
		Apr 1991			
0930131	K	K		k	
0940453	T	T		t	
0950912	F	G	F	g	
1010949		T	T	t	
1011023	E	E	E	e	
1040819	N	N	N	n	
1050813	R	R		r	
1051053	K	K		k	
1061256	A	A	A	a	
1071050	L	L	L	l	
1081030	O	O	O	o	
1091355	T	T	T	a	
1170332	B	B		b	
1190913	G	G		g	G
1191105		A		a	A
1191110		P		p	P
1191151		O		o	O

EVENT	G1	G2	G3	G4	G5
		May 1991			
1211146	J	J		j	
1211246	L	L		l	
1211357	A	A		a	
1212319		O	O	o	
1220126	A	A	A	a	
1220218	K	K	K	k	
1220229		L	L	l	
1220343	C	C	C	c	
1220431	M	L	L	m	
1220754	B	B	B	b	
1220901	C	C	C	c	
1220945	F	G	G	g	
1221158	D	D	D	d	
1221206	Q	R		q	
1230609		E	E	E	
1230613		L	L	L	
1230927		28A	O	O	
1232020	G	F	F	G	
1232341		N	N	N	
1240454		F	G	F	
1241330	E	E	E	E	
1241533		Q	Q	Q	
1251146	I	J		I	
1260755	K	K	K	K	
1261243	N	O	N	N	
1270902	B	B	B	A	
1270914	K	K	K	K	
1271324	F	F	F	F	
1280845	A	B	B	B	
1281213	K	K	L	L	
1300125		S	S	S	
1302052	T	A	T	T	
1310558	C	C	C		
1310633	P	P	P		
1330829	R	R	R		
1340937	A	A	A		
1341238	C	C	C		
1350839	B	B	B		
1351242	O	O	O	O	
1351429	I	I	J	I	
1361148	G	G		G	G
1501038	E	E	E	E	
1510919	M		M	M	
1511228	H	H		H	

EVENT	G1	G2	G3	G4	G5
		Jun 1991			
1541022	R	R	S	S	
1541031	O	O	P	O	
1541046	F	F	F	F	
1541144	E	E		E	
1550055	K	K	K	K	
1550114	F	F	F	F	
1550642	C	C	C	C	
1550708	L	L	L	L	
1571348	P	P	P	P	
1590112	E	E	E	E	
1592107	L	L	M	M	
1621053	O	O	O	O	
1631518	N	O	O	O	
1640433	G	G	G	G	
1640603	R	R		R	
1641137	L	L	L	L	
1660059	R	R	R	R	
1660250	J	J	I	J	
1660258	Q	Q	Q		
1670453	T	T	T		
1681239	C	D		C	
1681349	H	H	H	H	
1700640	Q	R	R	R	
1721154	L	L	L		
1721202	S	S	S	S	
1721443	A	A	A	A	
1730543	E	E	E	E	
1760754	H	H		H	
1781409	D	D	D	D	
		Jul 1991			
1841301	E	E	F	E	
1850627	D	D	D	D	
1851449	O	O	O	O	
1870748	R		R	R	
1950913	O		O	O	
1961300	S		S	S	
2021851	I		I	I	
		Nov 1991			
3052110	C	C	C		
3121119	P	P	P		
3160812	G	G	G		
3162036	I	J	I		
3321721	J	K	K		
		Dec 1991			
3420103	C	C	C		
3471910	M	M	M		
3501949	R	R	R		

Capital letter indicates both stations A & B. Lower case letter indicates station A only.

Table 3-2c. Listing of events recorded at 5 or more stations.

EVENT	G1	G2	G3	G4	G5
		Feb	**1992**		
0340623	M	M	M		
0411512	I	I	I		
0501109	T	T	T		
0562202	J	J	J		
		Mar	**1992**		
0621241	A	A	A		
0871921	P	P	P		
		Apr	**1992**		
0950217	H	G	H		
0961014	O	O	O		
0971048	K	L	K		
0992221	D	D	D		
0992252	R	Q	Q		
1061504	O	O	O		
1150712	G	G	H		
1171316	P	P	P		
1190844	J	J	J		
		May	**1992**		
1260622	D	D	D		
1261953	G	F	F		
1281916	F	F	F		
1331659	C	C	C		
1360812	Q	P	P		
1411225	L	L	L		

Capital letter indicates both stations A & B. Lower case letter indicates station A only.

Table 3-3a. Listing of all included records (events, calibrations, and noise tests).

EVENT	G1	G2	G3	G4	G5	G7	GA	GB	GC	GD
1780731							G			
1780732							C			
1781338							S			
1781356							A	a		
1790322							D	d		
1791622										N
1792335										A
1800007										K
1800147										S
1801230										S
1810343										N
1810815			T							
1810816			P							
1810906					L					07G
1811034	G									
1811035	C									
1811214		C								
1811602	R	R			R					
1811636	B									
1821138	P									
1821139	L									
1821219	B									
1821219	R									
1821226	K	K	k		K					
1821238		P								
1821239		K								
1821301		F								
1821302		B								
1821721	E									
1822118	F	G								
1830616			B							
1830616			R							
1830808					C					
1830808					S					
1830847	N									
1830957	K									
1831221	F									
1831225	I									
1840721				R						
1840722				N						
1841207				E						
1841208				A						
1841647	G	G		G	G					
1850133		C			C					
1850235	G	G	G	G	G					
1850700	N	O		N	N					
1850817	G		H	H	G					
1851021	K		K	K						
1851108					J					
1851109					F					
1851206	K	K		K						
1860508		A								
1860508		Q								
1860833		S								
1860918			B							
1860918			R							
1861011			E							
1861057		I	L							
1870512	Q									
1870725	R									
1870726	N									
1871129	E	E	E	E	E					
1871224			G	G	G					
1871234						c				
1871234						s				
1871936	C		G	G						
1872240	A									
1880147	E									
1880740	T		T	T	T					

EVENT	G1	G2	G3	G4	G5	G7
1881350	N					
1890310	R		R	R		
1891450	H		I	I	H	
1900743			L	L		
1900855	D		D	D		
1901518	J		K			
1910900	G		G	G		
1911254	G		H	I		
1920437	O					
1920712						s
1920713						o
1920805	A					
1920805	Q					
1920854					A	
1920854					Q	
1920904			H			
1920905			D			
1922359	T					
1930900	N	N	N	N	N	m
1930917	S	S	T	S	S	s
1930923			D			
1931442	N	N	N	N	N	n
1931516	D	D	D	D	D	d
1931638	O					
1932058	T					
1932155	B					
1940343			H			
1940522				I		
1940523				E		
1940828	F		F	F	F	
1940836					C	
1941043	S		S	S		
1941251	Q					
1941425	D		D	D	D	
1941433	G					
1941516	E		E	E	E	
1950605	K		K	K	K	
1950735	Q		Q	Q	Q	
1951021	S					
1951541			S	S	S	
1951627	N		N	O		
1970538			R			
1970539			N			
1970545					J	
1970546					E	
1970549				A		
1970549				Q		
1970552				S		
1970553				O		
1970627	N					
1970628	J					
1970633	C					
1970633	S					
1970649		F				
1970650		B				
1970737	P	P	Q	Q	Q	
1970835	E			E		
1970937	K	K	K	K		
1971047						c
1971154					O	
1971155		E	E	E		
1971155					K	
1971159	T	T	A	A	A	
1971245	R	R	R	R		
1971342	G	G				
1971956	J					
1980403	O	O	O			
1980958	O	O		P	P	
1981134	K	N				

EVENT	G1	G2	G3	G4	G5	G7
1981146	M		M	L	L	
1981149	B					
1981204				Q		
1981656	N		N	N	O	
1982125	R					
1990003	M					
1990811	H			H		
1990827			H	H	H	
1991007			C			
1991132	K					
1991306				K		
2000237			K	K		
2000540			S			
2000541			O			
2000549					N	
2000550					J	
2000843						q
2000844						m
2010321	H	H		H	H	
2011731	I				I	
2022233	P				P	
2022305	H				H	
2030242	L					
2030947	J					
2031131	F					
2040815	P			Q	P	
2041113		K				
2041114		G				
2041224	A	A	A	A	A	
2041445	M	M	M	M	M	
2041527	H	I	I	I	I	
2042055	O		P	Q	O	
2051003	A			A	A	
2051040					H	
2051041					D	
2060638				O		
2060741	N			N	N	
2060916						t
2060917						p
2061015		H				
2061016		D				
2061108		09B		Q		
2061111	R	R		A	S	
2061451	P				O	
2070558		K				
2070559		G				
2070658	P	P		P	P	
2070900	G	G		G	G	
2070917	F				E	
2071030				H		
2080532	J		J	J	J	
2080656	B		C			
2081149						r
2081150						n
2081256	P	P	P	P	P	
2081325	Q		Q			
2082307	I				I	
2090058	H		I		H	
2091131					N	
2091132					I	
2091922					F	
2100329	M					
2100634	G					
2100635	C					
2102138	E				E	
2110845	C	C	C	C	C	
2110920	P		N	N		
2111303	A		A	B	B	

Capital letter indicates both stations A & B. Lower case letter indicates station A only.

Table 3-3b. Listing of all included records (events, calibrations, and noise tests).

EVENT	G1	G2	G3	G4	G5	G7	EVENT	G1	G2	G3	G4	G5	G7	EVENT	G1	G2	G3	G4	G5	EVENT	G1	G2	G3	G4	G5
2120625	R		R				2272319	P						2400557	M		M	M	M	2610818	Q	Q	Q	Q	Q
2121143	T		T				2280058	K						2401235	Q					2610825	Q	Q	Q	P	P
2130555			M				2280209	I		I	I	I		2410717			K	K		2610832	Q	Q	P	P	P
2130556			I				2280506	M	N	M	N			2411109	N		O	O		2621235			H		
2130726	A		B	B	A		2280717	M		M	M			2411253	G		G	G		2641000			G		
2130820	E	E	E	E	E		2280751	O		O				2412053	M					2641101			A	A	
2131835	G						2280752			E				2421110				N		2641708			H		
2132218	M		M	M	M		2280938			P	P			2421111				J		2650246			L	L	
2132304	B						2281047	T						2421116					A	2651531		E			
2140317	G				F		2281147	F		F	F			2421116					P	2651531		T			
2140718	B	B	B	C	C		2301902	E						2421159		I				2651910		I			
2140734	A			A	A		2302317	F		F	F	F		2421200		E				2651911		E			
2140911	P		P	P	P		2310730			D				2421206	Q					2761059	T				
2140920	G						2310730			T				2421207	M					2761100	P				
2141214	R		Q	15H	R		2310858	P						2440743	Q		Q	Q		2780757			B		B
2141653	J						2310859	L						2460245	I					2810456			M		L
2141713	O				P		2310950						k	2460814	I					2810924		M			
2142118	E				F		2310951						g	2461013			F			2810925		I			
2142125	F						2311829			P	Q	Q		2461159	Q		Q	Q		2821046			C		
2150742	N	N	N	N			2312043	L	M	L	M	L		2462203	L					2831051			R		
2150856	P		P	Q	P		2312140			E	E	E		2470031	J					2831211		P	P	P	P
2150921	D						2312315			E		E		2470731	H		H	H		2831217		S	S	S	S
2151126				L			2320014	E				F		2470900					T	2831909			J		J
2151131		J		I	J		2320915	P		P	P	P		2470901					P	2851232			K		K
2151133				I			2321127	H	I	I	I	I		2471225		B				2861637	N				
2152129					N		2321221	N		O	P	N		2471225		Q				2861638	J				
2170753					H		2321236	E		E	E			2472255	P	P	P	P	P	2871808	A				
2170754					D		2330117	B				B		2481201			B			2871808	P				
2170811		F					2330348	T		A		S		2481201			R			2871917	N				
2170812		B					2330728			N	N	N		2481302				L		2871918	I				
2170819	B						2331234	C		D	D			2491050				S	S	2880749	T	S	T		T
2170819	Q						2331507	F		F	G			2491126				I		2881842	O	O	P	P	O
2170936						d	2332135					T		2491155					M	2911121	R	R	R	R	R
2170936						t	2340051					E		2491212	B				S	2921052	I				
2180205	Q				Q		2340705			C		C		2491225				E	E	2921401	E	E	E	E	E
2180716	F			F			2340718			F		F		2500019	L				L	2980458	M			N	
2180846	H			H			2340753			H		H		2500903	D					2991049					M
2181126	G						2340909			P				2510854	O	O	O	O	O	3000549	C	B	B	C	B
2190033	J				J		2350851					C		2511938	D	E		D	D	3021252	N		N	O	N
2191020	A			A			2350851					S		2520224	B					3030913	P		P	P	P
2201000				F			2350917		O					2530705	G				G	3030932	R		R		Q
2201001				B			2350918		K					2531053	G	G			G	3041220			B		
2201500	H	H	H	H	H	g	2350922		D					2540703	E	E	E		E	3091218	T		T		
2211305			C	C			2350922		T					2540849	Q					3100712		T			
2220237			B	B			2350925		A					2540850	M					3121935	I	I	I	J	
2220814			J				2350929				H	H		2560641			S		S	3161234	G		G		
2220908	T		A	A			2350929				O	O		2561113			J			3180629	M				
2221044	F						2350935	C						2561113					K	3180630	I				
2221157	N		N	O			2350935	S						2561113				Q		3200659	S		S	S	R
2221246	D		D	D			2350952						f	2561114			F			3200709	Q			Q	
2221555	L	L	L	L	L	l	2350953						b	2561114					G	3201500	L	L	L	L	L
2221556	S						2351124			P	P	P		2561114				M		3210756	S				
2222118	S						2351827	P	P	Q	Q	Q	p	2561119				C		3210757	O				
2240029	L		L	L			2352141					S		2561119				S		3240804					K
2242144	E		F		F		2352152	B	B	B	B	B		2572046					C	3240805					G
2250547	B						2360156	G						2600518				A		3242020			S		
2250547	R						2370705	P	P	P	P	P		2600518			G			3242021			O		
2250620	A		B	B			2371349	T						2600518				Q		3251224	E	E	E	E	E
2250702	R	R	R	R	R	r	2371600	H	H	H	H	H		2600519			B			3261136	M	M	M	M	M
2251056	K			K			2381234				G			2600533				T		3301221			O		
2252211	K	L	L	L	L		2390142	K	K	K	K	K		2600534				O		3310805	I	I	I		I
2260055	L			O			2390737			B				2600536			C			3330518	F	F	F		F
2260949				C			2390737			Q				2600536			R			3331036		B	B		
2260949				S			2390856	P	P	P	Q	P		2600537		A				3341206	S	S			
2261055	G						2391048	B	B	B	B	B		2600537		Q				3370827			L		L
2261523	S						2391108	L	L	L	L	L		2600806			L		L	3421143	J				
2262035	S						2391229	M	M			M		2601137	S	T	S	S	T	3440947			L		
2271036			H				2392130	T				T		2601208	M	M				3450823	J	I	J	J	I
2271313	P		P		P		2400335	M		M	N	M		2601347	R	R	R	R		3450948			M		

Capital letter indicates both stations A & B. Lower case letter indicates station A only.

Table 3-3c. Listing of all included records (events, calibrations, and noise tests).

EVENT	G1	G2	G3	G4	G5	EVENT	G1	G2	G3	G4	G5	EVENT	G1	G2	G3	G4	G5	EVENT	G1	G2	G3	G4	G5
3460809	K		K	K		0370714			H			1190913	G	G		g	G	1261241				G	
3461153	J	I	J		J	0370715			D			1191053		F		f		1261243	N	O	N	N	
3490939	B	B	B	C		0421318					I	1191105		A		a	A	1270857	A			A	
3491038	J	J	J	J	J	0511321			N			1191110		P		p	P	1270902	B	B	B	A	
3491541	D	D	D	D	D	0520814					Q	1191151		O		o	O	1270914	K	K	K	K	
3501546	A	A	A	A	A	0520815					M	1191200					J	1271017				J	
3502105			O			0550631					M	1191443					N	1271324	F	F	F	F	
3510116	T	T	T	T	T	0550743					T	1191823					Q	1280845	A	B	B	B	
3511742			R			0570730					F	1191831					F	1281057	M				
3520626		T				0591144					K	1210905				A		1281110	G	G			
3520627		P				0591230					N	1210905				P		1281213	K	K	L	L	
3520636			O			0611027					I	1210914		J				1300125		S	S	S	
3520637			K			0731053					H	1210915		F				1302031			H	H	
3541304	B	B	B	B	B	0731110		Q	Q		N	1210918	I					1302052	T	A	T	T	
3541940			Q			0800747	L					1210919	E					1302055		C			
3551143			B			0800748	H					1211146	J	J		j		1310457	O	O			
3572129		E	E	E	E	0800934	P		P			1211246	L	L		l		1310458	G				
3590826			A			0801040	N	N	N			1211357	A	A		a		1310558	C	C	C		
3591107		M				0811404			N	N		1211447			J			1310633	P	P	P		
3591320		T	T	T		0821025	E					1211448			F			1330829	R	R	R		
3600628				I		0841345			T	T	T	1212319		O	O	o		1340937	A	A	A		
3600629				E		0841353	N	N	N	N	N	1220126	A	A	A	a		1340939			G		
3601029		J	J	J	J	0851132	T			T	T	1220208			F			1341155	F	G			
3611328		I	I		H	0851150	K	K	K	K	K	1220218	K	K	K	k		1341238	C	C	C		
3620405		H	H		H	0851424	M	M				1220229		L	L	l		1350839	B	B	B		
3620945			K			0860910	M					1220343	C	C	C	c		1350852	J				
3621212		S				0860911	I					1220431	M	L	L	m		1350853	F				
3631154		C	C			0861351	R	R	R	R		1220754	B	B	B	b		1350859		B			
3632200			B		B	0862217	Q	Q		Q		1220901	C	C	C	c		1350907			H		
0010817			K			0871139				R		1220945	F	G	G	g		1350908			D		
0011919		P	O		O	0881328		A		B		1220948	F					1351242	O	O	O	O	
0040823					S	0881423		O		O		1221042	Q			q		1351429	I	I	J	I	
0040824					O	0900730				G		1221124	O					1361148	G	G		G	G
0070103		I	I	I		0910906				B		1221125	K					1380322	P				
0070435		M	M	M	M	0910913			Q			1221131		I				1400802	E				
0070615		T	T	T		0910914			M			1221132		E				1411738	J				J
0070817			A			0910916	J					1221134	M					1412019	G				G
0070937		N	N	N		0910917	F					1221137				J		1412345					E
0081055			Q	Q		0910923		H				1221138				F		1420151	N				N
0090811			T			0910924		C				1221158	D	D	D	d		1420822	F				
0090812			P			0930131	K	K		k		1221206	Q	R		q		1440800	B				
0090817			Q			0940453	T	T		t		1221242			K			1440843	I				
0090818			M			0940902	M			m		1221243			F			1441104	O				
0090825	I					0941339			M			1230609		E	E	E		1461429	M				
0090826	E					0950912	F	G	F	g		1230613		L	L	L		1470341	D				
0101528			S			0950922			N			1230927			O	O		1470649	D				
0110604	K	K	K	K		1010949		T	T	t		1230928		A				1500725				M	
0112102			S	S		1011023	E	E	E	e		1231140				H		1500726				I	
0131532		H				1020312			B			1232020	G	F	F	G		1500734			D		
0131533		D				1040819	N	N	N	n		1232341		N	N	N		1500734			T		
0140850			T			1050813	R	R		r		1240454			F	G	F	1500744		N			
0211126			F			1051053	K	K		k		1241330	E	E	E	E		1500745		J			
0261701			B			1061256	A	A	A	a		1241509		P				1500750	D				
0280632	K					1071050	L	L	L	l		1241510		L				1500750	T				
0280633	G					1081030	O	O	O	o		1241520				O		1500758	O				
0291120			E			1091355	T	T	T	a		1241521				K		1500759	K				
0291139			R			1122309			B			1241533		Q	Q	Q		1501038	E	E	E	E	
0291744			A			1130933			D			1250515		I		I		1510919	M		M	M	
0292000			F			1160851			K			1250708				L		1511228	H	H		H	
0300435			J			1160852			F			1250709				C		1541022	R	R	S	S	
0311207		H	H			1160857		I				1250750			I			1541031	O	O	P	O	
0312308	C	C	C	C		1160858		E				1250751			E			1541046	F	F	F	F	
0320535		P	Q			1160902	J					1250908	Q			R		1541144	E	E		E	
0321024	O		O			1160903	F					1251146	I	J		I		1550055	K	K	K	K	
0321241	R	R	R			1160914					K	1252007			R	R		1550114	F	F	F	F	
0360438			J			1160915					G	1260755	K	K	K	K		1550642	C	C	C	C	
0370210			A			1170332	B	B		b		1260806	N					1550708	L	L	L	L	
0370707					M	1181402	A					1260807	J					1550851				S	
0370708					I	1190857					K							1550852				O	

Capital letter indicates both stations A & B. Lower case letter indicates station A only.

Table 3-3d. Listing of all included records (events, calibrations, and noise tests).

EVENT	G1	G2	G3	G4	G5	EVENT	G1	G2	G3	G4	G5	EVENT	G1	G2	G3	G4	G5	EVENT	G1	G2	G3	G4	G5
1550855		N				1890623			L			2730540				H		3370753			Q		
1550856		J				1890624			H			2740812				K		3370754			L		
1550857	J					1890629		J				2761424			T	T		3371054		Q			
1550858	F					1890630		F				2761504			Q	Q		3381301		K	K		
1561113				A		1891036				J		2790140				K		3391111		D			
1570855	M		M			1891037				F		2790147			D	D		3400740		L			
1571348	P	P	P	P		1940553	Q			R		2790150			E			3411210		I			
1590112	E	E	E	E		1941406	O					2790326				L		3411427		H			
1590113			O			1941407	K					2790415				C		3420103	C	C	C		
1592107	L	L	M	M		1950913	O		O	O		2800746				L		3420757		L			
1592110	F					1951547	F			F		2800747				H		3450707		O			
1621053	O	O	O	O		1961021					I	2800750			I			3450708		K			
1621322	K					1961022					E	2800751			E			3451444		B			
1630635			M			1961300	S		S	S		2800915				L		3451506		G			
1630636			I			1962046			B	B		2810342			H			3470556		T			
1630816	I			I		1970404	M					2821019				D		3471910	M	M	M		
1631518	N	O	O	O		1970453	T			T		2821019				T		3472006		M			
1640433	G	G	G	G		1991102			L			2830245			D			3472009		Q			
1640603	R	R		R		1991102				T		2830929		M				3501543		G	I		
1641137	L	L	L	L		1991103			H			2830930		H				3501949	R	R	R		
1650837	H	H				1991103				P		2840959		J				3501959		J	K		
1660059	R	R	R	R		1991311				C		2841000		F				3511149		T			
1660250	J	J	I	J		2021851	I		I	I		2900841			L			3530145		C			
1660258	Q	Q	Q			2041954			K	K		2900842			H			3540615	S	S			
1660626	I	I				2050324			F	F		2900900				K		3540847		B			
1660720	K					2051156			S	S		2900901				F		3560854		N			
1661200	K					2060452			S	S		2900919		I				3571321		L			
1661556	J	J				2061130			O	O		2900920		D				3601147		G			
1670453	T	T	T			2150927			C	C		2961003			I			3610917		C			
1671107			I			2180920				Q		2961004			D			3630052		L			
1671356			O			2181553			S			2981151				Q		0022221	P	P			
1680305			F			2220858			M	N		2981152				M		0022222	F	G			
1681038				M		2221046				F		3021201	B					0022235		Q			
1681039				I		2221048			P	Q		3021201	R					0030028		Q			
1681043			I			2221054				P		3021238		T				0030040		L			
1681044			E			2221109			A	A		3021239		P				0030446		L			
1681048		J				2221123			K	K		3051350		F	F			0060152		B			
1681049		F				2261255			K			3051431		E				0070140	G				
1681053	I					2270330			K			3052110	C	C	C			0070544	C				
1681054	E					2320851			H			3060945		Q				0070614	H				
1681239	C	D		C		2331202			K			3081040		T	A			0331138	I				
1681349	H	H	H	H		2371023				S		3091231		C	D			0331139	E				
1700640	Q	R	R	R		2371024				O		3121004		S	S			0331147		T			
1701242				L		2371032			M			3121119	P	P	P			0331148		P			
1701308	K					2371033			I			3130453		L	L			0331335			T		
1710750	N			N		2371039		M				3141020		D	D			0331336			P		
1711219	Q			Q		2371040		I				3160812	G	G	G			0340027		B	B		
1711336	N			N		2371045	M					3162036	I	J	I			0340623	M	M	M		
1721154	L	L	L			2371046	H					3171119		H				0340627		K	K		
1721202	S	S	S	S		2381228			R	R		3171124		E				0350831		S	S		
1721443	A	A	A	A		2401047			M	N		3220624		C				0350837		B	B		
1730543	E	E	E	E		2401148				R		3231004		K	K			0350928		L	L		
1750728	I					2411238				H		3251250		M				0351100		A	A		
1750729	E					2420838				N		3290720		N				0351210		I	I		
1760754	H	H		H		2430933				O		3290721		J				0360921		H			
1761250				A		2442049				H		3301213		A				0361322		S	T		
1781409	D	D	D	D		2451040			M	M		3301255		B	B			0410401		K	K		
1790710				K		2470914				F		3311142			G			0411512	I	I	I		
1790711				G		2481213			F	F		3321721	J	K	K			0452032		E			
1812010			B	B		2481923			R	R		3331219			S			0461253	O	O			
1820716		M				2502346				N		3331241		Q				0461331	I	I			
1820717		I				2502347				J		3331242		N				0461338	K	J			
1831052				A		2511019				N		3331323		N	N			0461518	M	M			
1841301	E	E	F	E		2532203			H	I		3340401		I				0480551	L				
1850627	D	D	D	D		2671737		A				3340848		P	P			0490140	B				
1850851	L					2680311				K		3341309		C				0500807		N			
1851449	O	O	O	O		2680312				G		3350918		L				0500808		I			
1870748	R		R	R		2710527				B		3361220		I	I			0501109	T	T	T		
						2710602				H								0501446		E			

Capital letter indicates both stations A & B. Lower case letter indicates station A only.

Table 3-3e. Listing of all included records (events, calibrations, and noise tests).

EVENT	G1	G2	G3	G4	G5	EVENT	G1	G2	G3	G4	G5		
0510103		D				1201501		L					
0510816		F				1211148		H					
0511143		P				1212351			I				
0511240		T				1221212		L					
0511333		M				1260551	Q						
0511720		I	J			1260552	M						
0520037		H				1260604		R					
0520145		D	D			1260605		N					
0541104		Q				1260622	D	D	D				
0541204		R				1261110		O					
0542350		D				1261953	G	F	F				
0560751		K				1271241		J					
0560755		K				1281039		T	S				
0561444		H				1281916	F	F	F				
0562202	J	J	J			1310409		K	K				
0570128		M				1330718			J				
0570351		M				1331659	C	C	C				
0570934		E	E			1340629			R				
0571107		R				1340630			N				
0590903		Q				1341447		F	F				
0610914		P	Q			1350323		D	D				
0620606		Q				1360812	Q	P	P				
0621241	A	A	A			1381001		I	I				
0630137		F				1381027		M	N				
0650330	P	P				1401228		L	L				
0670937	D		D			1411220		T	T				
0672128	O					1411225	L	L	L				
0731719	O					1421123			N				
0841029	J					1471858	E		D				
0841030	F					1480803			F				
0841034		B				1490801	K		K				
0841034		R				1531113			F				
0841040			I			1791349		R					
0841041			E			1791350		N					
0851051		C				1791450	P						
0851152	R					1791451	L						
0860233		J	K			1950617	I						
0861039		B				1950713	Q						
0871921	P	P	P			2200627	T						
0880546		Q	Q			2201426				Q			
0911020		Q	Q			2201427				M			
0920826		A				2211425	D		D				
0950217	H	G	H			2230736					K		
0950505		L				2230737					F		
0951228		M	M			2231347				B			
0961014	O	O	O										
0971048	K	L	K										
0992119			R										
0992221	D	D	D										
0992238		G	H										
0992252	R	Q	Q										
0992307		K											
0992332		C											
1010801			M										
1010802			I										
1010802		M											
1010803		I											
1051350		K											
1060920		R											
1061227		B	B										
1061504	O	O	O										
1081146		A	A										
1121124		P											
1130305		B											
1131226		K											
1150712	G	G	H										
1171316	P	P	P										
1190844	J	J	J										
1201057		M	M										

Capital letter indicates both stations A & B. Lower case letter indicates station A only.

Table 3-4. Estimated or Reported 1991 Master-Clock Resynchs.

Time Range		Estimated Change
day hr mn	day hr mn	(ms)
084 05 35	084 07 08	-8
086 08 54	086 09 10	-7
091 03 48	091 06 58	-4
095 08 34	095 09 40	-2
098 12 34	098 15 44	-6
108 06 54	108 10 04	-13
116 09 13	116 21 14	-8
125 23 47	126 08 05	-5
149 22 05	150 07 57	-39
153 20 21	154 08 22	-6
160 21 29	161 09 30	-12
169 23 07	170 11 08	-5
175 04 33	175 07 28	-6
176 07 41	176 19 42	-5

Time	Before	After	Change
day hr mn	(ms)	(ms)	(ms)
283 19 12	3.3	0.1	-3.2
284 19 48	4.4	-0.1	-4.5
290 06 58	11.0	-0.1	-11.1
294 06 45	8.0	-0.1	-8.1
298 07 20	5.0	0.1	-4.9
301 07 07	5.6	-0.4	-6.0
303 06 50	4.2	-0.2	-4.4
309 07 11	7.3	-0.1	-7.4
310 07 00	2.3	-0.4	-2.7
311 10 00	2.0	-0.4	-2.4
316 07 11	6.0	0.4	-5.6

Table 3-5a. NEIC Parameters of Identified Events Sorted by Date.

Date	D.o.Y.	Hr	Mn	Sec		Latitude deg.		Longitude deg.		Depth km		Mag	Azi deg.	Epicentral Distance km	Epicentral Distance deg.	Travel m:ss	Phase	Region	
28 - JUN - 90	(179)	03:	20:	35.0		37 .085	N	49 .642	E	10	G	4.8	307	545	4.90	1:36	P	CASPIAN SEA	
28 - JUN - 90	(179)	03:	42:	01.9	*	37 .079	N	50 .147	E	10	G	4.7	304	581	5.22	1:39	P	CASPIAN SEA	
01 - JUL - 90	(182)	12:	24:	57.2		37 .181	N	49 .885	E	10	G	4.8	305	555	4.99	1:35	P	CASPIAN SEA	
01 - JUL - 90	(182)	17:	19:	44.1		37 .280	N	48 .818	E	10	G	4.6	310	476	4.28	1:30	P	CASPIAN SEA	
01 - JUL - 90	(182)	21:	16:	48.3		37 .285	N	48 .820	E	10	G	4.7	310	476	4.28	1:29	P	CASPIAN SEA	
04 - JUL - 90	(185)	02:	24:	41.9		25 .372	N	124 .473	E	133		5.6	256	7392	66.47	10:38	P	NORTHEAST OF TAIWAN	
06 - JUL - 90	(187)	05:	02:	27.9		45 .371	N	150 .170	E	42	D	5.7	226	7961	71.59	11:22	P	KURIL ISLANDS	
06 - JUL - 90	(187)	19:	34:	52.4		36 .861	N	49 .303	E	35	D	5.3	311	540	4.85	1:16	Pn	WESTERN IRAN	
09 - JUL - 90	(190)	15:	11:	20.3		5 .395	N	31 .654	E	13	G	6.4	22	4078	36.67	7:09	P	SUDAN	<MW>
11 - JUL - 90	(192)	04:	36:	08.6	*	37 .015	N	49 .530	E	33	N	4.5	308	543	4.88	1:35	P	CASPIAN SEA	
13 - JUL - 90	(194)	14:	20:	43.4		36 .415	N	70 .789	E	217	D	5.6	272	2304	20.72	4:28	P	HINDU KUSH REGION	
14 - JUL - 90	(195)	05:	54:	25.4		0 .003	N	17 .376	W	11	G	6.4	71	7676	69.03	11:07	P	NORTH OF ASCENCION ISLAND	<Msz>
14 - JUL - 90	(195)	07:	24:	39.6		0 .074	S	17 .523	W	12	G	5.8	71	7694	69.19	11:10	P	NORTH OF ASCENCION ISLAND	
16 - JUL - 90	(197)	07:	26:	34.6		15 .679	N	121 .172	E	25	D	7.9	266	7752	69.71	11:12	P	LUZON, PHILIPPINE ISLANDS	<MW>
16 - JUL - 90	(197)	13:	31:	13.2		16 .285	N	120 .457	E	13	D	5.7	266	7650	68.79	11:04	P	LUZON, PHILIPPINE ISLANDS	<Msz>
16 - JUL - 90	(197)	19:	45:	25.1		16 .365	N	120 .546	E	33	N	5.4	266	7652	68.81	11:04	P	LUZON, PHILIPPINE ISLANDS	
17 - JUL - 90	(198)	04:	02:	09.2		37 .137	N	49 .979	E	33	N	4.6	304	565	5.08	1:35	P	CASPIAN SEA	
17 - JUL - 90	(198)	21:	14:	43.8		16 .495	N	120 .981	E	23	G	6.7	266	7680	69.07	11:09	P	LUZON, PHILIPPINE ISLANDS	<MW>
18 - JUL - 90	(199)	08:	00:	12.8		16 .511	N	121 .007	E	14	G	5.8	266	7681	69.08	11:10	P	LUZON, PHILIPPINE ISLANDS	
18 - JUL - 90	(199)	11:	29:	24.9		36 .990	N	29 .595	E	17	D	5.2	80	1359	12.22	3:07	P	TURKEY	
20 - JUL - 90	(201)	17:	30:	36.2	?	42 .10	N	46 .77	E	33	N	4.2	217	278	2.50	0:50	P	EASTERN CAUCASUS	
22 - JUL - 90	(203)	09:	26:	14.6		23 .622	S	179 .893	W	531	G	5.9	260	15477	139.18	21:14	SKP	SOUTH OF FIJI ISLANDS	
22 - JUL - 90	(203)	11:	20:	09.6		16 .532	N	121 .045	E	33	N	5.3	266	7683	69.09	11:07	P	LUZON, PHILIPPINE ISLANDS	
23 - JUL - 90	(204)	20:	54:	56.6		42 .719	N	45 .947	E	33	N	4.8	199	305	2.74	0:47	Pn	EASTERN CAUCASUS	
26 - JUL - 90	(207)	06:	53:	56.3		27 .247	N	65 .508	E	19	G	5.8	300	2388	21.47	4:51	P	PAKISTAN	<2 events>
27 - JUL - 90	(208)	05:	31:	00.1		37 .318	N	49 .585	E	10	G	4.8	305	525	4.72	1:29	P	CASPIAN SEA	
27 - JUL - 90	(208)	12:	37:	59.5		15 .355	S	167 .464	E	126	G	7.5	261	13866	124.70	18:48	PKP	VANUATU ISLANDS	<MW;2 events>
02 - AUG - 90	(214)	17:	12:	48.5	*	38 .540	N	48 .186	E	33	N	4.2	300	346	3.12	0:56	P	N.W. IRAN-USSR BORDER REGION	
02 - AUG - 90	(214)	21:	17:	18.7	*	38 .398	N	48 .228	E	33	N	4.1	301	358	3.22	0:55	P	N.W. IRAN-USSR BORDER REGION	
03 - AUG - 90	(215)	09:	15:	06.1		47 .963	N	84 .961	E	33	G	6.1	241	3291	29.59	6:05	P	KAZAKH-XINJIANG BORDER REGION	<MW>
10 - AUG - 90	(222)	15:	44:	31.3		0 .333	N	126 .175	E	53		6.4	275	9258	83.25	12:25	P	MOLUCCA PASSAGE	<MW>
10 - AUG - 90	(222)	21:	11:	49.0		6 .572	N	60 .240	E	10	G	5.5	333	4040	36.33	7:07	P	CARLSBERG RIDGE	
12 - AUG - 90	(224)	21:	25:	21.9		19 .435	S	169 .132	E	140	G	6.3	263	14283	128.44	18:52	PKP	VANUATU ISLANDS	<2 events>
13 - AUG - 90	(225)	06:	18:	25.1		36 .663	N	49 .884	E	35	*	4.6	309	592	5.33	1:37	P	WESTERN IRAN	
14 - AUG - 90	(226)	00:	50:	39.2		27 .024	N	65 .969	E	21	D	5.2	300	2438	21.93	4:56	P	PAKISTAN	
14 - AUG - 90	(226)	15:	13:	28.6		35 .432	N	35 .648	W	10	G	6.0	114	6833	61.45	10:27	P	NORTH ATLANTIC RIDGE	<Msz>
15 - AUG - 90	(227)	23:	08:	56.0		43 .757	N	143 .297	E	162	D	5.4	230	7637	68.68	10:51	P	HOKKAIDO, JAPAN REGION	
16 - AUG - 90	(228)	04:	59:	57.6		41 .564	N	88 .770	E	0	G	6.2	253	3668	32.98	6:39	P	SOUTHERN XINJIANG, CHINA	
20 - AUG - 90	(232)	12:	20:	11.0	*	36 .956	N	49 .720	E	33	N	4.8	308	560	5.03	1:30	P	WESTERN IRAN	
21 - AUG - 90	(233)	03:	47:	26.2		37 .309	N	49 .685	E	10	G	4.8	305	533	4.79	1:30	P	CASPIAN SEA	
22 - AUG - 90	(234)	07:	51:	49.5	*	37 .056	N	49 .327	E	10	G	4.3	309	526	4.73	1:33	P	CASPIAN SEA	
25 - AUG - 90	(237)	15:	47:	53.8		0 .525	N	126 .084	E	11	G	6.5	275	9236	83.06	12:29	P	MOLUCCA PASSAGE	<MW>
29 - AUG - 90	(241)	20:	44:	23.0		11 .791	N	95 .034	E	25	D	5.2	288	5830	52.43	9:15	P	ANDAMAN ISLANDS REGION	
03 - SEP - 90	(246)	02:	40:	59.1		36 .409	N	70 .671	E	202	D	4.9	272	2294	20.63	4:27	P	HINDU KUSH REGION	
07 - SEP - 90	(250)	00:	12:	26.2		5 .443	N	31 .686	E	10	G	5.2	22	4072	36.62	7:09	P	SUDAN	
08 - SEP - 90	(251)	19:	33:	18.8		27 .500	N	66 .092	E	28	*	5.5	299	2412	21.69	4:52	P	PAKISTAN	
09 - SEP - 90	(252)	02:	14:	51.0		56 .654	N	34 .395	W	10	G	5.4	137	5765	51.84	9:14	P	NORTH ATLANTIC OCEAN	
14 - SEP - 90	(257)	20:	40:	18.3		13 .382	N	51 .456	E	10	G	5.4	346	3046	27.39	5:50	P	EASTERN GULF OF ADEN	
17 - SEP - 90	(260)	11:	57:	24.1		5 .917	S	103 .796	E	59	D	5.7	296	7902	71.06	11:14	P	SOUTHERN SUMATERA	
22 - SEP - 90	(265)	02:	46:	01.2	*	42 .538	N	46 .449	E	33	N	4.3	208	304	2.73	0:34	P	EASTERN CAUCASUS	
24 - SEP - 90	(267)	06:	35:	13.9	*	38 .253	N	47 .951	E	10	G	4.6	306	348	3.13		P	NORTHWESTERN IRAN	<PC only>
25 - OCT - 90	(298)	04:	52:	06.0	*	76 .243	N	8 .409	E	10	G	4.6	167	4382	39.41	?7:47	P	SVALBARD REGION	<within coda>
25 - OCT - 90	(298)	04:	53:	59.9		35 .121	N	70 .486	E	114	G	6.0	276	2327	20.93	4:38	P	HINDU KUSH REGION	
12 - NOV - 90	(316)	12:	28:	51.5		42 .959	N	78 .071	E	19	G	6.3	252	2774	24.95	5:28	P	ALMA-ATA REGION	<MW>
16 - DEC - 90	(350)	15:	45:	40.7		41 .361	N	43 .715	E	33	N	5.2	148	161	1.45	0:21	P	TURKEY-USSR BORDER REGION	
23 - DEC - 90	(357)	21:	28:	50.7	*	42 .115	N	44 .356	E	33	N	4.1	172	222	2.00	0:23	P	WESTERN CAUCASUS	
27 - DEC - 90	(361)	13:	26:	57.1		36 .539	N	48 .907	E	10	G	4.7	316	541	4.87	1:26	P	NORTHWESTERN IRAN	
28 - DEC - 90	(362)	04:	03:	53.6		37 .106	N	49 .227	E	10	G	5.0	309	516	4.64	1:29	P	CASPIAN SEA	

Table 3-5b. NEIC Parameters of Identified Events Sorted by Date.

Date	D.o.Y.	Hr	Mn	Sec		Latitude deg.		Longitude deg.		Depth km		Mag	Azi deg.	Epicentral Distance km	Distance deg.	Travel m:ss	Phase	Region	
01 - JAN - 91	(001)	19:	18:	56.4		39 .822	N	48 .439	E	61	D	4.9	275	318	2.86	0:48	P	N.W. IRAN-USSR BORDER REGION	
31 - JAN - 91	(031)	23:	03:	33.6		35 .993	N	70 .423	E	142	G	6.7	273	2288	20.57	4:31	P	HINDU KUSH REGION	<MW>
26 - FEB - 91	(057)	07:	25:	47.2		40 .186	N	13 .822	E	401		5.5	100	2613	23.49	4:30	P	TYRRHENIAN SEA	
27 - MAR - 91	(086)	22:	17:	55.0		40 .443	N	45 .443	E	33	N	4.3	240	70	0.63	-0:08	P	EASTERN CAUCASUS	<early>
14 - APR - 91	(104)	08:	08:	55.7		27 .155	N	127 .419	E	83	G	6.2	253	7519	67.62	10:45	P	RYUKYU ISLANDS	
15 - APR - 91	(105)	10:	48:	59.3		36 .340	N	71 .358	E	124	D	5.3	272	2355	21.18	4:30	P	AFGHANISTAN-USSR BORDER REGION	
27 - APR - 91	(117)	03:	31:	58.5	*	40 .093	N	43 .719	E	10	G	4.2	87	86	0.77	0:07	P	TURKEY-USSR BORDER REGION	
29 - APR - 91	(119)	09:	12:	48.1		42 .453	N	43 .673	E	17	G	7.2	162	272	2.45	0:29	P	WESTERN CAUCASUS	<MW>
29 - APR - 91	(119)	10:	52:	42.2		42 .712	N	44 .102	E	10	G	4.6	170	291	2.62	0:32	P	WESTERN CAUCASUS	
29 - APR - 91	(119)	11:	04:	28.9	*	42 .510	N	43 .816	E	10	G	4.3	164	275	2.47	0:35	P	WESTERN CAUCASUS	
29 - APR - 91	(119)	11:	10:	11.9		42 .584	N	43 .904	E	10	G	4.7	166	281	2.53	0:35	P	WESTERN CAUCASUS	
29 - APR - 91	(119)	11:	51:	10.3		42 .572	N	43 .816	E	10	G	4.9	165	281	2.53	0:34	P	WESTERN CAUCASUS	
29 - APR - 91	(119)	11:	59:	54.8		42 .625	N	43 .962	E	10	G	4.5	167	284	2.56	0:34	P	WESTERN CAUCASUS	
29 - APR - 91	(119)	14:	43:	06.3		42 .515	N	43 .937	E	10	G	5.4	166	273	2.45	0:35	P	WESTERN CAUCASUS	
29 - APR - 91	(119)	18:	23:	15.2		42 .583	N	43 .764	E	10	G	5.5	164	284	2.55	0:35	P	WESTERN CAUCASUS	
29 - APR - 91	(119)	18:	30:	41.5		42 .503	N	43 .899	E	14	G	6.0	166	272	2.45	0:36	P	WESTERN CAUCASUS	<Msz>
01 - MAY - 91	(121)	23:	19:	11.8	*	42 .719	N	44 .053	E	10	G	4.1	169	293	2.63	0:29	P	WESTERN CAUCASUS	
02 - MAY - 91	(122)	01:	25:	30.1		42 .541	N	43 .960	E	10	G	5.1	167	275	2.47	0:32	P	WESTERN CAUCASUS	
02 - MAY - 91	(122)	02:	07:	31.6	?	41 .34	N	45 .17	E	10	G	4.3	196	139	1.25	0:45	P	EASTERN CAUCASUS	
02 - MAY - 91	(122)	02:	18:	00.1	*	42 .211	N	43 .906	E	10	G	4.1	164	241	2.17	0:32	P	WESTERN CAUCASUS	
02 - MAY - 91	(122)	03:	42:	26.1	*	42 .608	N	43 .477	E	10	G	4.0	160	294	2.64	0:42	P	WESTERN CAUCASUS	
02 - MAY - 91	(122)	04:	30:	53.9	*	42 .481	N	43 .201	E	10	G	3.9	155	290	2.61	0:41	P	WESTERN CAUCASUS	
02 - MAY - 91	(122)	09:	00:	35.2	*	42 .704	N	43 .692	E	10	G	4.1	164	298	2.68	0:33	P	WESTERN CAUCASUS	
02 - MAY - 91	(122)	09:	44:	41.4		42 .507	N	43 .507	E	10	G	4.5	159	283	2.54	0:36	P	WESTERN CAUCASUS	
03 - MAY - 91	(123)	06:	08:	37.1		42 .482	N	43 .363	E	10	G	4.6	157	285	2.56	0:37	P	WESTERN CAUCASUS	
03 - MAY - 91	(123)	06:	12:	54.2	?	41 .93	N	43 .80	E	33	N	4.2	159	214	1.93	0:41	P	TURKEY-USSR BORDER REGION	
03 - MAY - 91	(123)	20:	19:	38.8		42 .683	N	43 .247	E	10	G	5.3	157	309	2.78	0:38	P	WESTERN CAUCASUS	
03 - MAY - 91	(123)	23:	41:	01.8		42 .647	N	43 .263	E	11	D	5.2	157	305	2.74	0:39	P	WESTERN CAUCASUS	
04 - MAY - 91	(124)	04:	53:	35.6	?	42 .15	N	43 .51	E	10	G	4.2	156	246	2.21	0:41	P	WESTERN CAUCASUS	
07 - MAY - 91	(127)	09:	01:	23.6	*	42 .606	N	43 .125	E	10	G	4.2	155	306	2.75	0:38	P	WESTERN CAUCASUS	
10 - MAY - 91	(130)	01:	25:	15.6		42 .496	N	43 .153	E	10	G	4.6	154	294	2.64	0:40	P	WESTERN CAUCASUS	
10 - MAY - 91	(130)	20:	30:	45.3		42 .627	N	43 .449	E	28	D	4.4	159	297	2.67	0:35	P	WESTERN CAUCASUS	
10 - MAY - 91	(130)	20:	52:	27.3		42 .534	N	43 .986	E	10	G	4.7	167	274	2.46	0:32	P	WESTERN CAUCASUS	
14 - MAY - 91	(134)	09:	36:	25.4	*	42 .609	N	43 .579	E	10	G	3.8	161	291	2.62	0:37	P	WESTERN CAUCASUS	
15 - MAY - 91	(135)	14:	28:	50.1		42 .565	N	43 .349	E	14	D	4.9	157	294	2.64	0:36	P	WESTERN CAUCASUS	
21 - MAY - 91	(141)	17:	37:	38.8		42 .867	N	48 .028	E	10	G	5.0	221	410	3.69	0:49	P	CASPIAN SEA	
24 - MAY - 91	(144)	07:	59:	38.8	*	42 .679	N	42 .908	E	10	G	3.9	152	321	2.89	0:26	P	WESTERN CAUCASUS	
27 - MAY - 91	(147)	03:	40:	45.5	?	42 .34	N	45 .86	E	10	G	3.7	201	263	2.37	0:26	P	EASTERN CAUCASUS	
03 - JUN - 91	(154)	10:	22:	40.4		40 .048	N	42 .859	E	28	D	5.0	87	159	1.43	0:13	P	TURKEY	
04 - JUN - 91	(155)	00:	55:	16.3		40 .600	N	42 .989	E	10	G	3.7	110	156	1.40	0:16	P	TURKEY	
08 - JUN - 91	(159)	01:	12:	01.8	*	41 .005	N	43 .563	E	33	N	4.2	135	138	1.24	0:12	P	TURKEY-USSR BORDER REGION	
15 - JUN - 91	(166)	00:	59:	20.3		42 .461	N	44 .009	E	9	G	6.3	167	266	2.39	0:33	P	WESTERN CAUCASUS	<MW;2 events>
16 - JUN - 91	(167)	11:	07:	10.6		39 .984	N	42 .875	E	26	D	4.6	85	158	1.42	0:15	P	TURKEY	
17 - JUN - 91	(168)	03:	04:	45.5	*	42 .252	N	44 .222	E	10	G	4.4	170	239	2.15	0:32	P	WESTERN CAUCASUS	
19 - JUN - 91	(170)	06:	40:	28.9		40 .282	N	42 .971	E	33	N	4.6	97	150	1.35	0:21	P	TURKEY	
30 - JUN - 91	(181)	20:	09:	18.3		42 .424	N	43 .688	E	10	G	4.5	162	269	2.42	0:47	P	WESTERN CAUCASUS	
04 - JUL - 91	(185)	06:	26:	31.8		42 .387	N	44 .116	E	20	D	5.0	169	256	2.30	0:39	P	WESTERN CAUCASUS	
14 - JUL - 91	(195)	09:	09:	11.9		36 .334	N	71 .119	E	213	G	6.4	272	2335	21.00	4:32	P	AFGHANISTAN-USSR BORDER REGION	
10 - AUG - 91	(222)	08:	57:	51.8	*	40 .052	N	42 .153	E	10	G	4.4	88	219	1.97	0:46	P	TURKEY	
20 - AUG - 91	(232)	08:	46:	40.5		37 .646	N	72 .150	E	135	D	5.2	268	2380	21.40	4:43	P	TAJIK SSR	
05 - SEP - 91	(248)	19:	23:	04.8		38 .847	N	41 .417	E	10	G	4.3	64	318	2.86	0:48	P	TURKEY	
08 - SEP - 91	(251)	10:	14:	58.8		36 .264	N	71 .324	E	133		5.0	272	2355	21.17	4:43	P	AFGHANISTAN-TAJIKISTAN BORD REG	
06 - OCT - 91	(279)	01:	46:	47.5		41 .096	N	43 .409	E	18	D	5.0	134	154	1.39	0:24	P	GEORGIA-ARMENIA-TURKEY BORD REG	
08 - OCT - 91	(281)	03:	31:	15.6		45 .587	N	149 .049	E	146	D	6.0	226	7878	70.84	11:07	P	KURIL ISLANDS	
10 - OCT - 91	(283)	02:	44:	49.6		41 .399	N	43 .259	E	10	G	4.4	139	187	1.68	0:21	P	GEORGIA-ARMENIA-TURKEY BORD REG	
12 - NOV - 91	(316)	20:	35:	59.6	*	39 .306	N	44 .936	E	33	N	4.3	349	94	0.84	0:26	P	ARMENIA-AZERBAIJAN-IRAN BORD REG	
13 - NOV - 91	(317)	11:	12:	13.2		8 .361	N	126 .371	E	36	G	6.6	269	8701	78.24	12:01	P	MINDANAO, PHILIPPINE ISLANDS	<MW>
21 - NOV - 91	(325)	12:	38:	28.5		5 .782	N	126 .832	E	73	G	6.1	271	8923	80.24	12:10	P	MINDANAO, PHILIPPINE ISLANDS	<MW>
28 - NOV - 91	(332)	17:	19:	55.5		36 .924	N	49 .603	E	16	D	5.6	309	554	4.99	1:34	P	WESTERN IRAN	

Table 3-5c. NEIC Parameters of Identified Events Sorted by Date.

Date	D.o.Y.	Hr	Mn	Sec		Latitude deg.		Longitude deg.		Depth km		Mag	Azi deg.	Epicentral Distance km	Epicentral Distance deg.	Travel m:ss	Phase	Region	
01 - DEC - 91	(335)	09:	17:	27.0		36 .373	N	45 .036	E	35	*	4.7	356	419	3.77	1:08	P	IRAN-IRAQ BORDER REGION	
07 - DEC - 91	(341)	11:	59:	00.9		45 .475	N	151 .391	E	50	D	6.0	225	8027	72.19	11:25	P	KURIL ISLANDS	<MW>
07 - DEC - 91	(341)	14:	22:	32.2		25 .191	N	62 .974	E	30	D	5.2	309	2374	21.35	4:51	P	SOUTHWESTERN PAKISTAN	
08 - DEC - 91	(342)	01:	02:	06.2	*	38 .335	N	48 .151	E	33	N	3.8	303	357	3.21	1:02	P	ARMENIA-AZERBAIJAN-IRAN BORD REG	
13 - DEC - 91	(347)	05:	45:	29.0		45 .567	N	151 .530	E	26	G	6.0	225	8029	72.20	11:30	P	KURIL ISLANDS	<2 events>
13 - DEC - 91	(347)	18:	59:	06.5		45 .521	N	151 .707	E	19	G	6.5	225	8043	72.33	11:32	P	KURIL ISLANDS	<MW>
13 - DEC - 91	(347)	19:	55:	09.5		45 .435	N	151 .270	E	48	D	6.4	225	8023	72.15	11:29	P	KURIL ISLANDS	<MW>
13 - DEC - 91	(347)	19:	58:	18.5		45 .439	N	151 .427	E	20	G	6.4	225	8032	72.23	11:32	P	KURIL ISLANDS	<Msz>
19 - DEC - 91	(353)	01:	33:	40.4		45 .253	N	151 .176	E	27	G	6.6	225	8030	72.21	11:28	P	KURIL ISLANDS	<MW>
20 - DEC - 91	(354)	08:	35:	37.3		45 .133	N	151 .248	E	48	D	6.0	225	8043	72.33	11:28	P	KURIL ISLANDS	<MW>
22 - DEC - 91	(356)	08:	43:	13.4		45 .533	N	151 .021	E	25	D	7.5	225	8001	71.95	11:28	P	KURIL ISLANDS	<MW>
23 - DEC - 91	(357)	13:	10:	04.9		45 .854	N	151 .962	E	24	D	6.0	224	8034	72.25	11:30	P	KURIL ISLANDS	
26 - DEC - 91	(360)	11:	35:	56.2		54 .382	N	162 .521	E	29	D	5.5	213	7957	71.55	11:24	P	NEAR EAST COAST OF KAMCHATKA	
27 - DEC - 91	(361)	09:	09:	37.5		51 .019	N	98 .150	E	14	D	6.5	235	4229	38.03	7:31	P	RUSSIA-MONGOLIA BORDER REGION	<MW*>
15 - FEB - 92	(046)	12:	52:	51.7	*	42 .803	N	46 .524	E	15	D	4.9	206	332	2.99	0:52	P	EASTERN CAUCASUS	
15 - FEB - 92	(046)	13:	30:	32.0	*	42 .462	N	46 .493	E	33	N	4.0	209	298	2.68	0:54	P	EASTERN CAUCASUS	
15 - FEB - 92	(046)	13:	37:	40.1		42 .934	N	46 .548	E	33	N	4.2	205	346	3.11	0:49	P	EASTERN CAUCASUS	
15 - FEB - 92	(046)	15:	18:	04.2	*	41 .434	N	46 .184	E	33	N	4.2	220	190	1.71	0:34	P	EASTERN CAUCASUS	
18 - FEB - 92	(049)	01:	39:	40.9	*	41 .477	N	43 .464	E	33	N	4.5	145	183	1.65	0:24	P	GEORGIA-ARMENIA-TURKEY BORD REG	
23 - FEB - 92	(054)	12:	03:	11.7	*	36 .391	N	49 .179	E	10	G	4.5	316	569	5.12	1:41	P	WESTERN IRAN	
26 - FEB - 92	(057)	03:	45:	19.7		11 .803	N	57 .764	E	10	G	5.8	334	3400	30.58	6:18	P	ARABIAN SEA	
02 - MAR - 92	(062)	12:	29:	40.2		52 .884	N	159 .997	E	44	D	6.9	215	7952	71.51	11:22	P	NEAR EAST COAST OF KAMCHATKA	<MW>
03 - MAR - 92	(063)	01:	18:	32.7		14 .265	S	167 .106	E	159	D	5.9	260	13761	123.75	18:44	PKP	VANUATU ISLANDS	<MW>
05 - MAR - 92	(065)	03:	30:	16.1		38 .263	N	44 .974	E	33	N	4.4	354	209	1.88	0:31	P	TURKEY-IRAN BORDER REGION	
13 - MAR - 92	(073)	17:	18:	40.1		39 .706	N	39 .570	E	28	D	7.1	85	442	3.98	1:04	P	TURKEY	<MW>
27 - MAR - 92	(087)	19:	21:	04.6		42 .456	N	43 .715	E	33	N	5.0	162	272	2.44	0:42	P	NORTHWESTERN CAUCASUS	
22 - APR - 92	(113)	03:	03:	47.6	*	39 .557	N	39 .557	E	10	G	4.5	83	446	4.01	1:17	P	TURKEY	
24 - APR - 92	(115)	07:	07:	25.1		27 .552	N	66 .057	E	33	N	6.1	299	2406	21.63	4:55	P	PAKISTAN	<MW>
26 - APR - 92	(117)	13:	15:	51.2	*	37 .663	N	47 .104	E	33	N	3.8	322	343	3.09	0:56	P	NORTHWESTERN IRAN	
30 - APR - 92	(121)	11:	44:	38.6		35 .070	N	26 .709	E	17	D	5.7	76	1680	15.11	3:44	P	CRETE	
07 - MAY - 92	(128)	19:	15:	02.3		38 .677	N	40 .130	E	10	G	5.0	69	427	3.84	1:15	P	TURKEY	
10 - MAY - 92	(131)	04:	04:	32.8		37 .193	N	72 .936	E	33	N	5.9	269	2461	22.13	4:59	P	TAJIKISTAN	<MW>
15 - MAY - 92	(136)	08:	08:	02.9		41 .003	N	72 .409	E	48	*	6.2	259	2331	20.96	4:44	P	KYRGYZSTAN	<Msz>
17 - MAY - 92	(138)	09:	49:	18.7		7 .260	N	126 .753	E	33	N	7.2	270	8811	79.24	12:07	P	MINDANAO, PHILIPPINE ISLANDS	<MW>
17 - MAY - 92	(138)	10:	15:	31.2		7 .169	N	126 .861	E	33	N	7.3	270	8827	79.38	12:08	P	MINDANAO, PHILIPPINE ISLANDS	<MW>
20 - MAY - 92	(141)	12:	20:	35.0		33 .324	N	71 .271	E	33	N	6.0	279	2473	22.24	5:00	P	PAKISTAN	
10 - AUG - 92	(223)	13:	42:	34.9		36 .053	N	69 .706	E	111	D	5.3	274	2225	20.01	4:30	P	HINDU KUSH REGION, AFGHANISTAN	

Table 3-6a. NEIC Parameters of Identified Events Sorted by Distance.

Date	D.o.Y.	Hr	Mn	Sec		Latitude deg.		Longitude deg.		Depth km		Mag	Azi deg.	Epicentral Distance km	Epicentral Distance deg.	Travel Time m:ss	Phase	Region	
27 - MAR - 91	(086)	22:	17:	55.0		40 .443	N	45 .443	E	33	N	4.3	240	70	0.63	-0:08	P	EASTERN CAUCASUS	<early>
27 - APR - 91	(117)	03:	31:	58.5	*	40 .093	N	43 .719	E	10	G	4.2	87	86	0.77	0:07	P	TURKEY-USSR BORDER REGION	
12 - NOV - 91	(316)	20:	35:	59.6	*	39 .306	N	44 .936	E	33	N	4.3	349	94	0.84	0:26	P	ARMENIA-AZERBAIJAN-IRAN BORD REG	
08 - JUN - 91	(159)	01:	12:	01.8	*	41 .005	N	43 .563	E	33	N	4.2	135	138	1.24	0:12	P	TURKEY-USSR BORDER REGION	
02 - MAY - 91	(122)	02:	07:	31.6	?	41 .34	N	45 .17	E	10	G	4.3	196	139	1.25	0:45	P	EASTERN CAUCASUS	
19 - JUN - 91	(170)	06:	40:	28.9		40 .282	N	42 .971	E	33	N	4.6	97	150	1.35	0:21	P	TURKEY	
06 - OCT - 91	(279)	01:	46:	47.5		41 .096	N	43 .409	E	18	D	5.0	134	154	1.39	0:24	P	GEORGIA-ARMENIA-TURKEY BORD REG	
04 - JUN - 91	(155)	00:	55:	16.3		40 .600	N	42 .989	E	10	G	3.7	110	156	1.40	0:16	P	TURKEY	
16 - JUN - 91	(167)	11:	07:	10.6		39 .984	N	42 .875	E	26	D	4.6	85	158	1.42	0:15	P	TURKEY	
03 - JUN - 91	(154)	10:	22:	40.4		40 .048	N	42 .859	E	28	D	5.0	87	159	1.43	0:13	P	TURKEY	
16 - DEC - 90	(350)	15:	45:	40.7		41 .361	N	43 .715	E	33	N	5.2	148	161	1.45	0:21	P	TURKEY-USSR BORDER REGION	
18 - FEB - 92	(049)	01:	39:	40.9	*	41 .477	N	43 .464	E	33	N	4.5	145	183	1.65	0:24	P	GEORGIA-ARMENIA-TURKEY BORD REG	
10 - OCT - 91	(283)	02:	44:	49.6		41 .399	N	43 .259	E	10	G	4.4	139	187	1.68	0:21	P	GEORGIA-ARMENIA-TURKEY BORD REG	
15 - FEB - 92	(046)	15:	18:	04.2	*	41 .434	N	46 .184	E	33	N	4.2	220	190	1.71	0:34	P	EASTERN CAUCASUS	
05 - MAR - 92	(065)	03:	30:	16.1		38 .263	N	44 .974	E	33	N	4.4	354	209	1.88	0:31	P	TURKEY-IRAN BORDER REGION	
03 - MAY - 91	(123)	06:	12:	54.2	?	41 .93	N	43 .80	E	33	N	4.2	159	214	1.93	0:41	P	TURKEY-USSR BORDER REGION	
10 - AUG - 91	(222)	08:	57:	51.8	*	40 .052	N	42 .153	E	10	G	4.4	88	219	1.97	0:46	P	TURKEY	
23 - DEC - 90	(357)	21:	28:	50.7	*	42 .115	N	44 .356	E	33	N	4.1	172	222	2.00	0:23	P	WESTERN CAUCASUS	
17 - JUN - 91	(168)	03:	04:	45.5	*	42 .252	N	44 .222	E	10	G	4.4	170	239	2.15	0:32	P	WESTERN CAUCASUS	
02 - MAY - 91	(122)	02:	18:	00.1	*	42 .211	N	43 .906	E	10	G	4.1	164	241	2.17	0:32	P	WESTERN CAUCASUS	
04 - MAY - 91	(124)	04:	53:	35.6	?	42 .15	N	43 .51	E	10	G	4.2	156	246	2.21	0:41	P	WESTERN CAUCASUS	
04 - JUL - 91	(185)	06:	26:	31.8		42 .387	N	44 .116	E	20	D	5.0	169	256	2.30	0:39	P	WESTERN CAUCASUS	
27 - MAY - 91	(147)	03:	40:	45.5	?	42 .34	N	45 .86	E	10	G	3.7	201	263	2.37	0:26	P	EASTERN CAUCASUS	
15 - JUN - 91	(166)	00:	59:	20.3		42 .461	N	44 .009	E	9	G	6.3	167	266	2.39	0:33	P	WESTERN CAUCASUS	<MW;2 events>
30 - JUN - 91	(181)	20:	09:	18.3		42 .424	N	43 .688	E	10	G	4.5	162	269	2.42	0:47	P	WESTERN CAUCASUS	
27 - MAR - 92	(087)	19:	21:	04.6		42 .456	N	43 .715	E	33	N	5.0	162	272	2.44	0:42	P	NORTHWESTERN CAUCASUS	
29 - APR - 91	(119)	18:	30:	41.5		42 .503	N	43 .899	E	14	G	6.0	166	272	2.45	0:36	P	WESTERN CAUCASUS	<Msz>
29 - APR - 91	(119)	09:	12:	48.1		42 .453	N	43 .673	E	17	G	7.2	162	272	2.45	0:29	P	WESTERN CAUCASUS	<MW>
29 - APR - 91	(119)	14:	43:	06.3		42 .515	N	43 .937	E	10	G	5.4	166	273	2.45	0:35	P	WESTERN CAUCASUS	
10 - MAY - 91	(130)	20:	52:	27.3		42 .534	N	43 .986	E	10	G	4.7	167	274	2.46	0:32	P	WESTERN CAUCASUS	
29 - APR - 91	(119)	11:	04:	28.9	*	42 .510	N	43 .816	E	10	G	4.3	164	275	2.47	0:35	P	WESTERN CAUCASUS	
02 - MAY - 91	(122)	01:	25:	30.1		42 .541	N	43 .960	E	10	G	5.1	167	275	2.47	0:32	P	WESTERN CAUCASUS	
20 - JUL - 90	(201)	17:	30:	36.2	?	42 .10	N	46 .77	E	33	N	4.2	217	278	2.50	0:50	P	EASTERN CAUCASUS	
29 - APR - 91	(119)	11:	10:	11.9		42 .584	N	43 .904	E	10	G	4.7	166	281	2.53	0:35	P	WESTERN CAUCASUS	
29 - APR - 91	(119)	11:	51:	10.3		42 .572	N	43 .816	E	10	G	4.9	165	281	2.53	0:34	P	WESTERN CAUCASUS	
02 - MAY - 91	(122)	09:	44:	41.4		42 .507	N	43 .507	E	10	G	4.5	159	283	2.54	0:36	P	WESTERN CAUCASUS	
29 - APR - 91	(119)	18:	23:	15.2		42 .583	N	43 .764	E	10	G	5.5	164	284	2.55	0:35	P	WESTERN CAUCASUS	
29 - APR - 91	(119)	11:	59:	54.8		42 .625	N	43 .962	E	10	G	4.5	167	284	2.56	0:34	P	WESTERN CAUCASUS	
03 - MAY - 91	(123)	06:	08:	37.1		42 .482	N	43 .363	E	10	G	4.6	157	285	2.56	0:37	P	WESTERN CAUCASUS	
02 - MAY - 91	(122)	04:	30:	53.9	*	42 .481	N	43 .201	E	10	G	3.9	155	290	2.61	0:41	P	WESTERN CAUCASUS	
29 - APR - 91	(119)	10:	52:	42.2		42 .712	N	44 .102	E	10	G	4.6	170	291	2.62	0:32	P	WESTERN CAUCASUS	
14 - MAY - 91	(134)	09:	36:	25.4	*	42 .609	N	43 .579	E	10	G	3.8	161	291	2.62	0:37	P	WESTERN CAUCASUS	
01 - MAY - 91	(121)	23:	19:	11.8	*	42 .719	N	44 .053	E	10	G	4.1	169	293	2.63	0:29	P	WESTERN CAUCASUS	
10 - MAY - 91	(130)	01:	25:	15.6		42 .496	N	43 .153	E	10	G	4.6	154	294	2.64	0:40	P	WESTERN CAUCASUS	
15 - MAY - 91	(135)	14:	28:	50.1		42 .565	N	43 .349	E	14	D	4.9	157	294	2.64	0:36	P	WESTERN CAUCASUS	
02 - MAY - 91	(122)	03:	42:	26.1	*	42 .608	N	43 .477	E	10	G	4.0	160	294	2.64	0:42	P	WESTERN CAUCASUS	
10 - MAY - 91	(130)	20:	30:	45.3		42 .627	N	43 .449	E	28	D	4.4	159	297	2.67	0:35	P	WESTERN CAUCASUS	
15 - FEB - 92	(046)	13:	30:	32.0	*	42 .462	N	46 .493	E	33	N	4.0	209	298	2.68	0:54	P	EASTERN CAUCASUS	
02 - MAY - 91	(122)	09:	00:	35.2	*	42 .704	N	43 .692	E	10	G	4.1	164	298	2.68	0:33	P	WESTERN CAUCASUS	
22 - SEP - 90	(265)	02:	46:	01.2	*	42 .538	N	46 .449	E	33	N	4.3	208	304	2.73	0:34	P	EASTERN CAUCASUS	
03 - MAY - 91	(123)	23:	41:	01.8		42 .647	N	43 .263	E	11	D	5.2	157	305	2.74	0:39	P	WESTERN CAUCASUS	
23 - JUL - 90	(204)	20:	54:	56.6		42 .719	N	45 .947	E	33	N	4.8	199	305	2.74	0:47	Pn	EASTERN CAUCASUS	
07 - MAY - 91	(127)	09:	01:	23.6	*	42 .606	N	43 .125	E	10	G	4.2	155	306	2.75	0:38	P	WESTERN CAUCASUS	
03 - MAY - 91	(123)	20:	19:	38.8		42 .683	N	43 .247	E	10	G	5.3	157	309	2.78	0:38	P	WESTERN CAUCASUS	
05 - SEP - 91	(248)	19:	23:	04.8		38 .847	N	41 .417	E	10	G	4.3	64	318	2.86	0:48	P	TURKEY	
01 - JAN - 91	(001)	19:	18:	56.4		39 .822	N	48 .439	E	61	D	4.9	275	318	2.86	0:48	P	N.W. IRAN-USSR BORDER REGION	
24 - MAY - 91	(144)	07:	59:	38.8	*	42 .679	N	42 .908	E	10	G	3.9	152	321	2.89	0:26	P	WESTERN CAUCASUS	
15 - FEB - 92	(046)	12:	52:	51.7	*	42 .803	N	46 .524	E	15	D	4.9	206	332	2.99	0:52	P	EASTERN CAUCASUS	

Table 3-6b. NEIC Parameters of Identified Events Sorted by Distance.

Date	D.o.Y.	Hr	Mn	Sec		Latitude deg.		Longitude deg.		Depth km	Mag	Azi deg.	Epicentral Distance km	Epicentral Distance deg.	Travel m:ss	Phase	Region	
26 - APR - 92	(117)	13:	15:	51.2	*	37 .663	N	47 .104	E	33 N	3.8	322	343	3.09	0:56	P	NORTHWESTERN IRAN	
15 - FEB - 92	(046)	13:	37:	40.1		42 .934	N	46 .548	E	33 N	4.2	205	346	3.11	0:49	P	EASTERN CAUCASUS	
02 - AUG - 90	(214)	17:	12:	48.5	*	38 .540	N	48 .186	E	33 N	4.2	300	346	3.12	0:56	P	N.W. IRAN-USSR BORDER REGION	
24 - SEP - 90	(267)	06:	35:	13.9	*	38 .253	N	47 .951	E	10 G	4.6	306	348	3.13		P	NORTHWESTERN IRAN	<PC only>
08 - DEC - 91	(342)	01:	02:	06.2	*	38 .335	N	48 .151	E	33 N	3.8	303	357	3.21	1:02	P	ARMENIA-AZERBAIJAN-IRAN BORD REG	
02 - AUG - 90	(214)	21:	17:	18.7	*	38 .398	N	48 .228	E	33 N	4.1	301	358	3.22	0:55	P	N.W. IRAN-USSR BORDER REGION	
21 - MAY - 91	(141)	17:	37:	38.8		42 .867	N	48 .028	E	10 G	5.0	221	410	3.69	0:49	P	CASPIAN SEA	
01 - DEC - 91	(335)	09:	17:	27.0		36 .373	N	45 .036	E	35 *	4.7	356	419	3.77	1:08	P	IRAN-IRAQ BORDER REGION	
07 - MAY - 92	(128)	19:	15:	02.3		38 .677	N	40 .130	E	10 G	5.0	69	427	3.84	1:15	P	TURKEY	
13 - MAR - 92	(073)	17:	18:	40.1		39 .706	N	39 .570	E	28 D	7.1	85	442	3.98	1:04	P	TURKEY	<MW>
22 - APR - 92	(113)	03:	03:	47.6	*	39 .557	N	39 .557	E	10 G	4.5	83	446	4.01	1:17	P	TURKEY	
01 - JUL - 90	(182)	21:	16:	48.3		37 .285	N	48 .820	E	10 G	4.7	310	476	4.28	1:29	P	CASPIAN SEA	
01 - JUL - 90	(182)	17:	19:	44.1		37 .280	N	48 .818	E	10 G	4.6	310	476	4.28	1:30	P	CASPIAN SEA	
28 - DEC - 90	(362)	04:	03:	53.6		37 .106	N	49 .227	E	10 G	5.0	309	516	4.64	1:29	P	CASPIAN SEA	
27 - JUL - 90	(208)	05:	31:	00.1		37 .318	N	49 .585	E	10 G	4.8	305	525	4.72	1:29	P	CASPIAN SEA	
22 - AUG - 90	(234)	07:	51:	49.5	*	37 .056	N	49 .327	E	10 G	4.3	309	526	4.73	1:33	P	CASPIAN SEA	
21 - AUG - 90	(233)	03:	47:	26.2		37 .309	N	49 .685	E	10 G	4.8	305	533	4.79	1:30	P	CASPIAN SEA	
06 - JUL - 90	(187)	19:	34:	52.4		36 .861	N	49 .303	E	35 D	5.3	311	540	4.85	1:16	Pn	WESTERN IRAN	
27 - DEC - 90	(361)	13:	26:	57.1		36 .539	N	48 .907	E	10 G	4.7	316	541	4.87	1:26	P	NORTHWESTERN IRAN	
11 - JUL - 90	(192)	04:	36:	08.6	*	37 .015	N	49 .530	E	33 N	4.5	308	543	4.88	1:35	P	CASPIAN SEA	
28 - JUN - 90	(179)	03:	20:	35.0		37 .085	N	49 .642	E	10 G	4.8	307	545	4.90	1:36	P	CASPIAN SEA	
28 - NOV - 91	(332)	17:	19:	55.5		36 .924	N	49 .603	E	16 D	5.6	309	554	4.99	1:34	P	WESTERN IRAN	
01 - JUL - 90	(182)	12:	24:	57.2		37 .181	N	49 .885	E	10 G	4.8	305	555	4.99	1:35	P	CASPIAN SEA	
20 - AUG - 90	(232)	12:	20:	11.0	*	36 .956	N	49 .720	E	33 N	4.8	308	560	5.03	1:30	P	WESTERN IRAN	
17 - JUL - 90	(198)	04:	02:	09.2		37 .137	N	49 .979	E	33 N	4.6	304	565	5.08	1:35	P	CASPIAN SEA	
23 - FEB - 92	(054)	12:	03:	11.7	*	36 .391	N	49 .179	E	10 G	4.5	316	569	5.12	1:41	P	WESTERN IRAN	
28 - JUN - 90	(179)	03:	42:	01.9	*	37 .079	N	50 .147	E	10 G	4.7	304	581	5.22	1:39	P	CASPIAN SEA	
13 - AUG - 90	(225)	06:	18:	25.1		36 .663	N	49 .884	E	35 *	4.6	309	592	5.33	1:37	P	WESTERN IRAN	
18 - JUL - 90	(199)	11:	29:	24.9		36 .990	N	29 .595	E	17 D	5.2	80	1359	12.22	3:07	P	TURKEY	
30 - APR - 92	(121)	11:	44:	38.6		35 .070	N	26 .709	E	17 D	5.7	76	1680	15.11	3:44	P	CRETE	
10 - AUG - 92	(223)	13:	42:	34.9		36 .053	N	69 .706	E	111 D	5.3	274	2225	20.01	4:30	P	HINDU KUSH REGION, AFGHANISTAN	
31 - JAN - 91	(031)	23:	03:	33.6		35 .993	N	70 .423	E	142 G	6.7	273	2288	20.57	4:31	P	HINDU KUSH REGION	<MW>
03 - SEP - 90	(246)	02:	40:	59.1		36 .409	N	70 .671	E	202 D	4.9	272	2294	20.63	4:27	P	HINDU KUSH REGION	
13 - JUL - 90	(194)	14:	20:	43.4		36 .415	N	70 .789	E	217 D	5.6	272	2304	20.72	4:28	P	HINDU KUSH REGION	
25 - OCT - 90	(298)	04:	53:	59.9		35 .121	N	70 .486	E	114 G	6.0	276	2327	20.93	4:38	P	HINDU KUSH REGION	
15 - MAY - 92	(136)	08:	08:	02.9		41 .003	N	72 .409	E	48 *	6.2	259	2331	20.96	4:44	P	KYRGYZSTAN	<Msz>
14 - JUL - 91	(195)	09:	09:	11.9		36 .334	N	71 .119	E	213 G	6.4	272	2335	21.00	4:32	P	AFGHANISTAN-USSR BORDER REGION	
08 - SEP - 91	(251)	10:	14:	58.8		36 .264	N	71 .324	E	133	5.0	272	2355	21.17	4:43	P	AFGHANISTAN-TAJIKISTAN BORD REG	
15 - APR - 91	(105)	10:	48:	59.3		36 .340	N	71 .358	E	124 D	5.3	272	2355	21.18	4:30	P	AFGHANISTAN-USSR BORDER REGION	
07 - DEC - 91	(341)	14:	22:	32.2		25 .191	N	62 .974	E	30 D	5.2	309	2374	21.35	4:51	P	SOUTHWESTERN PAKISTAN	
20 - AUG - 91	(232)	08:	46:	40.5		37 .646	N	72 .150	E	135 D	5.2	268	2380	21.40	4:43	P	TAJIK SSR	
26 - JUL - 90	(207)	06:	53:	56.3		27 .247	N	65 .508	E	19 G	5.8	300	2388	21.47	4:51	P	PAKISTAN	<2 events>
24 - APR - 92	(115)	07:	07:	25.1		27 .552	N	66 .057	E	33 N	6.1	299	2406	21.63	4:55	P	PAKISTAN	<MW>
08 - SEP - 90	(251)	19:	33:	18.8		27 .500	N	66 .092	E	28 *	5.5	299	2412	21.69	4:52	P	PAKISTAN	
14 - AUG - 90	(226)	00:	50:	39.2		27 .024	N	65 .969	E	21 D	5.2	300	2438	21.93	4:56	P	PAKISTAN	
10 - MAY - 92	(131)	04:	04:	32.8		37 .193	N	72 .936	E	33 N	5.9	269	2461	22.13	4:59	P	TAJIKISTAN	<MW>
20 - MAY - 92	(141)	12:	20:	35.0		33 .324	N	71 .271	E	33 N	6.0	279	2473	22.24	5:00	P	PAKISTAN	
26 - FEB - 91	(057)	07:	25:	47.2		40 .186	N	13 .822	E	401	5.5	100	2613	23.49	4:30	P	TYRRHENIAN SEA	
12 - NOV - 90	(316)	12:	28:	51.5		42 .959	N	78 .071	E	19 G	6.3	252	2774	24.95	5:28	P	ALMA-ATA REGION	<MW>
14 - SEP - 90	(257)	20:	40:	18.3		13 .382	N	51 .456	E	10 G	5.4	346	3046	27.39	5:50	P	EASTERN GULF OF ADEN	
03 - AUG - 90	(215)	09:	15:	06.1		47 .963	N	84 .961	E	33 G	6.1	241	3291	29.59	6:05	P	KAZAKH-XINJIANG BORDER REGION	<MW>
26 - FEB - 92	(057)	03:	45:	19.7		11 .803	N	57 .764	E	10 G	5.8	334	3400	30.58	6:18	P	ARABIAN SEA	
16 - AUG - 90	(228)	04:	59:	57.6		41 .564	N	88 .770	E	0 G	6.2	253	3668	32.98	6:39	P	SOUTHERN XINJIANG, CHINA	
10 - AUG - 90	(222)	21:	11:	49.0		6 .572	N	60 .240	E	10 G	5.5	333	4040	36.33	7:07	P	CARLSBERG RIDGE	
07 - SEP - 90	(250)	00:	12:	26.2		5 .443	N	31 .686	E	10 G	5.2	22	4072	36.62	7:09	P	SUDAN	
09 - JUL - 90	(190)	15:	11:	20.3		5 .395	N	31 .654	E	13 G	6.4	22	4078	36.67	7:09	P	SUDAN	<MW>
27 - DEC - 91	(361)	09:	09:	37.5		51 .019	N	98 .150	E	14 D	6.5	235	4229	38.03	7:31	P	RUSSIA-MONGOLIA BORDER REGION	<MW*>
25 - OCT - 90	(298)	04:	52:	06.0	*	76 .243	N	8 .409	E	10 G	4.6	167	4382	39.41	?7:47	P	SVALBARD REGION	<within coda>

Table 3-6c. NEIC Parameters of Identified Events Sorted by Distance.

Date	D.o.Y.	Hr	Mn	Sec	Latitude deg.	Longitude deg.	Depth km	Mag	Azi deg.	Epicentral Distance km	Epicentral Distance deg.	Travel m:ss	Phase	Region	
09 - SEP - 90	(252)	02:	14:	51.0	56 .654 N	34 .395 W	10 G	5.4	137	5765	51.84	9:14	P	NORTH ATLANTIC OCEAN	
29 - AUG - 90	(241)	20:	44:	23.0	11 .791 N	95 .034 E	25 D	5.2	288	5830	52.43	9:15	P	ANDAMAN ISLANDS REGION	
14 - AUG - 90	(226)	15:	13:	28.6	35 .432 N	35 .648 W	10 G	6.0	114	6833	61.45	10:27	P	NORTH ATLANTIC RIDGE	<Msz>
04 - JUL - 90	(185)	02:	24:	41.9	25 .372 N	124 .473 E	133	5.6	256	7392	66.47	10:38	P	NORTHEAST OF TAIWAN	
14 - APR - 91	(104)	08:	08:	55.7	27 .155 N	127 .419 E	83 G	6.2	253	7519	67.62	10:45	P	RYUKYU ISLANDS	
15 - AUG - 90	(227)	23:	08:	56.0	43 .757 N	143 .297 E	162 D	5.4	230	7637	68.68	10:51	P	HOKKAIDO, JAPAN REGION	
16 - JUL - 90	(197)	13:	31:	13.2	16 .285 N	120 .457 E	13 D	5.7	266	7650	68.79	11:04	P	LUZON, PHILIPPINE ISLANDS	<Msz>
16 - JUL - 90	(197)	19:	45:	25.1	16 .365 N	120 .546 E	33 N	5.4	266	7652	68.81	11:04	P	LUZON, PHILIPPINE ISLANDS	
14 - JUL - 90	(195)	05:	54:	25.4	0 .003 N	17 .376 W	11 G	6.4	71	7676	69.03	11:07	P	NORTH OF ASCENCION ISLAND	<Msz>
17 - JUL - 90	(198)	21:	14:	43.8	16 .495 N	120 .981 E	23 G	6.7	266	7680	69.07	11:09	P	LUZON, PHILIPPINE ISLANDS	<MW>
18 - JUL - 90	(199)	08:	00:	12.8	16 .511 N	121 .007 E	14 G	5.8	266	7681	69.08	11:10	P	LUZON, PHILIPPINE ISLANDS	
22 - JUL - 90	(203)	11:	20:	09.6	16 .532 N	121 .045 E	33 N	5.3	266	7683	69.09	11:07	P	LUZON, PHILIPPINE ISLANDS	
14 - JUL - 90	(195)	07:	24:	39.6	0 .074 S	17 .523 W	12 G	5.8	71	7694	69.19	11:10	P	NORTH OF ASCENCION ISLAND	
16 - JUL - 90	(197)	07:	26:	34.6	15 .679 N	121 .172 E	25 D	7.9	266	7752	69.71	11:12	P	LUZON, PHILIPPINE ISLANDS	<MW>
08 - OCT - 91	(281)	03:	31:	15.6	45 .587 N	149 .049 E	146 D	6.0	226	7878	70.84	11:07	P	KURIL ISLANDS	
17 - SEP - 90	(260)	11:	57:	24.1	5 .917 S	103 .796 E	59 D	5.7	296	7902	71.06	11:14	P	SOUTHERN SUMATERA	
02 - MAR - 92	(062)	12:	29:	40.2	52 .884 N	159 .997 E	44 D	6.9	215	7952	71.51	11:22	P	NEAR EAST COAST OF KAMCHATKA	<MW>
26 - DEC - 91	(360)	11:	35:	56.2	54 .382 N	162 .521 E	29 D	5.5	213	7957	71.55	11:24	P	NEAR EAST COAST OF KAMCHATKA	
06 - JUL - 90	(187)	05:	02:	27.9	45 .371 N	150 .170 E	42 D	5.7	226	7961	71.59	11:22	P	KURIL ISLANDS	
22 - DEC - 91	(356)	08:	43:	13.4	45 .533 N	151 .021 E	25 D	7.5	225	8001	71.95	11:28	P	KURIL ISLANDS	<MW>
13 - DEC - 91	(347)	19:	55:	09.5	45 .435 N	151 .270 E	48 D	6.4	225	8023	72.15	11:29	P	KURIL ISLANDS	<MW>
07 - DEC - 91	(341)	11:	59:	00.9	45 .475 N	151 .391 E	50 D	6.0	225	8027	72.19	11:25	P	KURIL ISLANDS	<MW>
13 - DEC - 91	(347)	05:	45:	29.0	45 .567 N	151 .530 E	26 G	6.0	225	8029	72.20	11:30	P	KURIL ISLANDS	<2 events>
19 - DEC - 91	(353)	01:	33:	40.4	45 .253 N	151 .176 E	27 G	6.6	225	8030	72.21	11:28	P	KURIL ISLANDS	<MW>
13 - DEC - 91	(347)	19:	58:	18.5	45 .439 N	151 .427 E	20 G	6.4	225	8032	72.23	11:32	P	KURIL ISLANDS	<Msz>
23 - DEC - 91	(357)	13:	10:	04.9	45 .854 N	151 .962 E	24 D	6.0	224	8034	72.25	11:30	P	KURIL ISLANDS	
13 - DEC - 91	(347)	18:	59:	06.5	45 .521 N	151 .707 E	19 G	6.5	225	8043	72.33	11:32	P	KURIL ISLANDS	<MW>
20 - DEC - 91	(354)	08:	35:	37.3	45 .133 N	151 .248 E	48 D	6.0	225	8043	72.33	11:28	P	KURIL ISLANDS	<MW>
13 - NOV - 91	(317)	11:	12:	13.2	8 .361 N	126 .371 E	36 G	6.6	269	8701	78.24	12:01	P	MINDANAO, PHILIPPINE ISLANDS	<MW>
17 - MAY - 92	(138)	09:	49:	18.7	7 .260 N	126 .753 E	33 N	7.2	270	8811	79.24	12:07	P	MINDANAO, PHILIPPINE ISLANDS	<MW>
17 - MAY - 92	(138)	10:	15:	31.2	7 .169 N	126 .861 E	33 N	7.3	270	8827	79.38	12:08	P	MINDANAO, PHILIPPINE ISLANDS	<MW>
21 - NOV - 91	(325)	12:	38:	28.5	5 .782 N	126 .832 E	73 G	6.1	271	8923	80.24	12:10	P	MINDANAO, PHILIPPINE ISLANDS	<MW>
25 - AUG - 90	(237)	15:	47:	53.8	0 .525 N	126 .084 E	11 G	6.5	275	9236	83.06	12:29	P	MOLUCCA PASSAGE	<MW>
10 - AUG - 90	(222)	15:	44:	31.3	0 .333 N	126 .175 E	53	6.4	275	9258	83.25	12:25	P	MOLUCCA PASSAGE	<MW>
03 - MAR - 92	(063)	01:	18:	32.7	14 .265 S	167 .106 E	159 D	5.9	260	13761	123.75	18:44	PKP	VANUATU ISLANDS	<MW>
27 - JUL - 90	(208)	12:	37:	59.5	15 .355 S	167 .464 E	126 G	7.5	261	13866	124.70	18:48	PKP	VANUATU ISLANDS	<MW;2 events>
12 - AUG - 90	(224)	21:	25:	21.9	19 .435 S	169 .132 E	140 G	6.3	263	14283	128.44	18:52	PKP	VANUATU ISLANDS	<2 events>
22 - JUL - 90	(203)	09:	26:	14.6	23 .622 S	179 .893 W	531 G	5.9	260	15477	139.18	21:14	SKP	SOUTH OF FIJI ISLANDS	

Table 3-7a. NEIC Parameters of Identified Events Sorted by Magnitude.

Date	D.o.Y.	Hr	Mn	Sec	Latitude deg.		Longitude deg.		Depth km		Mag	Azi deg.	Epicentral Distance km	Epicentral Distance deg.	Travel m:ss	Phase	Region	
16 - JUL - 90	(197)	07:	26:	34.6	15 .679	N	121 .172	E	25	D	7.9	266	7752	69.71	11:12	P	LUZON, PHILIPPINE ISLANDS	<MW>
22 - DEC - 91	(356)	08:	43:	13.4	45 .533	N	151 .021	E	25	D	7.5	225	8001	71.95	11:28	P	KURIL ISLANDS	<MW>
27 - JUL - 90	(208)	12:	37:	59.5	15 .355	S	167 .464	E	126	G	7.5	261	13866	124.70	18:48	PKP	VANUATU ISLANDS	<MW;2 events>
17 - MAY - 92	(138)	10:	15:	31.2	7 .169	N	126 .861	E	33	N	7.3	270	8827	79.38	12:08	P	MINDANAO, PHILIPPINE ISLANDS	<MW>
29 - APR - 91	(119)	09:	12:	48.1	42 .453	N	43 .673	E	17	G	7.2	162	272	2.45	0:29	P	WESTERN CAUCASUS	<MW>
17 - MAY - 92	(138)	09:	49:	18.7	7 .260	N	126 .753	E	33	N	7.2	270	8811	79.24	12:07	P	MINDANAO, PHILIPPINE ISLANDS	<MW>
13 - MAR - 92	(073)	17:	18:	40.1	39 .706	N	39 .570	E	28	D	7.1	85	442	3.98	1:04	P	TURKEY	<MW>
02 - MAR - 92	(062)	12:	29:	40.2	52 .884	N	159 .997	E	44	D	6.9	215	7952	71.51	11:22	P	NEAR EAST COAST OF KAMCHATKA	<MW>
31 - JAN - 91	(031)	23:	03:	33.6	35 .993	N	70 .423	E	142	G	6.7	273	2288	20.57	4:31	P	HINDU KUSH REGION	<MW>
17 - JUL - 90	(198)	21:	14:	43.8	16 .495	N	120 .981	E	23	G	6.7	266	7680	69.07	11:09	P	LUZON, PHILIPPINE ISLANDS	<MW>
19 - DEC - 91	(353)	01:	33:	40.4	45 .253	N	151 .176	E	27	G	6.6	225	8030	72.21	11:28	P	KURIL ISLANDS	<MW>
13 - NOV - 91	(317)	11:	12:	13.2	8 .361	N	126 .371	E	36	G	6.6	269	8701	78.24	12:01	P	MINDANAO, PHILIPPINE ISLANDS	<MW>
27 - DEC - 91	(361)	09:	09:	37.5	51 .019	N	98 .150	E	14	D	6.5	235	4229	38.03	7:31	P	RUSSIA-MONGOLIA BORDER REGION	<MW*>
13 - DEC - 91	(347)	18:	59:	06.5	45 .521	N	151 .707	E	19	G	6.5	225	8043	72.33	11:32	P	KURIL ISLANDS	<MW>
25 - AUG - 90	(237)	15:	47:	53.8	0 .525	N	126 .084	E	11	G	6.5	275	9236	83.06	12:29	P	MOLUCCA PASSAGE	<MW>
14 - JUL - 91	(195)	09:	09:	11.9	36 .334	N	71 .119	E	213	G	6.4	272	2335	21.00	4:32	P	AFGHANISTAN-USSR BORDER REGION	
09 - JUL - 90	(190)	15:	11:	20.3	5 .395	N	31 .654	E	13	G	6.4	22	4078	36.67	7:09	P	SUDAN	<MW>
14 - JUL - 90	(195)	05:	54:	25.4	0 .003	N	17 .376	W	11	G	6.4	71	7676	69.03	11:07	P	NORTH OF ASCENCION ISLAND	<Msz>
13 - DEC - 91	(347)	19:	55:	09.5	45 .435	N	151 .270	E	48	D	6.4	225	8023	72.15	11:29	P	KURIL ISLANDS	<MW>
13 - DEC - 91	(347)	19:	58:	18.5	45 .439	N	151 .427	E	20	G	6.4	225	8032	72.23	11:32	P	KURIL ISLANDS	<Msz>
10 - AUG - 90	(222)	15:	44:	31.3	0 .333	N	126 .175	E	53		6.4	275	9258	83.25	12:25	P	MOLUCCA PASSAGE	<MW>
15 - JUN - 91	(166)	00:	59:	20.3	42 .461	N	44 .009	E	9	G	6.3	167	266	2.39	0:33	P	WESTERN CAUCASUS	<MW;2 events>
12 - NOV - 90	(316)	12:	28:	51.5	42 .959	N	78 .071	E	19	G	6.3	252	2774	24.95	5:28	P	ALMA-ATA REGION	<MW>
12 - AUG - 90	(224)	21:	25:	21.9	19 .435	S	169 .132	E	140	G	6.3	263	14283	128.44	18:52	PKP	VANUATU ISLANDS	<2 events>
15 - MAY - 92	(136)	08:	08:	02.9	41 .003	N	72 .409	E	48	*	6.2	259	2331	20.96	4:44	P	KYRGYZSTAN	<Msz>
16 - AUG - 90	(228)	04:	59:	57.6	41 .564	N	88 .770	E	0	G	6.2	253	3668	32.98	6:39	P	SOUTHERN XINJIANG, CHINA	
14 - APR - 91	(104)	08:	08:	55.7	27 .155	N	127 .419	E	83	G	6.2	253	7519	67.62	10:45	P	RYUKYU ISLANDS	
24 - APR - 92	(115)	07:	07:	25.1	27 .552	N	66 .057	E	33	N	6.1	299	2406	21.63	4:55	P	PAKISTAN	<MW>
03 - AUG - 90	(215)	09:	15:	06.1	47 .963	N	84 .961	E	33	G	6.1	241	3291	29.59	6:05	P	KAZAKH-XINJIANG BORDER REGION	<MW>
21 - NOV - 91	(325)	12:	38:	28.5	5 .782	N	126 .832	E	73	G	6.1	271	8923	80.24	12:10	P	MINDANAO, PHILIPPINES ISLANDS	<MW>
29 - APR - 91	(119)	18:	30:	41.5	42 .503	N	43 .899	E	14	G	6.0	166	272	2.45	0:36	P	WESTERN CAUCASUS	<Msz>
25 - OCT - 90	(298)	04:	53:	59.9	35 .121	N	70 .486	E	114	G	6.0	276	2327	20.93	4:38	P	HINDU KUSH REGION	
20 - MAY - 92	(141)	12:	20:	35.0	33 .324	N	71 .271	E	33	N	6.0	279	2473	22.24	5:00	P	PAKISTAN	
14 - AUG - 90	(226)	15:	13:	28.6	35 .432	N	35 .648	W	10	G	6.0	114	6833	61.45	10:27	P	NORTH ATLANTIC RIDGE	<Msz>
08 - OCT - 91	(281)	03:	31:	15.6	45 .587	N	149 .049	E	146	D	6.0	226	7878	70.84	11:07	P	KURIL ISLANDS	
07 - DEC - 91	(341)	11:	59:	00.9	45 .475	N	151 .391	E	50	D	6.0	225	8027	72.19	11:25	P	KURIL ISLANDS	<MW>
13 - DEC - 91	(347)	05:	45:	29.0	45 .567	N	151 .530	E	26	G	6.0	225	8029	72.20	11:30	P	KURIL ISLANDS	<2 events>
23 - DEC - 91	(357)	13:	10:	04.9	45 .854	N	151 .962	E	24	D	6.0	224	8034	72.25	11:30	P	KURIL ISLANDS	
20 - DEC - 91	(354)	08:	35:	37.3	45 .133	N	151 .248	E	48	D	6.0	225	8043	72.33	11:28	P	KURIL ISLANDS	<MW>
10 - MAY - 92	(131)	04:	04:	32.8	37 .193	N	72 .936	E	33	N	5.9	269	2461	22.13	4:59	P	TAJIKISTAN	<MW>
03 - MAR - 92	(063)	01:	18:	32.7	14 .265	S	167 .106	E	159	D	5.9	260	13761	123.75	18:44	PKP	VANUATU ISLANDS	<MW>
22 - JUL - 90	(203)	09:	26:	14.6	23 .622	S	179 .893	W	531	G	5.9	260	15477	139.18	21:14	SKP	SOUTH OF FIJI ISLANDS	
26 - JUL - 90	(207)	06:	53:	56.3	27 .247	N	65 .508	E	19	G	5.8	300	2388	21.47	4:51	P	PAKISTAN	<2 events>
26 - FEB - 92	(057)	03:	45:	19.7	11 .803	N	57 .764	E	10	G	5.8	334	3400	30.58	6:18	P	ARABIAN SEA	
18 - JUL - 90	(199)	08:	00:	12.8	16 .511	N	121 .007	E	14	G	5.8	266	7681	69.08	11:10	P	LUZON, PHILIPPINE ISLANDS	
14 - JUL - 90	(195)	07:	24:	39.6	0 .074	S	17 .523	W	12	G	5.8	71	7694	69.19	11:10	P	NORTH OF ASCENCION ISLAND	
30 - APR - 92	(121)	11:	44:	38.6	35 .070	N	26 .709	E	17	D	5.7	76	1680	15.11	3:44	P	CRETE	
16 - JUL - 90	(197)	13:	31:	13.2	16 .285	N	120 .457	E	13	D	5.7	266	7650	68.79	11:04	P	LUZON, PHILIPPINE ISLANDS	<Msz>
17 - SEP - 90	(260)	11:	57:	24.1	5 .917	S	103 .796	E	59	D	5.7	296	7902	71.06	11:14	P	SOUTHERN SUMATERA	
06 - JUL - 90	(187)	05:	02:	27.9	45 .371	N	150 .170	E	42	D	5.7	226	7961	71.59	11:22	P	KURIL ISLANDS	
28 - NOV - 91	(332)	17:	19:	55.5	36 .924	N	49 .603	E	16	D	5.6	309	554	4.99	1:34	P	WESTERN IRAN	
13 - JUL - 90	(194)	14:	20:	43.4	36 .415	N	70 .789	E	217	D	5.6	272	2304	20.72	4:28	P	HINDU KUSH REGION	
04 - JUL - 90	(185)	02:	24:	41.9	25 .372	N	124 .473	E	133		5.6	256	7392	66.47	10:38	P	NORTHEAST OF TAIWAN	
29 - APR - 91	(119)	18:	23:	15.2	42 .583	N	43 .764	E	10	G	5.5	164	284	2.55	0:35	P	WESTERN CAUCASUS	
08 - SEP - 90	(251)	19:	33:	18.8	27 .500	N	66 .092	E	28	*	5.5	299	2412	21.69	4:52	P	PAKISTAN	
26 - FEB - 91	(057)	07:	25:	47.2	40 .186	N	13 .822	E	401		5.5	100	2613	23.49	4:30	P	TYRRHENIAN SEA	
10 - AUG - 90	(222)	21:	11:	49.0	6 .572	N	60 .240	E	10	G	5.5	333	4040	36.33	7:07	P	CARLSBERG RIDGE	
26 - DEC - 91	(360)	11:	35:	56.2	54 .382	N	162 .521	E	29	D	5.5	213	7957	71.55	11:24	P	NEAR EAST COAST OF KAMCHATKA	

Table 3-7b. NEIC Parameters of Identified Events Sorted by Magnitude.

Date	D.o.Y.	Hr	Mn	Sec		Latitude deg.		Longitude deg.		Depth km		Mag	Azi deg.	Epicentral Distance km	Epicentral Distance deg.	Travel Time m:ss	Phase	Region	
29 - APR - 91	(119)	14:	43:	06.3		42 .515	N	43 .937	E	10	G	5.4	166	273	2.45	0:35	P	WESTERN CAUCASUS	
14 - SEP - 90	(257)	20:	40:	18.3		13 .382	N	51 .456	E	10	G	5.4	346	3046	27.39	5:50	P	EASTERN GULF OF ADEN	
09 - SEP - 90	(252)	02:	14:	51.0		56 .654	N	34 .395	W	10	G	5.4	137	5765	51.84	9:14	P	NORTH ATLANTIC OCEAN	
15 - AUG - 90	(227)	23:	08:	56.0		43 .757	N	143 .297	E	162	D	5.4	230	7637	68.68	10:51	P	HOKKAIDO, JAPAN REGION	
16 - JUL - 90	(197)	19:	45:	25.1		16 .365	N	120 .546	E	33	N	5.4	266	7652	68.81	11:04	P	LUZON, PHILIPPINE ISLANDS	
03 - MAY - 91	(123)	20:	19:	38.8		42 .683	N	43 .247	E	10	G	5.3	157	309	2.78	0:38	P	WESTERN CAUCASUS	
06 - JUL - 90	(187)	19:	34:	52.4		36 .861	N	49 .303	E	35	D	5.3	311	540	4.85	1:16	Pn	WESTERN IRAN	
10 - AUG - 92	(223)	13:	42:	34.9		36 .053	N	69 .706	E	111	D	5.3	274	2225	20.01	4:30	P	HINDU KUSH REGION, AFGHANISTAN	
15 - APR - 91	(105)	10:	48:	59.3		36 .340	N	71 .358	E	124	D	5.3	272	2355	21.18	4:30	P	AFGHANISTAN-USSR BORDER REGION	
22 - JUL - 90	(203)	11:	20:	09.6		16 .532	N	121 .045	E	33	N	5.3	266	7683	69.09	11:07	P	LUZON, PHILIPPINE ISLANDS	
16 - DEC - 90	(350)	15:	45:	40.7		41 .361	N	43 .715	E	33	N	5.2	148	161	1.45	0:21	P	TURKEY-USSR BORDER REGION	
03 - MAY - 91	(123)	23:	41:	01.8		42 .647	N	43 .263	E	11	D	5.2	157	305	2.74	0:39	P	WESTERN CAUCASUS	
18 - JUL - 90	(199)	11:	29:	24.9		36 .990	N	29 .595	E	17	D	5.2	80	1359	12.22	3:07	P	TURKEY	
07 - DEC - 91	(341)	14:	22:	32.2		25 .191	N	62 .974	E	30	D	5.2	309	2374	21.35	4:51	P	SOUTHWESTERN PAKISTAN	
20 - AUG - 91	(232)	08:	46:	40.5		37 .646	N	72 .150	E	135	D	5.2	268	2380	21.40	4:43	P	TAJIK SSR	
14 - AUG - 90	(226)	00:	50:	39.2		27 .024	N	65 .969	E	21	D	5.2	300	2438	21.93	4:56	P	PAKISTAN	
07 - SEP - 90	(250)	00:	12:	26.2		5 .443	N	31 .686	E	10	G	5.2	22	4072	36.62	7:09	P	SUDAN	
29 - AUG - 90	(241)	20:	44:	23.0		11 .791	N	95 .034	E	25	D	5.2	288	5830	52.43	9:15	P	ANDAMAN ISLANDS REGION	
02 - MAY - 91	(122)	01:	25:	30.1		42 .541	N	43 .960	E	10	G	5.1	167	275	2.47	0:32	P	WESTERN CAUCASUS	
06 - OCT - 91	(279)	01:	46:	47.5		41 .096	N	43 .409	E	18	D	5.0	134	154	1.39	0:24	P	GEORGIA-ARMENIA-TURKEY BORD REG	
03 - JUN - 91	(154)	10:	22:	40.4		40 .048	N	42 .859	E	28	D	5.0	87	159	1.43	0:13	P	TURKEY	
04 - JUL - 91	(185)	06:	26:	31.8		42 .387	N	44 .116	E	20	D	5.0	169	256	2.30	0:39	P	WESTERN CAUCASUS	
27 - MAR - 92	(087)	19:	21:	04.6		42 .456	N	43 .715	E	33	N	5.0	162	272	2.44	0:42	P	NORTHWESTERN CAUCASUS	
21 - MAY - 91	(141)	17:	37:	38.8		42 .867	N	48 .028	E	10	G	5.0	221	410	3.69	0:49	P	CASPIAN SEA	
07 - MAY - 92	(128)	19:	15:	02.3		38 .677	N	40 .130	E	10	G	5.0	69	427	3.84	1:15	P	TURKEY	
28 - DEC - 90	(362)	04:	03:	53.6		37 .106	N	49 .227	E	10	G	5.0	309	516	4.64	1:29	P	CASPIAN SEA	
08 - SEP - 91	(251)	10:	14:	58.8		36 .264	N	71 .324	E	133		5.0	272	2355	21.17	4:43	P	AFGHANISTAN-TAJIKISTAN BORD REG	
29 - APR - 91	(119)	11:	51:	10.3		42 .572	N	43 .816	E	10	G	4.9	165	281	2.53	0:34	P	WESTERN CAUCASUS	
15 - MAY - 91	(135)	14:	28:	50.1		42 .565	N	43 .349	E	14	D	4.9	157	294	2.64	0:36	P	WESTERN CAUCASUS	
01 - JAN - 91	(001)	19:	18:	56.4		39 .822	N	48 .439	E	61	D	4.9	275	318	2.86	0:48	P	N.W. IRAN-USSR BORDER REGION	
15 - FEB - 92	(046)	12:	52:	51.7	*	42 .803	N	46 .524	E	15	D	4.9	206	332	2.99	0:52	P	EASTERN CAUCASUS	
03 - SEP - 90	(246)	02:	40:	59.1		36 .409	N	70 .671	E	202	D	4.9	272	2294	20.63	4:27	P	HINDU KUSH REGION	
23 - JUL - 90	(204)	20:	54:	56.6		42 .719	N	45 .947	E	33	N	4.8	199	305	2.74	0:47	Pn	EASTERN CAUCASUS	
27 - JUL - 90	(208)	05:	31:	00.1		37 .318	N	49 .585	E	10	G	4.8	305	525	4.72	1:29	P	CASPIAN SEA	
21 - AUG - 90	(233)	03:	47:	26.2		37 .309	N	49 .685	E	10	G	4.8	305	533	4.79	1:30	P	CASPIAN SEA	
28 - JUN - 90	(179)	03:	20:	35.0		37 .085	N	49 .642	E	10	G	4.8	307	545	4.90	1:36	P	CASPIAN SEA	
01 - JUL - 90	(182)	12:	24:	57.2		37 .181	N	49 .885	E	10	G	4.8	305	555	4.99	1:35	P	CASPIAN SEA	
20 - AUG - 90	(232)	12:	20:	11.0	*	36 .956	N	49 .720	E	33	N	4.8	308	560	5.03	1:30	P	WESTERN IRAN	
10 - MAY - 91	(130)	20:	52:	27.3		42 .534	N	43 .986	E	10	G	4.7	167	274	2.46	0:32	P	WESTERN CAUCASUS	
29 - APR - 91	(119)	11:	10:	11.9		42 .584	N	43 .904	E	10	G	4.7	166	281	2.53	0:35	P	WESTERN CAUCASUS	
01 - DEC - 91	(335)	09:	17:	27.0		36 .373	N	45 .036	E	35	*	4.7	356	419	3.77	1:08	P	IRAN-IRAQ BORDER REGION	
01 - JUL - 90	(182)	21:	16:	48.3		37 .285	N	48 .820	E	10	G	4.7	310	476	4.28	1:29	P	CASPIAN SEA	
27 - DEC - 90	(361)	13:	26:	57.1		36 .539	N	48 .907	E	10	G	4.7	316	541	4.87	1:26	P	NORTHWESTERN IRAN	
28 - JUN - 90	(179)	03:	42:	01.9	*	37 .079	N	50 .147	E	10	G	4.7	304	581	5.22	1:39	P	CASPIAN SEA	
19 - JUN - 91	(170)	06:	40:	28.9		40 .282	N	42 .971	E	33	N	4.6	97	150	1.35	0:21	P	TURKEY	
16 - JUN - 91	(167)	11:	07:	10.6		39 .984	N	42 .875	E	26	D	4.6	85	158	1.42	0:15	P	TURKEY	
03 - MAY - 91	(123)	06:	08:	37.1		42 .482	N	43 .363	E	10	G	4.6	157	285	2.56	0:37	P	WESTERN CAUCASUS	
29 - APR - 91	(119)	10:	52:	42.2		42 .712	N	44 .102	E	10	G	4.6	170	291	2.62	0:32	P	WESTERN CAUCASUS	
10 - MAY - 91	(130)	01:	25:	15.6		42 .496	N	43 .153	E	10	G	4.6	154	294	2.64	0:40	P	WESTERN CAUCASUS	
24 - SEP - 90	(267)	06:	35:	13.9	*	38 .253	N	47 .951	E	10	G	4.6	306	348	3.13		P	NORTHWESTERN IRAN	<PC only>
01 - JUL - 90	(182)	17:	19:	44.1		37 .280	N	48 .818	E	10	G	4.6	310	476	4.28	1:30	P	CASPIAN SEA	
17 - JUL - 90	(198)	04:	02:	09.2		37 .137	N	49 .979	E	33	N	4.6	304	565	5.08	1:35	P	CASPIAN SEA	
13 - AUG - 90	(225)	06:	18:	25.1		36 .663	N	49 .884	E	35	*	4.6	309	592	5.33	1:37	P	WESTERN IRAN	
25 - OCT - 90	(298)	04:	52:	06.0	*	76 .243	N	8 .409	E	10	G	4.6	167	4382	39.41	?7:47	P	SVALBARD REGION	<within coda>

Table 3-7c. NEIC Parameters of Identified Events Sorted by Magnitude.

Date	D.o.Y.	Hr	Mn	Sec		Latitude deg.		Longitude deg.		Depth km	Mag	Azi deg.	Epicentral Distance km	Epicentral Distance deg.	Travel m:ss	Phase	Region
18 - FEB - 92	(049)	01:	39:	40.9	*	41 .477	N	43 .464	E	33 N	4.5	145	183	1.65	0:24	P	GEORGIA-ARMENIA-TURKEY BORD REG
30 - JUN - 91	(181)	20:	09:	18.3		42 .424	N	43 .688	E	10 G	4.5	162	269	2.42	0:47	P	WESTERN CAUCASUS
02 - MAY - 91	(122)	09:	44:	41.4		42 .507	N	43 .507	E	10 G	4.5	159	283	2.54	0:36	P	WESTERN CAUCASUS
29 - APR - 91	(119)	11:	59:	54.8		42 .625	N	43 .962	E	10 G	4.5	167	284	2.56	0:34	P	WESTERN CAUCASUS
22 - APR - 92	(113)	03:	03:	47.6	*	39 .557	N	39 .557	E	10 G	4.5	83	446	4.01	1:17	P	TURKEY
11 - JUL - 90	(192)	04:	36:	08.6	*	37 .015	N	49 .530	E	33 N	4.5	308	543	4.88	1:35	P	CASPIAN SEA
23 - FEB - 92	(054)	12:	03:	11.7	*	36 .391	N	49 .179	E	10 G	4.5	316	569	5.12	1:41	P	WESTERN IRAN
10 - OCT - 91	(283)	02:	44:	49.6		41 .399	N	43 .259	E	10 G	4.4	139	187	1.68	0:21	P	GEORGIA-ARMENIA-TURKEY BORD REG
05 - MAR - 92	(065)	03:	30:	16.1		38 .263	N	44 .974	E	33 N	4.4	354	209	1.88	0:31	P	TURKEY-IRAN BORDER REGION
10 - AUG - 91	(222)	08:	57:	51.8	*	40 .052	N	42 .153	E	10 G	4.4	88	219	1.97	0:46	P	TURKEY
17 - JUN - 91	(168)	03:	04:	45.5	*	42 .252	N	44 .222	E	10 G	4.4	170	239	2.15	0:32	P	WESTERN CAUCASUS
10 - MAY - 91	(130)	20:	30:	45.3		42 .627	N	43 .449	E	28 D	4.4	159	297	2.67	0:35	P	WESTERN CAUCASUS
27 - MAR - 91	(086)	22:	17:	55.0		40 .443	N	45 .443	E	33 N	4.3	240	70	0.63	-0:08	P	EASTERN CAUCASUS <early>
12 - NOV - 91	(316)	20:	35:	59.6	*	39 .306	N	44 .936	E	33 N	4.3	349	94	0.84	0:26	P	ARMENIA-AZERBAIJAN-IRAN BORD REG
02 - MAY - 91	(122)	02:	07:	31.6	?	41 .34	N	45 .17	E	10 G	4.3	196	139	1.25	0:45	P	EASTERN CAUCASUS
29 - APR - 91	(119)	11:	04:	28.9	*	42 .510	N	43 .816	E	10 G	4.3	164	275	2.47	0:35	P	WESTERN CAUCASUS
22 - SEP - 90	(265)	02:	46:	01.2	*	42 .538	N	46 .449	E	33 N	4.3	208	304	2.73	0:34	P	EASTERN CAUCASUS
05 - SEP - 91	(248)	19:	23:	04.8		38 .847	N	41 .417	E	10 G	4.3	64	318	2.86	0:48	P	TURKEY
22 - AUG - 90	(234)	07:	51:	49.5	*	37 .056	N	49 .327	E	10 G	4.3	309	526	4.73	1:33	P	CASPIAN SEA
27 - APR - 91	(117)	03:	31:	58.5	*	40 .093	N	43 .719	E	10 G	4.2	87	86	0.77	0:07	P	TURKEY-USSR BORDER REGION
08 - JUN - 91	(159)	01:	12:	01.8	*	41 .005	N	43 .563	E	33 N	4.2	135	138	1.24	0:12	P	TURKEY-USSR BORDER REGION
15 - FEB - 92	(046)	15:	18:	04.2	*	41 .434	N	46 .184	E	33 N	4.2	220	190	1.71	0:34	P	EASTERN CAUCASUS
03 - MAY - 91	(123)	06:	12:	54.2	?	41 .93	N	43 .80	E	33 N	4.2	159	214	1.93	0:41	P	TURKEY-USSR BORDER REGION
04 - MAY - 91	(124)	04:	53:	35.6	?	42 .15	N	43 .51	E	10 G	4.2	156	246	2.21	0:41	P	WESTERN CAUCASUS
20 - JUL - 90	(201)	17:	30:	36.2	?	42 .10	N	46 .77	E	33 N	4.2	217	278	2.50	0:50	P	EASTERN CAUCASUS
07 - MAY - 91	(127)	09:	01:	23.6	*	42 .606	N	43 .125	E	10 G	4.2	155	306	2.75	0:38	P	WESTERN CAUCASUS
15 - FEB - 92	(046)	13:	37:	40.1		42 .934	N	46 .548	E	33 N	4.2	205	346	3.11	0:49	P	EASTERN CAUCASUS
02 - AUG - 90	(214)	17:	12:	48.5	*	38 .540	N	48 .186	E	33 N	4.2	300	346	3.12	0:56	P	N.W. IRAN-USSR BORDER REGION
23 - DEC - 90	(357)	21:	28:	50.7	*	42 .115	N	44 .356	E	33 N	4.1	172	222	2.00	0:23	P	WESTERN CAUCASUS
02 - MAY - 91	(122)	02:	18:	00.1	*	42 .211	N	43 .906	E	10 G	4.1	164	241	2.17	0:32	P	WESTERN CAUCASUS
01 - MAY - 91	(121)	23:	19:	11.8	*	42 .719	N	44 .053	E	10 G	4.1	169	293	2.63	0:29	P	WESTERN CAUCASUS
02 - MAY - 91	(122)	09:	00:	35.2	*	42 .704	N	43 .692	E	10 G	4.1	164	298	2.68	0:33	P	WESTERN CAUCASUS
02 - AUG - 90	(214)	21:	17:	18.7	*	38 .398	N	48 .228	E	33 N	4.1	301	358	3.22	0:55	P	N.W. IRAN-USSR BORDER REGION
02 - MAY - 91	(122)	03:	42:	26.1	*	42 .608	N	43 .477	E	10 G	4.0	160	294	2.64	0:42	P	WESTERN CAUCASUS
15 - FEB - 92	(046)	13:	30:	32.0	*	42 .462	N	46 .493	E	33 N	4.0	209	298	2.68	0:54	P	EASTERN CAUCASUS
02 - MAY - 91	(122)	04:	30:	53.9	*	42 .481	N	43 .201	E	10 G	3.9	155	290	2.61	0:41	P	WESTERN CAUCASUS
24 - MAY - 91	(144)	07:	59:	38.8	*	42 .679	N	42 .908	E	10 G	3.9	152	321	2.89	0:26	P	WESTERN CAUCASUS
14 - MAY - 91	(134)	09:	36:	25.4	*	42 .609	N	43 .579	E	10 G	3.8	161	291	2.62	0:37	P	WESTERN CAUCASUS
26 - APR - 92	(117)	13:	15:	51.2	*	37 .663	N	47 .104	E	33 N	3.8	322	343	3.09	0:56	P	NORTHWESTERN IRAN
08 - DEC - 91	(342)	01:	02:	06.2	*	38 .335	N	48 .151	E	33 N	3.8	303	357	3.21	1:02	P	ARMENIA-AZERBAIJAN-IRAN BORD REG
04 - JUN - 91	(155)	00:	55:	16.3		40 .600	N	42 .989	E	10 G	3.7	110	156	1.40	0:16	P	TURKEY
27 - MAY - 91	(147)	03:	40:	45.5	?	42 .34	N	45 .86	E	10 G	3.7	201	263	2.37	0:26	P	EASTERN CAUCASUS

```
   LOG.G3       3-JUN-92   16:25:19     Rdgeos V10.02: GEOS Tape Log File

  Default  Chan 1  Chan 2  Chan 3  Chan 4  Chan 5  Chan 6
    G3     G3A(4)  G3A(5)  G3A(6)  G3B(4)  G3B(5)  G3B(6)

Experiment    Location    Serial No.    Year
     28           3            5         1991

File Evt    Type          Time & Standard    Corr   DR100 name   Duration  Srate Pre-event Volts Trg ch   STA    LTA  Ratio

  1    1  Sensor Cal  121:14:47:27.382 EXT.  0.000 1211447Jn.G3    00:37   1200.     2.06 None
                                             Ch 1: VEL, 54 dB,  50 Hz | Ch 2: VEL, 54 dB,  50 Hz | Ch 3: VEL, 54 dB,  50 Hz |
                                             Ch 4: VEL, 54 dB,  50 Hz | Ch 5: VEL, 54 dB,  50 Hz | Ch 6: VEL, 54 dB,  50 Hz |

 ***  506 null values filled in
  2    2  Amp Calib   121:14:48:15.683 EXT.  0.000 1211448Fn.G3    00:41   1200.     2.06 None
                                             Ch 1: VEL, 54 dB,  50 Hz | Ch 2: VEL, 54 dB,  50 Hz | Ch 3: VEL, 54 dB,  50 Hz |
                                             Ch 4: VEL, 54 dB,  50 Hz | Ch 5: VEL, 54 dB,  50 Hz | Ch 6: VEL, 54 dB,  50 Hz |

File    Clock event   Clock time & Standard     Old Time & Standard                  - - - Internal/External Skew - - -
  3     VB Synch TMO 121:14:55:35.717  NONE
  4     WWVB Corr.   121:14:56:44.000  NONE                          0.001  0.000  0.000  0.000  0.001  0.000  0.000  0.000
                                                                    Mean: 0.000    Std. dev:      1.225  Corr: 0.000
  5     VB Synch TMO 121:18:05:35.750  NONE
  6     VB Synch TMO 121:21:15:35.816  NONE

File Evt    Type          Time & Standard    Corr   DR100 name   Duration  Srate Pre-event Volts Trg ch   STA    LTA  Ratio

  7    3  Trigger     121:23:19:44.228 EXT.  0.000 1212319On.G3    00:26   1200.     2.06  26.66    1     0.4    20.  2**3
                                             Ch 1: VEL, 54 dB,  50 Hz | Ch 2: VEL, 54 dB,  50 Hz | Ch 3: VEL, 54 dB,  50 Hz |
                                             Ch 4: VEL, 54 dB,  50 Hz | Ch 5: VEL, 54 dB,  50 Hz | Ch 6: VEL, 54 dB,  50 Hz |

File    Clock event   Clock time & Standard     Old Time & Standard                  - - - Internal/External Skew - - -
  8     VB Synch TMO 122:00:25:35.889  NONE

File Evt    Type          Time & Standard    Corr   DR100 name   Duration  Srate Pre-event Volts Trg ch   STA    LTA  Ratio

  9    4  Trigger     122:01:26:00.618 EXT.  0.000 1220126An.G3    03:27   1200.     2.06  26.94    1     0.4    20.  2**3
                                             Ch 1: VEL, 54 dB,  50 Hz | Ch 2: VEL, 54 dB,  50 Hz | Ch 3: VEL, 54 dB,  50 Hz |
                                             Ch 4: VEL, 54 dB,  50 Hz | Ch 5: VEL, 54 dB,  50 Hz | Ch 6: VEL, 54 dB,  50 Hz |

 10    5  Trigger     122:02:08:17.838 EXT.  0.000 1220208Fn.G3    00:26   1200.     2.06  26.94    1     0.4    20.  2**3
                                             Ch 1: VEL, 54 dB,  50 Hz | Ch 2: VEL, 54 dB,  50 Hz | Ch 3: VEL, 54 dB,  50 Hz |
                                             Ch 4: VEL, 54 dB,  50 Hz | Ch 5: VEL, 54 dB,  50 Hz | Ch 6: VEL, 54 dB,  50 Hz |

 11    6  Trigger     122:02:18:31.458 EXT.  0.000 1220218Kn.G3    01:42   1200.     2.06  26.94    1     0.4    20.  2**3
                                             Ch 1: VEL, 54 dB,  50 Hz | Ch 2: VEL, 54 dB,  50 Hz | Ch 3: VEL, 54 dB,  50 Hz |
                                             Ch 4: VEL, 54 dB,  50 Hz | Ch 5: VEL, 54 dB,  50 Hz | Ch 6: VEL, 54 dB,  50 Hz |

 12    7  Trigger     122:02:29:34.222 EXT.  0.000 1220229Ln.G3    00:28   1200.     2.06  26.82    1     0.4    20.  2**3
                                             Ch 1: VEL, 54 dB,  50 Hz | Ch 2: VEL, 54 dB,  50 Hz | Ch 3: VEL, 54 dB,  50 Hz |
                                             Ch 4: VEL, 54 dB,  50 Hz | Ch 5: VEL, 54 dB,  50 Hz | Ch 6: VEL, 54 dB,  50 Hz |

File    Clock event   Clock time & Standard     Old Time & Standard                  - - - Internal/External Skew - - -
 13     WWVB Corr.   122:02:57:52.004  NONE                           0.004  0.004  0.004  0.004  0.004  0.004  0.004  0.004
                                                                    Mean: 0.004    Std. dev:      0.000  Corr: 0.004
 14     VB Synch TMO 122:03:35:35.959  NONE

   LOG.G3       3-JUN-92   16:25:19     Rdgeos V10.02: GEOS Tape Log File

File Evt    Type          Time & Standard    Corr   DR100 name   Duration  Srate Pre-event Volts Trg ch   STA    LTA  Ratio

 15    8  Trigger     122:03:43:07.589 EXT.  0.004 1220343Cn.G3    00:16   1200.     2.06  26.90    1     0.4    20.  2**3
                                             Ch 1: VEL, 54 dB,  50 Hz | Ch 2: VEL, 54 dB,  50 Hz | Ch 3: VEL, 54 dB,  50 Hz |
                                             Ch 4: VEL, 54 dB,  50 Hz | Ch 5: VEL, 54 dB,  50 Hz | Ch 6: VEL, 54 dB,  50 Hz |

 16    9  Trigger     122:04:31:33.992 EXT.  0.004 1220431Ln.G3    01:21   1200.     2.06  26.94    1     0.4    20.  2**3
                                             Ch 1: VEL, 54 dB,  50 Hz | Ch 2: VEL, 54 dB,  50 Hz | Ch 3: VEL, 54 dB,  50 Hz |
                                             Ch 4: VEL, 54 dB,  50 Hz | Ch 5: VEL, 54 dB,  50 Hz | Ch 6: VEL, 54 dB,  50 Hz |

 17   10  Trigger     122:06:26:54.759 EXT.  0.004 1220626Sn.G3    00:18   1200.     2.06  26.99    1     0.4    20.  2**3
                                             Ch 1: VEL, 54 dB,  50 Hz | Ch 2: VEL, 54 dB,  50 Hz | Ch 3: VEL, 54 dB,  50 Hz |
                                             Ch 4: VEL, 54 dB,  50 Hz | Ch 5: VEL, 54 dB,  50 Hz | Ch 6: VEL, 54 dB,  50 Hz |

File    Clock event   Clock time & Standard     Old Time & Standard                  - - - Internal/External Skew - - -
 18     VB Synch TMO 122:06:45:36.042  NONE

File Evt    Type          Time & Standard    Corr   DR100 name   Duration  Srate Pre-event Volts Trg ch   STA    LTA  Ratio

 19   11  Trigger     122:07:54:04.183 EXT.  0.004 1220754Bn.G3    00:54   1200.     2.06  26.96    1     0.4    20.  2**3
                                             Ch 1: VEL, 54 dB,  50 Hz | Ch 2: VEL, 54 dB,  50 Hz | Ch 3: VEL, 54 dB,  50 Hz |
                                             Ch 4: VEL, 54 dB,  50 Hz | Ch 5: VEL, 54 dB,  50 Hz | Ch 6: VEL, 54 dB,  50 Hz |

 20   12  Trigger     122:09:01:07.788 EXT.  0.004 1220901Cn.G3    02:11   1200.     2.06  26.94    1     0.4    20.  2**3
                                             Ch 1: VEL, 54 dB,  50 Hz | Ch 2: VEL, 54 dB,  50 Hz | Ch 3: VEL, 54 dB,  50 Hz |
                                             Ch 4: VEL, 54 dB,  50 Hz | Ch 5: VEL, 54 dB,  50 Hz | Ch 6: VEL, 54 dB,  50 Hz |

 21   13  Trigger     122:09:45:18.411 EXT.  0.004 1220945Gn.G3    02:13   1200.     2.06  26.93    1     0.4    20.  2**3
                                             Ch 1: VEL, 54 dB,  50 Hz | Ch 2: VEL, 54 dB,  50 Hz | Ch 3: VEL, 54 dB,  50 Hz |
                                             Ch 4: VEL, 54 dB,  50 Hz | Ch 5: VEL, 54 dB,  50 Hz | Ch 6: VEL, 54 dB,  50 Hz |

File    Clock event   Clock time & Standard     Old Time & Standard                  - - - Internal/External Skew - - -
 22     VB Synch TMO 122:09:55:36.110  NONE

File Evt    Type          Time & Standard    Corr   DR100 name   Duration  Srate Pre-event Volts Trg ch   STA    LTA  Ratio

 23   14  Trigger     122:11:58:09.178 EXT.  0.004 1221158Dn.G3    00:35   1200.     2.06  26.94    1     0.4    20.  2**3
                                             Ch 1: VEL, 54 dB,  50 Hz | Ch 2: VEL, 54 dB,  50 Hz | Ch 3: VEL, 54 dB,  50 Hz |
                                             Ch 4: VEL, 54 dB,  50 Hz | Ch 5: VEL, 54 dB,  50 Hz | Ch 6: VEL, 54 dB,  50 Hz |

*** No. files processed:   23. ***
```

Figure 3-1a. Log-file of G3 tape #28.

```
   LOG.G1      18-MAR-91   12:52:21     PCGEOS V04.07: GEOS Tape Log File

  Default  Chan 1  Chan 2  Chan 3  Chan 4  Chan 5  Chan 6
    G1     G1A(4)  G1A(5)  G1A(6)  G1B(4)  G1B(5)  G1B(6)

 ** Corrupted first GEOS header.  Use header file —>..\..\G1.GHD
**
 ** 2 time cell errors detected **
 ** Corrupted first GEOS header.  Use header file —>..\..\G1.GHD
**
 ** 1 time cell errors detected **
 ** Corrupted first GEOS header.  Use header file —>..\..\G1.GHD
**
 ** 2 time cell errors detected **

Experiment    Location    Serial No.    Year
      0           0           99         1990

File Evt    Type          Time & Standard    Corr   DR100 name   Duration  Srate Pre-event Volts Trg ch   STA    LTA  Ratio
  3    1  Trigger     183:07:50:43.264 WWVB   .000 1830750On.G1    00:16   1200.     2.06  20.00    4      .5    10.  2**3
                                            Ch 1: VEL, 54 dB,  50 Hz | Ch 2: VEL, 54 dB,  50 Hz | Ch 3: VEL, 54 dB,  50 Hz |
                                            Ch 4: VEL, 54 dB,  50 Hz | Ch 5: VEL, 54 dB,  50 Hz | Ch 6: VEL, 54 dB,  50 Hz |

Experiment    Location    Serial No.    Year
      0           1           43         1990
  4    2  Trigger     183:08:17:20.104 MAN.   .000 1830817Gn.G1    00:16   1200.     2.06  24.38    1      .4    20.  2**3
                                            Ch 1: VEL, 60 dB,  50 Hz | Ch 2: VEL, 60 dB,  50 Hz | Ch 3: VEL, 60 dB,  50 Hz |
                                            Ch 4: VEL, 60 dB,  50 Hz | Ch 5: VEL, 60 dB,  50 Hz | Ch 6: VEL, 60 dB,  50 Hz |

File    Clock event   Clock time & Standard     Old Time & Standard                  - - - Internal/External Skew - - -
  5     Master Synch 183:08:26:00.000  EXT.     0:00:00:**.007 WWVB      .000   .000   .000   .000   .000   .000   .000   .000
                                                                        Mean:  .000    Std. dev:       .000  Corr:  .000

File Evt    Type          Time & Standard    Corr   DR100 name   Duration  Srate Pre-event Volts Trg ch   STA    LTA  Ratio
  6    3  Trigger     183:08:28:23.031 EXT.   .000 1830828Hn.G1    00:24   1200.     2.06  24.30    1      .4    20.  2**3
                                            Ch 1: VEL, 60 dB,  50 Hz | Ch 2: VEL, 60 dB,  50 Hz | Ch 3: VEL, 60 dB,  50 Hz |
                                            Ch 4: VEL, 60 dB,  50 Hz | Ch 5: VEL, 60 dB,  50 Hz | Ch 6: VEL, 60 dB,  50 Hz |
```

Figure 3-1b. Log-file of G1 tape #03.

```
   LOG.G1      02-APR-91   16:57:22     PCGEOS V04.07: GEOS Tape Log File

  Default  Chan 1  Chan 2  Chan 3  Chan 4  Chan 5  Chan 6
    G1     G1A(4)  G1A(5)  G1A(6)  G1B(4)  G1B(5)  G1B(6)


File    Clock event   Clock time & Standard     Old Time & Standard                  - - - Internal/External Skew - - -
  1     Master Synch 261:08:57:00.000  EXT.   ***:**:**:**.000 NONE      .090   .090   .090   .090   .090   .090   .090   .090
                                                                        Mean:  .090    Std. dev:       .000  Corr:  .090
  2     WWVB Corr.   261:08:58:39.000  EXT.                               .000   .000   .000   .000   .000   .000   .000   .000
                                                                        Mean:  .000    Std. dev:       .000  Corr:  .000
  3     WWVB Corr.   261:11:59:47.000  EXT.                               .000   .000   .000   .000   .000   .000   .000   .000
                                                                        Mean:  .000    Std. dev:       .000  Corr:  .000

Experiment    Location    Serial No.    Year
      0           1         3096         1990

File Evt    Type          Time & Standard    Corr   DR100 name   Duration  Srate Pre-event Volts Trg ch   STA    LTA  Ratio
  4    1  Continuous  261:12:33:00.878 EXT.   .000 2611233An.G1    00:18   1200.     2.06  26.30
                                            Ch 1: VEL, 54 dB,  50 Hz | Ch 2: VEL, 54 dB,  50 Hz | Ch 3: VEL, 54 dB,  50 Hz |
                                            Ch 4: VEL, 54 dB,  50 Hz | Ch 5: VEL, 54 dB,  50 Hz | Ch 6: VEL, 54 dB,  50 Hz |

File    Clock event   Clock time & Standard     Old Time & Standard                  - - - Internal/External Skew - - -
  5     Master Synch 261:14:20:00.000  EXT.     0:00:00:**.003 MAN.      .000   .000   .000   .000   .000   .000   .000   .000
                                                                        Mean:  .000    Std. dev:       .000  Corr:  .000
  6     WWVB Corr.   261:14:22:45.000  EXT.                               .000   .001   .000   .000   .000   .000   .000   .000
                                                                        Mean:  .000    Std. dev:       .935  Corr:  .000
```

Figure 3-1c. Log-file of G1 tape #22.

```
   LOG.G2      04-APR-91   13:04:07     PCGEOS V04.07: GEOS Tape Log File

  Default  Chan 1  Chan 2  Chan 3  Chan 4  Chan 5  Chan 6
    G2     G2A(4)  G2A(5)  G2A(6)  G2B(4)  G2B(5)  G2B(6)


Experiment    Location    Serial No.    Year
      6           2           3          1990                          .002   .999   .999   .999   .999   .999   .999   .999
                                                                        Mean:  .999    Std. dev:      2.806  Corr:  .999

File Evt    Type          Time & Standard    Corr   DR100 name   Duration  Srate Pre-event Volts Trg ch   STA    LTA  Ratio
  1    1  Trigger     186:13:27:20.632 EXT.  -.001 1861327Gn.G2    00:16   1200.     2.06  32.75    4      .7    30.  2**3
                                            Ch 1: VEL, 54 dB,  50 Hz | Ch 2: VEL, 54 dB,  50 Hz | Ch 3: VEL, 54 dB,  50 Hz |
                                            Ch 4: VEL, 54 dB,  50 Hz | Ch 5: VEL, 54 dB,  50 Hz | Ch 6: VEL, 54 dB,  50 Hz |
  2    2  Trigger     186:13:43:35.032 EXT.  -.001 1861343Ln.G2    00:19   1200.     2.06  32.75    4      .7    30.  2**3
                                            Ch 1: VEL, 54 dB,  50 Hz | Ch 2: VEL, 54 dB,  50 Hz | Ch 3: VEL, 54 dB,  50 Hz |
                                            Ch 4: VEL, 54 dB,  50 Hz | Ch 5: VEL, 54 dB,  50 Hz | Ch 6: VEL, 54 dB,  50 Hz |

File    Clock event   Clock time & Standard     Old Time & Standard                  - - - Internal/External Skew - - -
  3     VB Skew TMO  186:13:54:29.043  NONE
  4     WWVB Corr.   186:14:20:23.849  NONE                              .849   .849   .849   .849   .849   .849   .849   .849
                                                                        Mean:  .849    Std. dev:       .000  Corr:  .849

File Evt    Type          Time & Standard    Corr   DR100 name   Duration  Srate Pre-event Volts Trg ch   STA    LTA  Ratio
  5    3  Trigger     186:15:04:59.974 EXT.  -.151 1861504Tn.G2    05:42   1200.     2.06  32.75    4      .7    30.  2**3
                                            Ch 1: VEL, 54 dB,  50 Hz | Ch 2: VEL, 54 dB,  50 Hz | Ch 3: VEL, 54 dB,  50 Hz |
                                            Ch 4: VEL, 54 dB,  50 Hz | Ch 5: VEL, 54 dB,  50 Hz | Ch 6: VEL, 54 dB,  50 Hz |
```

Figure 3-1d. Log-file of G2 tape #06.

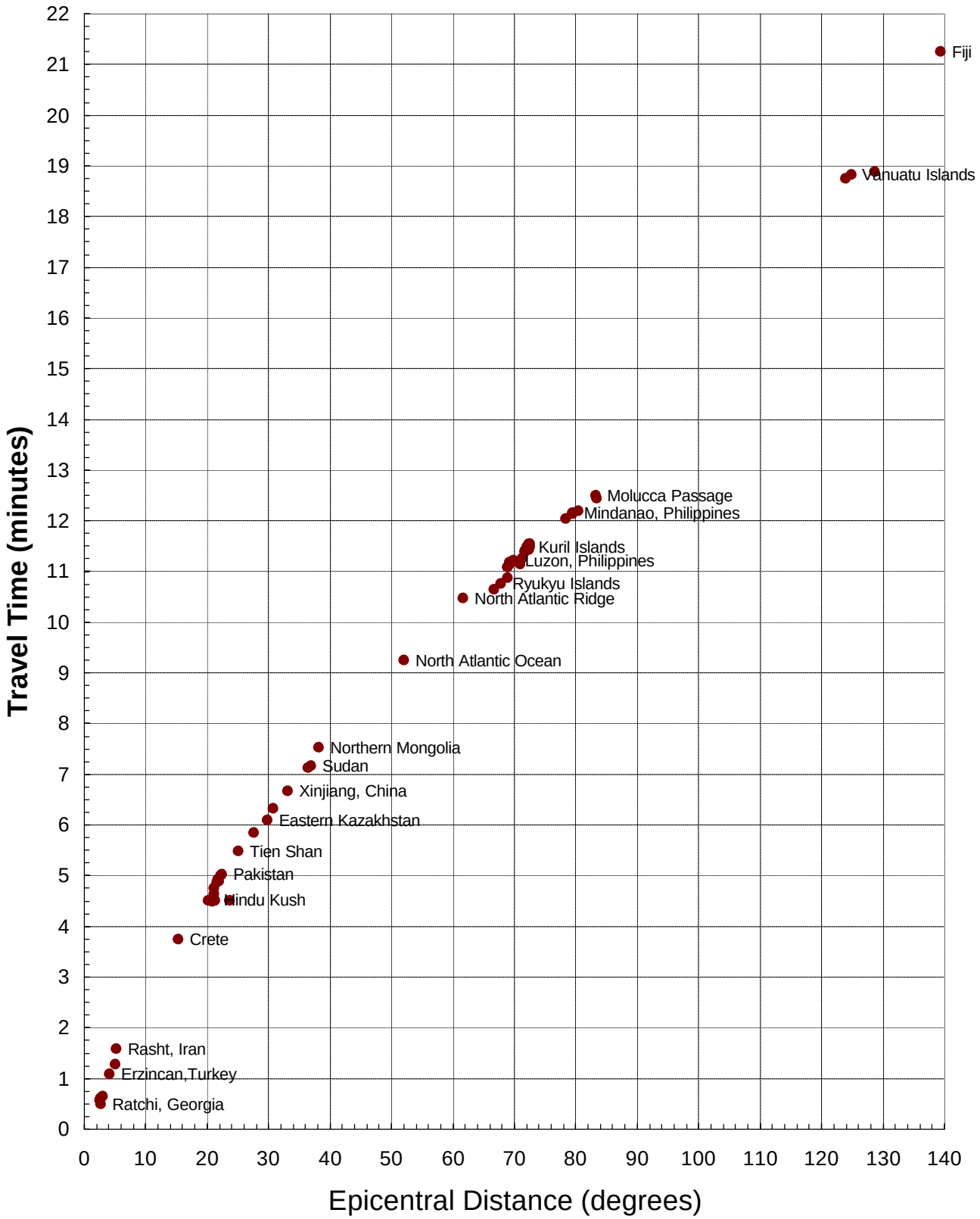

Figure 3-2. Identified Teleseismic Triggers.

Plots of GEOS records for events

at five or more sensor locations

from 26 June 1990 through 10 August 1992

Plots not available in PDF-file.

CHAPTER IV

A PC-Based Seismic System for Armenia

W. H. K. Lee and E. Cranswick,
(U. S. Geological Survey)

R. Banfill
(Small Systems Support, Big Water, Utah)

INTRODUCTION

Personal-computer-based seismic systems are playing an increasing role in seismic data acquisition and processing. In the past the computer used was usually a mini-computer with specialized hardware and software (costing hundreds of thousands of dollars, and taking several weeks to install). Because personal computers (PCs) are now inexpensive, a PC-based seismic system can be implemented for as little as $5,000 and requires less than one hour to install.

A PC-based seismic system expects multiple channels of analog signals (either hard-wired or telemetered) as inputs. The analog signals are usually a few volts in amplitude (peak-to-peak), and will be digitized at a prescribed sampling rate. The system records the digital data either continuously or by event trigger.

THE PC-QUAKE SYSTEM

The PC-Quake system (Lee, 1989) is a general-purpose seismic system, with the following characteristics:

(1) Uses IBM-compatible 286, 386sx, 386, or 486 PCs with an 8-MHz AT bus.

(2) Uses analog-to-digital (A/D) boards (DT 282x series) made by Data Translation, Inc.

(3) Digitizes 16 analog channels (upgradable to 128 channels) at user selectable rate.

(4) Digitizes up to a few thousand samples per second per channel.

(5) Displays digitized data continuously and in real time.

(6) Saves digitized data continuously or by event triggering.

(7) Automatically picks P-arrivals and locates events.

(8) Offline analysis includes manual picking, filtering, FFT, and coda Q.

(9) Channel to digitize, or display, or trigger is user selectable.

Readers are referred to Lee and Dodge (1992) for more detail.

A PC-BASED SEISMIC SYSTEM FOR ARMENIA

In 1990, a PC-Quake system was implemented in Armenia. This system consists of two identical IBM-compatible 286 PCs with 12-bit, 16-channel A/D boards made by Data Translation. One PC is used for on-line data acquisition and the other PC is used for off-line data processing and analysis. The two PCs are linked by a high-speed local area network (LANtastic kit by Artisoft), and an optical WORM drive (IBM 3363) is used to archive the digitized data on 200-megabyte removable cartridges. The off-line PC also serves as a backup to the on-line unit. A multiplexer could be used to increase the number of channels to a maximum of 256 channels for the 12-bit A/D board (or 64 channels for a 16-bit A/D board).

Table 4-1 lists the events recorded on the PC system from 21 September 1990 through 1 January 1991. For those events simultaneously recorded on the GEOS systems the GEOS event

name is indicated. Magnitudes as found in the USGS's National Earthquake Information Center's (NEIC's) monthly Preliminary Determination of Epicenters, Arefiev *et al*. (1991), or as determined in Chapter V of this report are also provided. Note that PC trigger times are based on the relatively inaccurate PC internal clock that drift by several seconds per day.

Plots of the PC-XDETECT records follow this chapter. Start-of-record times are indicated on the upper left corner of each plot page (*e.g.* 09/21/90 07:15 30.359). The plots show the IRIG time signal, ten vertical components (G1AZ to G5BZ), the horizontal components from G1A and G4A (G1AN, G1AE, G4AN, and G4AE), and the sine-wave trigger signal that is activated by a multi-component algorithm. "N" and "E" components are nominally north and east; refer to Table 2-1 for their true orientations. Peak digital counts and relative component scaling factors are indicated at the left of each trace. The time scale shown at the bottom of the page is in seconds. Long events can appear as multiple records across several pages.

Table 4-1. Events Recorded by the PC-XDETECT System.

PC Trigger Time				GEOS Event	Magnitude
day	hr	mn	sec	day hr mn	
264	07	15	30.359		1.2
265	02	46	27.049	2650246	4.3
267	06	36	05.487		4.6
278	07	55	09.042	2780757	
282	20	53	57.755		0.8
288	07	46	41.022	2880749	0.9
288	18	39	27.696	2881842	1.7
291	11	18	33.428	2911121	2.3
292	13	57	52.289	2921401	
300	05	44	32.206	3000549	3.0
312	19	29	39.690	3121935	
312	20	37	18.465		1.6
320	06	53	07.991	3200659	1.8
320	07	03	03.516	3200709	1.8
320	14	53	36.909	3201500	2.2
320	14	59	19.400		
325	12	24	02.742	3251224	
345	08	23	13.789	3450823	
349	09	38	49.638	3490939	
349	10	38	12.568	3491038	3.3
349	15	40	52.267	3491541	
350	15	45	43.419	3501546	5.2
351	01	16	40.201	3510116	
351	17	42	49.379	3511742	
354	13	02	22.628	3541304	3.5
357	21	27	09.430	3572129	4.1
359	13	18	53.218	3591320	
360	10	27	22.928	3601029	
363	11	52	03.405	3631154	
001	19	17	34.945	0011919	4.9

PC trigger times are much less accurate than the GEOS times. Magnitudes above 4 are M_B from NEIC Monthly Listings. Other magnitudes above 3 are from Arefiev *et al.*, 1991. Smaller magnitudes are M_L from Chapter V of this report.

Plots of PC-XDETECT records

from 21 September 1990 through 01 January 1991

Plots not available in PDF-file.

CHAPTER V

Near-Surface Measurements of P- and S-Wave Velocities from the Dense Three-Dimensional Array near Garni, Armenia

J. Mori, J. Filson, E. Cranswick, R. D. Borcherdt, G. Glassmoyer, and W. H. K. Lee,
(U. S. Geological Survey)

R. Amirbekian, V. Aharonian
(Yerevan Seismic Station)

L. Hachverdian
(Armenian Academy of Sciences)

ABSTRACT

P- and S-wave arrivals from local earthquakes were studied using an array of ten three-component instruments in and around a tunnel at Garni Observatory, Armenia. The array has a three-dimensional configuration with lateral dimensions of 300 to 500 m and a depth extent of 100 m. Estimates of the horizontal and vertical components of slowness for P and S wavefronts were used to determine the angles of approach and the propagation velocity. The results show that the region around the array has low average velocities for both P (1.43 km/sec) and S (0.61 km/sec) waves, so wavefronts approach the array at steep angles of incidence. Waveforms from one event show clear reflections from the free surface for both P and S waves. The timing of these reflections gives the velocity variation with depth within the array. We estimate a P-wave velocity of 0.33 km/sec within a few meters of the surface increasing to 6.0 km/sec for the deepest portion of the array. Local site variations can greatly complicate the high-frequency waveforms even for tunnel stations in bedrock. The S waves exhibit stronger site-dependent waveforms and time delays than do the P waves.

INTRODUCTION

An array of ten three-component instruments was installed in and around a 200 meter horizontal tunnel (Figure 5-1) at Garni Observatory, Armenia (40.136^{o}N, 44.724^{o}E). The Garni array is located on the lower southwestern slope of Mt. Azhdahak in the Gegham Range of central Armenia. Mt. Azhdahak is a Cenozoic volcanic center with layered tuffs dominating the geology near the tunnel. With horizontal spacings of 60 to 480 meters and vertical spacings of 14 to 100 meters, this dense array provides one of the few opportunities to record three-components of ground motion in a three-dimensional array. We have used these data to make measurements of the three-dimensional slowness for incoming P and S arrivals from eleven earthquakes at distances of 10 to 60 km. These three-dimensional slowness estimates are useful because they show the angle of incidence with which the wavefront approaches the array and also directly give the velocity of the material in the region of the array. The predominant frequencies of the data used in this study are from 3 to 20 Hz which correspond to wavelengths of 90 to 570 meters for the P wave and 30 to 170 meters for the S wave. The instrument spacing is comparable to these wavelengths, so we are able to accurately map wavefronts as they pass through the upper 100 meters of the near-surface material.

The first part of this paper treats the data as single incoming wavefronts and we estimate the directions of approach and the average propagation velocity across the array. The second part of the paper looks at one specific detail of the waveforms, the free-surface reflections. The relative arrival time of the reflection as a function of station depth gives more information about the depth dependent velocity variation within the array.

DATA

The data for this study were recorded by 1 Hz (Mark Products L4C) velocity transducers both on a triggered IBM-compatible personal computer (PC) system at 200 samples/second/channel with 12-bit resolution (Tottingham and Lee, 1989) and on the General Earthquake Observations System

(GEOS) recorders (Borcherdt *et al*., 1985) at 200 samples/second/channel with 16-bit resolution. The PC system recorded all ten vertical and four horizontal components with a common time base. The five GEOS instruments recorded the complete three-component data for all ten sites. Comparisons between the two systems show spectral coherence above 0.9 in the frequency range of 1 to 50 Hz. The P-wave data used in this study were primarily taken from the PC system. The S-wave data were taken from horizontal components recorded by the GEOS system.

We studied eleven earthquakes recorded by the array from September through November 1990 (Table 5-1). Approximate hypocentral distances (km) were determined by multiplying the S-P time (seconds) by 7.8. Magnitudes were determined by convolving a Wood-Anderson instrument response with the data to produce equivalent Wood-Anderson amplitudes (Kanamori and Jennings, 1978). Amplitudes from all the available horizontal components (four to twenty per event) were used with the Richter (1937) distance correction to obtain the magnitudes. Based on the similarity of the waveforms and the relative arrival times, three of the earthquakes were located closely together at a hypocentral distance of about 12 km, nearly under the array (events 4, 5, and 8 in Table 5-1). Another two events (9,10), located 20 km to the east, also have similar hypocenters. The remaining 6 earthquakes arrived from a wide spread of azimuths (Table 5-1).

Figure 5-2 shows an example of the data for event 11. The P waves show similar impulsive waveforms across the array that are well suited for timing arrivals. The S waves on the horizontal components are also fairly clear, although some procedure of waveform matching is needed to accurately estimate arrival times. There are significant differences both in waveform and amplitude among these sites, which are located within a few hundred meters of each other. Differences in site response for closely spaced stations have also been noted at other arrays, such as in New York state (Menke *et al.*, 1990) and southern California (Vernon *et al.*, 1991; Mori, 1993). These site-response characteristics, especially for the S wave, are an indication of the problems that will be encountered in studying coherent wavefronts across the array.

THREE-DIMENSIONAL SLOWNESS MEASUREMENTS

For a plane wave traveling across a three-dimensional array of stations, the arrival time (t_i) at station *i* can be written as,

$$t_i = S_x x_i + S_y y_i + S_z z_i ,$$

where S_x, S_y, S_z are the three components of slowness and x_i, y_i, z_i are the spatial coordinates of the *i* th station. With arrival times measured at four or more sites distributed in space, the slowness in three dimensions can be determined. For the data used in this study, we determine the slowness vector using a grid search method that tests the correlation of the waveform data for each value of the three-component slowness. This is a three-dimensional extension of the two-dimensional method used by Frankel *et al.* (1991) to study apparent velocities with a small aperture array. The procedure used in this study consists of:

1. Calculating the relative arrival times at each station for the given value of slowness.
2. Shifting the waveforms by these time lags.
3. Calculating the cross correlation of each pair of stations and summing the values. For 10 arrivals, this involved 45 cross correlations.

The combined cross correlation for all the station pairs is a measure of how well the relative arrival times fit the given value of slowness. In this manner we searched for the three components of slowness that that give the highest correlation of the waveforms. After determining the slowness vector, the back azimuth (ϕ) to the event is,

$$\phi = \arctan(S_x/S_y) \ .$$

The incoming angle of incidence (θ) from vertical is,

$$\theta = \arctan((S_x^2 + S_y^2)^{1/2} / S_z) \ .$$

The apparent velocity (V_a) is,

$$V_a = 1/(S_x^2 + S_y^2)^{1/2} \ .$$

The material velocity (V_o) is,

$$V_o = 1/(S_x^2 + S_y^2 + S_z^2)^{1/2} \ .$$

We used time windows of 0.5 sec for the P wave and 0.7 sec for the S wave to compute cross correlations. The slowness was tested in increments of 0.03 sec/km. An example of the grid search for the P-wave window of the event recorded at 1500 on 11/16/90 is shown in Figure 5-3. The contoured values of the combined correlation are shown for horizontal and vertical slices out of the three-dimensional slowness space that was searched. The contour interval is 0.05. The highest values of the correlation for the P wave (shaded areas) show an incoming wavefront with a horizontal slowness of 0.12 sec/km (corresponding to an apparent velocity of 8.3 km/sec) moving toward the southwest in the horizontal slice. In the vertical slice the P wave is approaching the surface at an incidence angle of 11 degrees with a total slowness of 0.64 sec/km (P-wave velocity of 1.56 km/sec). The S-wave window (Figure 5-4) shows a wavefront of similar orientation moving with a horizontal slowness of 0.30 sec/km (apparent velocity of 3.3 km/sec) in the horizontal slice and total slowness of 1.71 sec/km (S-wave velocity of 0.58 km/sec) in the vertical slice.

In the horizontal slices, the contours are elongated in the east-west direction, indicating that there is better resolution for the north-south slowness than for the east-west slowness. This is due to the geometry of the array. The stations tend to be lined up in the direction along the axis of the tunnel, so that there is good station spacing in the north-south direction and more limited distribution of stations in the east-west direction. The contours in the vertical slice show contours that are elongated in the vertical direction, which is also probably due to station geometry. Since the vertical extent of the array is only 100 meters compared to the larger horizontal extent of 300-500 meters, there is a better constraint on the horizontal slowness compared to the vertical slowness. Another reason for poorer resolution in the vertical direction could be due to strong velocity variations as a function of depth.

In addition to the grid search method described above, we checked our results by picking the onset times and directly determined the slowness using a least-squares fit to the arrival times. In

general the two methods give consistent results. The advantage of the more tedious grid search method is that the cross correlations look at a larger portion of the waveform and are particularly useful for emergent P and S waves, where it is difficult to accurately pick the onset of the arrival. Also, searching through the whole slowness space shows the range of values that is consistent with the data and is useful for identifying directions from which secondary energy is arriving across the array.

SLOWNESS RESULTS

Using the grid search method, we determined the P-wave slowness for the eleven earthquakes and also the S-wave slowness for six earthquakes. There were incomplete horizontal data to determine S-wave slowness for the other five events. The cross correlation values generally have well-defined maxima, giving good estimates of the horizontal and vertical slowness.

For the P waves, the results presented in Table 5-1 show a large spread of incoming azimuths with steep incidence angles. 6 of the events (1, 4, 5, 7, 8, and 11) have large apparent velocities (>10 km/sec), indicating relatively deep earthquakes with raypaths to the array that take-off upward from the source. The other events, even to a distance of greater than 60 km, also have steep incidence angles (< 20 degrees) which is an indication of low-velocity material in the near-surface region. The low-velocity material will bend the ray paths toward the vertical as they approach the surface. One consistent result for all events is the P-wave velocity for the region near the array. For the wide range of incoming azimuths the estimates for the P-wave velocity had a standard deviation of 15%. The average velocity was determined to be 1.43 ± 0.22 km/sec. The stated uncertainty is one standard deviation.

For the S waves, the north and east horizontal components were rotated into a transverse direction assuming the back-azimuth obtained from the P wave, before the cross correlation procedure was run on the waveforms. The estimates of the incoming S wavefronts are generally in agreement with the P wavefonts. However, there is more variation among the S waveforms compared to the P, thus the correlation values were lower indicating more uncertainty in the results. The determinations for the back azimuth to the event and the vertical incidence angle are within 14 degrees of the values from the P waves. This indicates that the P and S wavefronts are approaching from approximately the same angle. The average S-wave velocity is 0.61 ± 0.06 km/sec. This gives a high P to S velocity ratio of 2.3 ± 0.2.

As mentioned above there tends to be more uncertainty in the S-wave estimates because of the variation in waveforms across the array. At a given frequency, the S waves might be expected to show more variations than the P waves, because the S-wave velocity is slower than the P-wave velocity and the wavelength is correspondingly shorter. For this reason, the S waves might also be more sensitive to site-dependent time delays. Figure 5-5 shows the P- and S-wave arrivals for the event at 1839 on 10/15/90. Note that the pattern of relative arrival times across the array is quite similar for the P and S, with the exception of G5A, where the S wave arrives late. This significant S-wave site delay appears to be azimuthally dependent and is strong for events 5 and 8, which approach the array steeply from the northwest. For these two events, G5A was not used in the S-wave slowness analyses. There is also some evidence that the delay could be due to phase response problems in the instrumentation at G5A.

FREE-SURFACE REFLECTIONS

Figure 5-6 shows the P- and S- wave arrival from the event at 1839 on 10/15/90 as recorded on the tunnel stations and one surface station directly above, plotted as a function of station depth. The instrument response was removed to convert the data to ground displacement and the waveforms were aligned on the first arrival. Note that there is a secondary arrival (dashed line) following both the initial P and S arrivals on the tunnel stations, but not on the surface station. This arrival is interpreted to be the downward reflection from the free surface, since it moves out with station depth. The timing and polarity of this arrival is also consistent with the direct arrivals at the surface station G4A and the tunnel station G1A located 60 meters directly below. Between these two stations there is a 0.04 sec time difference in the direct P arrival which corresponds to the 0.08 sec two-way travel time of the surface reflection seen on G1A (Figure 5-6). This type of arrival has been previously observed from borehole data (Hauksson *et al.*, 1987). The amplitude of the first arrival at the tunnel stations is about half that of the surface station. This difference can be partly explained because the energy is divided between the direct and reflected arrivals for the sub-surface stations, while for the stations on the surface all the energy is contained in the direct arrival. Also, there is an amplitude difference because the surface station is sited on lower-velocity material. At these high frequencies, the tunnel sites show more complicated waveforms than the surface sites. These differences in waveforms may affect the estimated slowness, if the waveform correlations are dominated by these high-frequency characteristics. To avoid this, we use relatively long (0.5 to 0.7 sec) time windows to give more weight to the lower-frequency components.

We can use this secondary arrival to estimate the P-wave velocity in the material between the tunnel stations and the surface. Assuming that the ray is traveling at a near-vertical angle of incidence as indicated by the slowness results, the time difference between the direct and reflected arrivals is the two-way travel time from the station to the surface. The measured times give average velocities of 0.33, 0.70, 1.1, and 1.5 km/sec for the material between the surface and stations G3A, G2A, G2B, and G1A, respectively, as shown in the top portion of Figure 5-7. If we assume that the velocity structure is parallel to the topography, the data can also be interpreted as a layered structure shown in the bottom portion of Figure 5-7, with velocities ranging from 0.33 km/sec at the surface to 6.0 km/sec at a depth of 60 m. The layer thicknesses in this model were arbitrarily set to match the station spacings. The actual velocity structure may be quite different from either of the simple models shown in Figure 5-7, especially given the various layers of volcanic tuff that are observed in the local geology near the tunnel. However, at present we do not have data to constrain the velocity of these more complicated structures.

The S waveforms in Figure 5-6 are very similar to the P waveforms, therefore the timing of the reflection phases gives an S-wave velocity structure similar to the the P-wave velocity structure but with 0.5 times the velocity. This P to S velocity ratio of 2.0 is the same as obtained from the slowness analysis for this event. The ratio of 2.0 measured from the reflected arrivals is probably the more reliable estimate because it is a direct measurement of the time differences of P and S waves arriving along similar paths.

DISCUSSION

We do not have independent determinations for the locations of these events, so it is difficult to judge the accuracy in the estimates for back azimuth and incidence angles. The estimates of the P- and S-wave velocities are much better constrained. The largest time differences are between the tunnel and surface stations, indicating that most of the arrivals have steep angles of incidence. Therefore, small errors in the back azimuth and incidence angle do not affect the velocity estimates significantly. This is reflected in our consistent estimates of the material velocity. Determination of apparent velocity for steep incidence angles are strongly dependent on the angle of incidence, so there is much more uncertainty in these values.

The slowness analysis used in this study assumes a plane wave incident on the array. This assumption breaks down for any vertical or lateral variations in velocity near the array, as was clearly inferred from analysis of the reflected phases. However, the values from the slowness analyses are still meaningful as velocities for the near-surface region averaged over the dimensions of the array. In particular, since the largest time differences are measured between the tunnel and surface stations, the velocity estimates in our study are dominated by the near-surface material above the tunnel. The consistent results we obtain for a wide range of P-wave azimuths indicate that lateral variations are not strong enough to affect the P-wave velocity estimates. However, there appear to be stronger lateral variations in the S-wave velocity structure to the extent that incoming wavefronts are not as well approximated by a plane wave.

The velocities estimated by the slowness method are also frequency dependent, since lower frequencies, corresponding to longer wavelengths, will sample material properties deeper in the crust. We see this effect in the higher P-wave velocity for event 2, which was the most distant event (S-P time > 9 seconds) and had P waves with the lowest frequencies. This is further evidence that the low velocities are associated with the near-surface material. In additon, the most direct evidence for the very low velocities near the surface are the time delays from the free-surface reflections at tunnel stations. Using four tunnel stations at various depths below the surface, we see a strong increase of both the P- and S-wave velocities with depth (Figure 5-7). The range of values we obtain are similar to the results from a borehole experiment at Anza, California (Fletcher *et al.*, 1990) and show P-wave velocities near the surface of a few hundred meters per second and increasing to several kilometers per second at 50 to 100 meters depth. This strong depth dependence of the velocity is some of the detailed velocity structure that is blurred together in our average P-wave velocity of 1.43 km/sec obtained from the slowness method.

This three-dimensional array experiment has been useful for making direct estimates of the P- and S-wave velocities and providing approximate locations of local earthquakes (Figure 5-8). Knowledge of the near-surface velocities is important for evaluating the site effects associated with strong ground-motions. However, in the slowness analysis we assume that the region around the tunnel was a uniform medium, and thus obtain only average near-surface velocities. Denser instrumentation would be useful for studying the lateral variations that exist on the scale of tens to hundreds of meters. These site conditions affect the ampltudes of the high-frequency waves and also affect our direction estimates of the incoming wavefronts. Further, for the purposes of more accurately locating earthquakes, the aperture of the array should be expanded to several kilometers. Even in that case, it would be necessary to have some indepently known source locations to detemine the individual site delays.

CONCLUSIONS

Estimates of slowness for incoming P and S waves recorded on the Garni three-dimensional array show steep incidence angles from local earthquakes. These arrivals give average P- and S-wave velocities of 1.43 $\pm$ 0.22 and 0.61 $\pm$ 0.06 km/sec, respectively, for the region around the array. Since the data used for slowness correlations have relatively high predominant frequencies (3-20 Hz), these values reflect the material close to the ground surface. This result was confirmed by measurements of the time delays from free-surface reflections observed on the tunnel stations. The P-wave velocity profile inferred from the surface reflections varied from 0.33 km/sec near the surface to 6.0 km/sec at 60 meters depth. At the higher frequencies used in this study, the tunnel sites have more complicated waveforms than the surface sites, because of the reflection off the ground surface. In addition to differences in waveform and amplitude between the closely spaced instruments, there are also arrival-time delays which are particularly strong for the S wave and affect the ability of the array to resolve the incoming azimuth of seismic waves.

Despite the high frequency complexities observed in the incoming wavefronts, the array was still useful for giving approximate locations of small earthquakes in the immediate region, which may be important for seismic hazard assessments. Garni lies on the northern edge of a narrow, east-west trending valley, a strong topographic feature that may be due to active faulting. This feature extends west to the outskirts of Yerevan, a city of 1.2 million people.

ACKNOWLEDGEMENTS

E. Sembera, C. Dietel, K. Safarian, H. Galagian, G. Apoian, and K. Kirakossian supplied technical support for the instrumentation. R. Banfill wrote much of the software for the PC system. The research is part of the Joint Seismic Program led by the Incorporated Research Institutions for Seismology (IRIS). This research was sponsored by the Defense Advanced Research Projects Agency and the Air Force Office of Scientific Research through the Air Force Geophysical Laboratory and the National Science Foundation. The work was carried out under the aegis of Area IX of the U.S./U.S.S.R Agreement on Cooperation in the field of Environmental Protection. D. Eberhart-Phillips and S. Hough provided helpful comments on this paper.

Table 5-1. Parameters of incident plane waves from events recorded on the Garni array. Distances were estimated from S-P times. Magnitudes were determined by convolving a Wood-Anderson instrument response with the data.

No.	Date	Time	Distance (km)	Magnitude	P wave				S wave			
					Back Azimuth (deg)	Apparent Velocity (km/s)	Velocity (km/s)	Incidence Angle (deg)	Back Azimuth (deg)	Apparent Velocity (km/s)	Velocity (km/s)	Incidence Angle (deg)
1.	09/21/90	0715	16	1.2	282	16.7	1.28	4				
2.	10/05/90	0755	>60		294	8.3	2.02	14				
3.	10/09/90	2054	12	0.8	176	4.2	1.27	18				
4.	10/15/90	0746	12	0.9	338	11.1	1.44	7				
5.	10/15/90	1839	12	1.7	338	11.1	1.44	7	326	6.7	0.71	6
6.	10/18/90	1118	30	2.3	82	6.7	1.21	11	90	3.3	0.55	10
7.	10/27/90	0544	42	3.0	204	11.1	1.44	7	198	10.0	0.62	4
8.	11/08/90	2037	12	1.6	354	16.7	1.33	5	8	5.0	0.62	4
9.	11/16/90	0653	20	1.8	74	6.7	1.36	12	80	3.3	0.58	10
10.	11/16/90	0703	20	1.8	74	6.7	1.36	12				
11.	11/16/90	1500	14	2.2	32	8.3	1.56	11	34	3.3	0.58	10

Figure 5-1. Approximate station configuration for the three-dimensional Garni Array. G5B which appears to be above the ground is on a hillside slope east of the array.

Figure 5-2. Example of the three-component velocity data for the event at 1500 on 11/16/90.

Figure 5-3. Contoured plots of combined cross correlation values for tested values of slowness from the P-wave window of the event at 1500 on 11/16/90. Vertical (top) and horizontal (bottom) slices of the three-dimensional slowness space are shown. High correlation values (shaded areas) correspond to values of slowness which are consistent with a plane-wave propagating across the array.

Figure 5-4. Contoured plots of combined correlation values from the S-wave window of the event at 1500 on 11/16/90.

Figure 5-5. P- and S-wave arrivals for the event at 0746 on 10/15/90. Note that the relative arrivals for the P and S are similar, except at G5A where the S wave arrives significantly late.

Figure 5-6. Ground displacements of the P and S waves for the event at 1839 on 10/15/90. Reflections from the free surface (dashed line) can be seen following both the P- and S-wave arrivals at the tunnel stations.

Figure 5-7. (Top) Average P-wave velocities between the tunnel stations and the ground surface from time delays of surface reflections.

(Bottom) Velocity model consistent with the time delays of the surface relections, assuming a layered structure parallel to the topography.

Figure 5-8. Rough locations of the numbered events from Table 5-1 shown on a map of northern Armenia.

Wave-slowness contour plots for selected events

Plots not available in PDF-file.

REFERENCES

Arefiev, S., I. Parini, K. Pletnev, A. Romanov, D. Mayer-Rosa, and P. Smit (1991). "Spitak (Armenia, USSR) 1988 Earthquake Region: Strong-Motion Data of Selected Earthquakes June 1990 - April 1991", *Technical Report No. 104, Publication Series of the Swiss Seismological Service,* Federal Institute of Technology, Zurich, Switzerland.

Borcherdt, R. D., J. B. Fletcher, E. G. Jensen, G. L. Maxwell, J. R. VanSchaak, R. E. Warrick, E. Cranswick, M. J. S. Johnston, and R. McClearn (1985). A general earthquake observation system (GEOS), *Bull. Seismol. Soc. Am.*, **75**, 1783-1826.

Borcherdt, R. D. (Editor), (1989), Results and data from seismologic and geologic studies following earthquakes of December 7, 1988, near Spitak, Armenian S. S. R.

Fletcher, J. B., T. Fumal, H.-P. Liu, and L. C. Haar (1990). Near-surface velocities and attenuation at two boreholes near Anza, California, from logging data, *Bull. Seismol. Soc. Am.*, **80**, 807-832.

Frankel, A., S. Hough, P. Friberg, and R. Busby (1991). Observations of Loma Prieta aftershocks from a dense array in Sunnyvale, California, *Bull. Seismol. Soc. Am.*, **81**, 1900-1922.

Hauksson, E., T. Teng, and T. L. Henyey (1987). Results from a 1500m deep, three-level downhole seismometer array: site response, low Q values and f_{max}, *Bull. Seismol. Soc. Am.*, **77**, 1883-1904.

Kanamori, H. and P. C. Jennings (1978). Determination of local magnitude, M_L, from strong-motion accelerograms, *Bull. Seismol. Soc. Am.*, **68**, 471-485.

Lee, W. H. K. (Editor), (1989). "Toolbox for Seismic Data Acquisition, Processing, and Analysis", *IASPEI Software Library Volume 1*, Seism. Soc. Am., El Cerrito, CA.

Lee, W. H. K. and D. A. Dodge (Editors), (1992). A course on: PC-based seismic networks, *U. S. Geol. Surv. Open-File Report 92-441*, 535 pp.

Lee, W. H. K., D. M. Tottingham, and J. O. Ellis, (1988). A PC-based seismic data acquisition and processing system, *U. S. Geol. Surv. Open-File Report 88-751*, 31 pp.

Menke, W., A. L. Lerner-Lam, B. Dubendorff, and J. Pacheco (1990). Polarization and coherence of 5 to 30 Hz seismic wave fields at a hard-rock site and their relevance to velocity heterogeneities in the crust, *Bull. Seismol. Soc. Am.*, **80**, 430-449.

Mori, J. (1993). Waveform coherence of near-field waveforms on a small-aperture array in Upland, California, in preparation.

Richter, C. F. (1937). *Elementary Seismology*, W.H. Freeman and Company, San Francisco.

Tottingham, D. M. and W. H. K. Lee, (1989). XDETECT: A fast seismic data acquistion and processing program, *U. S. Geol. Surv. Open-File Report 89-205*, 8 pp.

United States Geological Survey, (1990-1992). Preliminary Determination of Epicenters.

Vernon, F. L., J. Fletcher, L. Carroll, A. Chave, and E. Sembera (1991). Coherence of seismic body waves from local events as measured by a small-aperture array, *J. Geophys. Res.*, **96**, 11981-11996.